

Influence of plasma pre-treatment of
polytetrafluoroethylene (PTFE) micropowders on the
mechanical and tribological performance of
polyethersulfone (PESU)-PTFE and impact modified
polyamide (PA66)-PTFE compounds

Published works submitted in partial fulfilment of the requirements of the
University of Bolton for the degree of Doctor of Philosophy on the basis of
published work

By

Harald Hunke

May 2017

Institute for Materials Research and Innovation (IMRI),
University of Bolton,
Deane Road,
Bolton BL3 5AB, United Kingdom

Acknowledgement

This PhD by publication would never have been completed without the contribution of many individuals, to whom I am deeply indebted. Firstly, I would like to express my deep gratitude to my PhD supervisors, Professor Tahir Shah, Professor Elias Siores and Dr Navneet Soin from the University of Bolton, who gave me the opportunity, the encouragement and the strong support to conduct this work. I am extremely grateful to Professor Erich Kramer from the University of Applied Sciences, Northwestern Switzerland, for initiating the idea for this project and for introducing me to the field of tribology years ago, when I wrote my master thesis. I would also wish to thank Mr Christof Diener and Mrs Nicole Müller from Diener GmbH for providing the access to plasma treatment equipment, their support and for sharing their knowledge of the subject. The research programme would not have been realized without compounding of the materials and I am therefore indebted to Mr Tim Henken and Mr. Markus Warzel of Sitraplas GmbH for providing the compounding facilities. I would like to thank Dr Alfons Pascual (University of Applied Sciences, Northwestern Switzerland) for the support with the DSC analysis, Dr MSL Karuna (IICT, Hyderabad, India) for the contact angle measurements and Dr Kurt Witan (University of Applied Sciences in Darmstadt) for providing the support to conduct the dart drop tests and preliminary ball on plate tribology tests. I would like to thank my friends Andreas Tatar for the development and construction of the pin carrier for the tribological pin on disc tests and Marco Prigandt for the support with the mechanical trials. My thanks are also due to Mrs Regina Straessle and Mr Fabian Meier (KATZ Training and Technology Centre in Aarau, Switzerland) for their help with tribology measurements of the PESU-PTFE samples.

Many thanks to Mr. Andreas Gebhard (Tribologic GmbH in Kaiserslautern) who helped in obtaining the tribological results for the polyamide samples and for helping me with his great knowledge of tribology. I would also like to thank the University of Newcastle for the X-ray photoelectron spectra, which were obtained at the National EPSRC XPS User's Service (NEXUS) facility, and Anand Arcot Narasimulu (University of Bolton) who helped in the EDAX analysis of the compounded samples. I gratefully acknowledge the support of companies BASF SE, EMS Grivory and Sitraplas GmbH for the supply of the materials used in this study.

My endless gratitude to my dad, who died prematurely, and who would have been extremely happy to see me complete my PhD programme, and to my dear mom for their continual support on all my ways! I owe you everything! Special thanks to my parents- in-laws, who always supported our family especially when I was busy with this research project. Finally, I want to express my thanks to my dear wife Nicole and my sons, Mats and Tom for their love and understanding, which allowed me to pursue my time consuming scientific interests in addition to my job. Thank you for giving me the hope, the courage and the support, especially at times of my weakness, to complete this work.

Dedicated to my parents Marlies and Eberhard,
my wife Nicole, and our sons Mats and Tom.

Declaration

I declare that this work is not the same as any that I have previously submitted or am currently submitting in any form, or for any qualification, at any university or other educational institution. None of this work, nor parts of this work, have previously been submitted for an award of a qualification through any university or other educational institution.

Signed: Oerlinghausen, May the 06th 2017

A handwritten signature in blue ink, appearing to read "Harald Funke". The signature is written in a cursive style with a long, sweeping underline.

Abstract

Polytetrafluoroethylene (PTFE), $(\text{CF}_2\text{-CF}_2)_n$ exhibits a low coefficient of friction (CoF, 0.07 - 0.15) and is therefore widely used as an additive in polymer compounds to improve their friction and wear properties. However, its applications in polymer compounds are limited due to the PTFE's inherent poor chemical reactivity, low wettability and poor adhesion with other polymers preventing the establishment of good interfacial bonding. To overcome this, the work introduces plasma treatment of PTFE micropowders in a low-pressure 2.45 GHz microwave plasma reactor, using NH_3 and H_2 as process gasses to chemically modify their surface by introducing surface nitrogen and oxygen polar groups leading to more hydrophilic surfaces. The presence of these functional groups enhances the surface energy of the plasma treated PTFE and enhances the compatibility with thermoplastic polymers. It must be emphasised that nearly all the literature existing on the surface functionalisation of PTFE focuses on the PTFE films only. The first publication from this research work, in the group of three, reports on the effects of the H_2 , NH_3 plasma processing time (2.5, 10 h), resulting defluorination (1.13 for $\text{NH}_3/10\text{h}$, 1.30 for $\text{H}_2/10\text{h}$ as compared to 1.86 for pristine PTFE) and measurement of changes in wettability and crystallinity of the PTFE micropowders. The resulting plasma modified PTFE micropowders were further used as dry lubricants to enhance the tribological and mechanical properties of amorphous polyethersulfone (PESU) and semi-crystalline α -olefin-copolymer impact-modified polyamide 66 (PA66i) polymer compounds resulting in the next two publications. At the same loading levels (10wt%) of PTFE, prepared using twin-screw compounding, the pin-on-disc tribological measurements of the PESU-PTFE compounds revealed a lower

CoF from 0.55 for pristine PESU to 0.20 along with corresponding reduction in the wear rates from $5.75 \times 10^{-06} \text{ mm}^3/\text{Nm}$ (pristine PTFE) to $4.70 \times 10^{-06} \text{ mm}^3/\text{Nm}$ (for H_2 treated PTFE) to $3.42 \times 10^{-06} \text{ mm}^3/\text{Nm}$ (for NH_3 treated PTFE). In the PA66i matrix, the wear rates of the pristine and plasma treated PTFE were observed to be similar for the sliding speeds up to 2 m/s. However, at the higher sliding speeds, the benefits of plasma treatment became more apparent. At the sliding speed of 3 m/s, the wear rate of pristine PTFE-PA66i compound was $1.1 \times 10^{-06} (\pm 0.2) \text{ mm}^3/\text{Nm}$ whereas the wear rate of H_2 treated PTFE was $0.7 \times 10^{-06} (\pm 0.1) \text{ mm}^3/\text{Nm}$ and the wear rate of NH_3 treated PTFE was $0.6 \times 10^{-06} (\pm 0.1) \text{ mm}^3/\text{Nm}$. These improvements in the tribological and mechanical properties have been ascribed to the enhanced dispersion of PTFE in the host matrix with the plasma processing introduced functional polar groups providing enhanced intermolecular bonding (as confirmed using Fourier transform infrared spectroscopy, differential scanning calorimetry and dynamic mechanical-thermal analysis) between the components. Therefore, the incorporation of functional groups into PTFE micro-powders by plasma treatment is an effective and efficient route for enhancing the mechanical and tribological properties of engineering polymer compounds such as PESU-PTFE and PA66i-PTFE offering significant cost and environmental benefits over the existing e- beam and wet chemical technologies.

Table of Contents

Acknowledgement.....	II
Declaration	V
List of Figures.....	XI
List of Tables	XVI
Abbreviations.....	XVIII
Structure of the Thesis	XXI
1 Introduction	23
1.1 Literature review.....	23
1.2 Aims of the research	28
1.3 Research Objectives.....	28
1.4 Accomplishment of material production and tests.....	29
2 Tribology: Fundamentals	32
2.1 Economic aspects of tribology.....	33
2.2 The tribological system.....	35
2.2.1 Theory of friction.....	39
2.2.2 Friction mechanism.....	42
2.2.3 Stick-slip-phenomenon	46
2.2.4 Theory of wear.....	46
2.2.5 Mechanism of Wear.....	48
2.2.6 Measurement of wear.....	50
2.3 Classification of tribological tests.....	51
3 Materials in Tribology	55
3.1 Polymers in tribological applications.....	57
3.2 Polyamide 66 (PA66).....	61
3.3 Polyethersulfone (PESU).....	65
3.4 Polytetrafluorethylene (PTFE).....	67
3.4.1 Tribological aspects of PTFE as a solid lubricant	71
3.4.2 PTFE micro powder.....	73
4 Plasma modification of polymers.....	77
4.1 The plasma process	77
4.1.1 Plasma treatment of polymer powders.....	84
5 Experimental set-up.....	88
5.1 Plasma Treatment of PTFE Powder.....	88

5.2	Composition and compounding of samples	91
5.3	Injection moulding of test specimens	95
6	Analytical Methods	97
6.1	Powder characterisation	97
6.1.1	Fourier transform infrared spectroscopy (FTIR)	97
6.1.2	Differential scanning calorimetry (DSC).....	98
6.1.3	X-ray photoelectron spectroscopy (XPS)	99
6.1.4	Thermal stability of plasma induced functional groups.....	100
6.1.5	Contact angle measurement of PTFE powders	100
6.2	Compound characterisation	103
6.2.1	Tensile test	103
6.2.2	Melt volume-flow Rate (MVR)	103
6.2.3	Dart drop test.....	105
6.2.4	Dynamic-mechanical thermal analysis (DMA)	106
6.2.5	Scanning Electron Microscopy (SEM)	106
6.3	Tribological testing	107
6.3.1	Pin-on-disc test.....	107
6.3.2	Block-on-ring test	110
6.3.3	Statistical methods for result evaluation	113
6.3.3.1	Statistical outlier test according Nalimov	113
6.3.3.2	Standard deviation and confidence interval	114
6.3.4	Raw data analysis.....	116
6.3.5	Number of tests	117
7	Experimental results and discussion	118
7.1	Results of PTFE plasma treatment.....	118
7.1.1	Fourier transform infrared spectroscopy (FTIR)	118
7.1.2	Differential scanning calorimetry (DSC).....	120
7.1.3	X-ray photoelectron spectroscopy (XPS)	124
7.1.4	Thermal stability of plasma induced functional groups.....	129
7.1.5	Contact angle measurement of PTFE powders	131
7.2	Compound characterisation	132
7.2.1	Tensile test	132
7.2.2	Melt volume-flow rate (MVR).....	134
7.2.3	Dart drop test.....	136
7.2.4	Dynamic-mechanical thermal analysis (DMA)	139
7.2.5	Scanning electron microscopy (SEM)	140
7.3	Tribological testing	143
7.3.1	Pin-on-disc test.....	143
7.3.2	Block-on-ring test	147
8	Conclusions and recommendations for further work	153

8.1	Contents of the work.....	153
8.1.1	Goals achieved.....	153
8.2	Conclusions.....	155
8.3	Recommendations for further work.....	159
A	Appendix.....	161
A.1	Paper in Materials 2015, volume 8, pages 2258–2275	161
	Low-Pressure H ₂ , NH ₃ Microwave Plasma Treatment of Polytetrafluoroethylene (PTFE) Powders: Chemical, Thermal and Wettability Analysis.....	161
A.2	Paper in Wear 2015, volumes 328-329, pages 480–487.....	162
	Influence of plasma pre-treatment of polytetrafluoroethylene (PTFE) micropowders on the mechanical and tribological performance of Polyethersulfone (PESU)–PTFE composites.....	162
A.3	Paper in Wear 2015, volumes 338-339, page 122–132	149
	Plasma modified Polytetrafluoroethylene (PTFE) lubrication of α -olefin-copolymer impact-modified Polyamide 66.....	149
A.4	Collaborative work.....	198
A.5	Non published results.....	216
A.5.1	SEM images of counter discs.....	216
A.6	Statistical values.....	217
A.6.1	r-table	217
A.6.2	Table of student t-factor.....	218
9	References.....	219

List of Figures

Figure 2.1 Real contact area of a Polyamide-PTFE sample 2-PA66-T2 before (left) and subsequent (right) to a ball on plate tribological test. AFM atomic force microscopy area: 30 μm x 30 μm	35
Figure 2.2 Schematic view of two surfaces in contact (left) and upon load and motion (right)	36
Figure 2.3 Tribological system and influences thereof based on: Uetz Wiedemeyer [67]	37
Figure 2.4 Phases of energy dissipation [66].	38
Figure 2.5 Stribeck curve with phase I: solid friction, phase II.: mixed friction and phase III.: hydrodynamic friction.....	40
Figure 2.6 Schematic illustration of the basic friction mechanism [70]	42
Figure 2.7 Influence of surface roughness [73]	44
Figure 2.8 Model concept of deformation by tangential stress according to Erhard [77]	45
Figure 2.9 Categories of wear classified by the type of relative motion according to Blau [82]	47
Figure 2.10 Wear mechanisms according to DIN 50320 [70]	48
Figure 2.11 Measurement of wear [87].....	50
Figure 2.12 Classification of tribological tests according Uetz et al. [67].....	52
Figure 2.13 Simplified model tests according DIN ISO 7148-2 [89].....	52
Figure 2.14 Simplified model tests for material evaluation: Block on ring (left), ball on flat (middle) and pin on disk (right).....	53

Figure 3.1 Engineering plastics in tribological applications and their continuous service temperature	56
Figure 3.2 Structure of polyamide 66	61
Figure 3.3 Structure of PESU with aromatic rings linked via sulfone group with ether linkages	65
Figure 3.4 Structure of polytetrafluoroethylene PTFE	68
Figure 3.5 Helix structure of PTFE molecule [129]	70
Figure 4.1 Microwave (MW) plasma treatment of PTFE with hydrogen as process gas	78
Figure 4.2 Inter molecular interaction between functionalised PTFE and polyamide 66 (left) and PESU (right).....	83
Figure 4.3 Inter molecular interaction between functionalised PTFE and polyamide 66 (left) and PESU (right).....	83
Figure 4.4 Reactor configurations for plasma treatments of polymer powders according to [181]. 1.) Fluidized bed reactor 2.) Circulating fluidized bed 3.) Rotating drum reactor 4.) Batch reactor	86
Figure 5.1 (a) Photograph of Microwave plasma device used during the study, (b) glass drum with the excited microwave plasma.....	88
Figure 5.2 Schematic view of a co-rotating twin screw extruder (left) and kneading and conveying element (right)	93
Figure 5.3 Schematic set up of the compounding line	94
Figure 6.1 Hydrophilic (left) vs. hydrophobic droplet (right).....	101
Figure 6.2 Balance of forces at liquid droplet on a surface (Young's equation)	101
Figure 6.3 Dart drop test apparatus.....	105
Figure 6.4 WAZAU tribometer (left); schematic of the pin-on-disc measurement (right)	107

Figure 6.5 Tribo pins with carrier before test (left) and subsequent to the test (right)	108
Figure 6.6 Schematic of the block on ring test (left); Atlas TT block on ring tester (right)	110
Figure 6.7 Side view of Atlas TT tester (left); schematic set-up of Atlas TT (right)	110
Figure 7.1 ATR FTIR spectrum of treated and pristine PTFE samples (a) In the region between 1250 cm^{-1} and 1450 cm^{-1} showing the slightly stronger reflection of the bands of PTFE $\text{H}_2/10\text{ h}$ and PTFE $\text{NH}_3/2.5\text{ h}$ in the vicinity of 1300 cm^{-1} . (b) in the region between 1050 cm^{-1} and 1400 cm^{-1} showing the shifted bands of PTFE $\text{H}_2/10\text{ h}$.	120
Figure 7.2 DSC curves of 1st heating cycles of (a) H_2 plasma treated PTFE sample. (b) NH_3 plasma treated PTFE sample. (c) MAX H_2 plasma treated PTFE powders. The expanded curves on the left show the post-crystallization peaks observed for the plasma treated samples.	123
Figure 7.3 (a) High resolution C1s spectra of pristine and NH_3 plasma treated PTFE powders. (b) Deconvolution of C1s spectra of pristine and PTFE/ $\text{NH}_3/10\text{ h}$ samples. (c) Increase in the N1s signal intensity as a function of NH_3 plasma treatment time. (d) XPS valence band spectra of pristine and PTFE/ $\text{NH}_3/10\text{ h}$ samples.	125
Figure 7.4 (a) High resolution C1s spectra of pristine and H_2 plasma treated PTFE powders showing the efficacy of the process. (b) High resolution C1s spectra of PTFE/ $\text{H}_2/2011$ and PTFE/ $\text{H}_2/2012$ samples showing the degeneration of plasma treated surfaces.	129
Figure 7.5 Temperature dependent XPS of pristine and plasma modified PTFE (a) C1s core level XPS spectra for pristine PTFE. (b) C1s core level XPS	

spectra for PTFE/H₂/10h sample. **(c)** C1s core level XPS spectra for PTFE/NH₃/10h sample. **(d)** N1s core level XPS spectra showing the decrease in the signal intensity. **(e)** Changes in the O/C and N/C atomic ratios for PTFE/NH₃/10h sample as function of temperature. **(f)** Evolution of F/C atomic ratio for pristine and plasma treated PTFE as a function of temperature. 130

Figure 7.6 **(a)** Variation of contact angle for pristine and plasma treated samples in various testing media, **(b)** Pristine PTFE powders are poorly dispersible in water (**left**); upon H₂ (**middle**) and NH₃ plasma treatment (**right**), the dispersion is significantly improved. 132

Figure 7.7 **(a)** Magnification of impact data of PESU-PTFE compounds with 10% modification (pristine and plasma treated), **(b)** Impact test data of all PESU and PESU-PTFE compounds. 136

Figure 7.8 Impact test data of all Pa66i compounds. 137

Figure 7.9 Plots of storage modulus and tan δ versus temperature for impact modified PA66 and its compounds with pristine and plasma treated PTFE powders. 140

Figure 7.10 SEM pictures of the fractured surface of tensile test bars. PESU-PTFE composites with 10% pristine PTFE (**left**), PESU-H₂ (**middle**) and PESU-NH₃ 141

Figure 7.11 SEM analysis of the fracture surface of **(a, b)** 1-PA66-T0, **(c, d)** 2-PA66-T2, **(c)** 6-PA66-H2 and **(d)** 28-PA66-NH3 samples. 143

Figure 7.12 Mean friction coefficient as a function of time of PESU-PTFE compounds 145

Figure 7.13 Wear loss of PESU-PTFE compounds vs. sliding distance in pin on disc set up 146

Figure 7.14 Mean friction coefficient as a function of time of PA66i-PTFE compounds	148
Figure 7.15 Average curves (dark blue) of test specimen height loss (top), CoF (middle) and counter body temperature (bottom) and upper and lower boundaries (light blue) of the corresponding confidence intervals. From left to right sliding speed increases from 1 m/s to 3 m/s in steps of 1 m/s.	150
Figure 7.16 Wear rate of PA66i-PTFE compounds vs. sliding speed	151
Figure 8.1 SEM pictures of transfer film on discs after sliding against (a) sample 15-PESU-T2, (b) sample 30-PESU-NH3	216

List of Tables

Table 3.1 Operating temperature (short term and long term) and sliding surface temperature [92].....	57
Table 3.2 Mechanical properties of PA 66 according to [106]	62
Table 3.3 Mechanical properties of impact modified PA66 compound	65
Table 3.4 Properties of PESU according [121]	67
Table 3.5 Bond energies in polymers according to [122]	69
Table 3.6 Mechanical properties of PTFE according to [123,127].....	70
Table 3.7 Properties of Dyneon PTFE TF 9201Z	75
Table 4.1 Chemical assignments of C1s peak positions on PTFE treatment with hydrogen and ammonia	79
Table 5.1 Parameters for Plasma treatment of PTFE samples	90
Table 5.2 Polyamide processing conditions	94
Table 5.3 Polyethersulfone processing conditions	94
Table 5.4 Composition of polyamide 66 samples	95
Table 5.5 Composition of polyethersulfone samples	95
Table 5.6 Injection moulding parameters and moulding times for polyamide 66	96
Table 5.7 Injection moulding parameters and moulding times for polyethersulfone samples.....	96
Table 6.1 Parameter of tribological tests.....	109
Table 6.2 Parameter of tribological tests.....	111
Table 6.3 r values and corresponding outlier classification	114
Table 6.4 Report of Atlas tribo tester for sample 1-PA66-T0 at 2 MPa and a sliding velocity of [m / s].....	116

Table 6.5 Number of tests conducted and standards used.....	117
Table 7.1 Summary of various differential scanning calorimetric values of different PTFE samples	121
Table 7.2 Atomic percentages and associated elemental ratios of PTFE samples..	124
Table 7.3 Mechanical properties of PA66i samples.....	133
Table 7.4 Mechanical properties of PESU samples	134
Table 7.5 Melt volume rate of PESU and PA66i samples	135
Table 7.6 Glass transition temperature of impact polyamide samples.....	139
Table 7.7 Coefficients of friction of the samples as a function of sliding speed	148
Table 7.8 Counter body temperatures of the samples as a function of sliding speed.	149
Table 7.9 Linear wear rate w_t in [$\mu\text{m}/\text{h}$] and specific wear rate w_s in [$10^{-6} \text{ mm}^3/\text{Nm}$] of the samples as a function of sliding speed.....	151

Abbreviations

ASTM	American Society for Testing and Materials
\bar{x}	mean value
°C	Degree Celsius
C	Capillary constant of the powder
CF	Carbon fibre
CO ₂	Carbon dioxide
DIN	Deutsches Institut für Normung
DSC	Differential Scanning Calorimetry
ESCA	Electron Spectroscopy for Chemical Analysis
F	Fluorine
F _{ad}	Adhesion component of friction
F _{def}	Deformation component of friction
F _{dyn}	Dynamic coefficient of friction
F _n	Normal load
F _R	Friction force
f _{stat}	Static coefficient of friction
FTIR	Fourier Transformation Infra-Red
GDP	Gross domestic product
GF	Glass fibre
GHz	Gigahertz
H	Hydrogen
J/m	Joule per meter
K	Wear rate
kJ/mol	Kilojoule per Mol
LCP	Liquid crystal polymer

M	Mass in capillary rise method
m/sec.	Meter per second
Min	Minute
Mm	Millimetre
MoS ₂	Molybdenum disulphide
MPa	Mega Pascal
MVR	Melt Volume-flow Rate
MW	Micro wave
<i>N</i>	number of values
NH ₃	Ammonia
PA	Polyamide
PA46	Polyamide 4.6
PA66	Polyamide 66
PA66i	α -olefin-copolymer impact-modified polyamide 66
PBT	Polybutylene terephthalate
PE	Polyethylene
PEEK	Poly(etheretherketone)
PEI	Polyetherimide
PESU	Polyethersulfone
PET	Polyethylene terephthalate
PI	Polyimide
POM	Polyoxymethylene; acetal
PPE	Polyphenyl ether
PTFE	Poly(tetrafluoroethylene)
pv value	pressure * velocity value
<i>r</i> *	comparison value
S	Sliding distance

S	standard deviation
Sec.	Seconds
SEM	Scanning Electron Microscopy
T	Flow time in capillary rise method
Temp.	Temperature
T_g	Glass transition temperature
T_m	Melting point
UHMW-PE	Ultra High Molecular Polyethylene
UK	United Kingdom
Uv	Ultraviolet
W	Watt
W_{ad}	Work of adhesion
W_L	Linear wear
W_s	Specific wear rate
W_v	Volumetric wear
XPS	X-Ray Photo Electron Spectroscopy
H	Viscosity of the liquid
Θ	Contact angle
P	Density of the test liquid
Σ	Surface tension
σ^d	Disperse component
σ_l	Surface tension of liquid
σ^p	Polar component
σ_s	Surface tension of solid
σ_{sl}	Interfacial tension
γ_{lv}	Liquid surface free energy
γ_{sl}	Solid / liquid interfacial free energy

Structure of the Thesis

This thesis is in the design for a PhD by publication and therefore containing some of the results in the published papers, only. The aims and objectives of the thesis titled “Influence of plasma pre-treatment of polytetrafluoroethylene (PTFE) micro powders on the mechanical and tribological performance of polyethersulfone (PESU)–PTFE and polyamide (PA66)-PTFE composites” are described in Chapter 1.

The fundamentals of tribology encompassed by the economic background and the history of tribology are summarized in Chapter 2. The set-up of a tribological system is illustrated and the mechanism of friction and the mechanism of wear are explained in detail. The important phenomenon of stick-slip is particularly described. The measurements of wear as well as the classification of tribological tests complete the chapter.

Chapter 3 covers the types of polymers and modifications used in tribological applications in general and the polymers chosen in this work as matrix polymers. Polytetrafluoroethylene as polymer and the micro powders thereof as tribological modifications in compounds are also described.

Chapter 4 deals with the theoretical background of plasma treatment of polymers and the challenges and types of plasma treatment of polymer powders in particular.

The experimental set up of the plasma treatment of PTFE powder and its compounding into the matrix polymers as well as the composition of compounds are explained in Chapter 5. The injection moulding of tensile test bars and test plates for the analysis of the compounds is described as well.

Chapter 6 discusses the analytical methods used for the characterization of the plasma altered PTFE powder and the characterization of the compounds using the altered powders as lubricants.

The conclusions and recommendations for further work of the influence of plasma pre-treatment of polytetrafluoroethylene (PTFE) micro powders on the mechanical and tribological performance of Polyethersulfone (PESU)-PTFE and Polyamide (PA66)-PTFE composites are made in Chapter 7.

In the Appendix, unpublished results as well as some statistical auxiliary tables can be found. The peer reviewed papers published in the journals “*Material*” and “*Wear*” are listed in the appendix as well as the literature references used for this research.

1 Introduction

1.1 Literature review

Polymers are gaining an ever-increasing importance in the mechanical engineering applications of our modern world. They offer high strength-to-weight ratio, good chemical resistance and relatively low production cost compared to other engineering materials, such as metal alloys, aluminium, zinc or brass. In the second half of the 20th century, plastics became one of the most universally-used and multi-purpose materials in the global economy [1]. In fact, the global polymer production rose from 1.7 million tons in 1950 to 299 million tons in 2013 [1]. The modification with fibres as reinforcements widens the scope of structural applications, and therefore they are widely used in the fields of metal substitution to reach today's targets of energy and carbon dioxide reduction. More recently, the polymers are increasingly playing an important role as tribo-engineering materials for mechanical engineering components that are subject to friction and wear processes, such as gears, cams, bearings, bushes and bearing cages. Polymers are preferred in tribo-systems due to their low coefficient of friction, ability to sustain loads and relatively low costs. In tribological systems, the parts made out of polymers are often exposed to wear and these are easily exchanged at the end of their life. This enables the complete tribological component to survive longer. The current state of the art of engineering polymer modification for tribological applications now encompasses addition of lubricants such as molybdenum disulphide [2], waxes [3], graphite [4] or polytetrafluoroethylene (PTFE) [5–7]. Especially, PTFE modification of engineering polymers for tribological applications has gained a huge interest due to PTFE's low coefficient of friction. However, PTFE's applications are hampered in some cases

due to its inherent poor chemical reactivity, low wettability and poor adhesion with other materials. Hence, a considerable amount of effort has been made to modify the surface of PTFE and improve its surface activity by means of chemical etching (for ex. reduction with sodium naphthalene), electron beam irradiation or treatment with different plasma techniques [8–15]. While the chemical and UV treatment processes of polymers are well established on laboratory scale, they are not used on commercial scale, as they are difficult to perform in mass production. Electron beam irradiation is already a common commercial method for converting high molecular weight PTFE to a grind-able form for the production process of micro powders [16]. The PTFE resin is irradiated on a conveyor belt subsequent to the reaction process of tetrafluoroethylene to the polymer PTFE. The long chain PTFE molecules are cut (chain scission) by the irradiation process and then grinded to micro powders. However, the scission can be achieved with a relatively low irradiation time and simple equipment. For the incorporation of desired functional groups on a commercial scale, an industrial electron beam accelerator irradiating under ammonia, air or vacuum atmosphere is needed [17]. The electron beam equipment is capital intensive and in fact, the electron beam irradiated PTFE costs anywhere between Euro 50-80/kg. Therefore, it is desirable to develop a more consistent and cost-effective process to incorporate functional groups onto the PTFE surface for their subsequent use as lubricants in engineering thermoplastics. Plasma treatment of polymers is a versatile method to create novel surface functionalities by incorporating polar groups without altering their bulk properties. The technique is environmentally friendly, unlike the chemical treatment processes, it does not release toxic organic components to the environment. Moreover, the plasma treatment can be performed at room temperature, with the process being relatively easy to control and low in cost [18]. The plasma treatment of polymer surfaces of films and parts is state

of the art and subject of many publications with relevance to adhesion [19–22] and tribology [23]. Yasuda et al. showed that functional groups can also be incorporated into PTFE films by plasma treatment with different process gasses such as argon, nitrogen, ammonia, or hydrogen [24]. From a technological point of view, as compared to polymer films, the plasma treatment of powders is inherently difficult owing to the three-dimensional geometry of the particles. Sophisticated mixing techniques are required to overcome the agglomeration phenomenon and to ensure that the large surface area of the powder is uniformly exposed to the plasma [12]. While the plasma treatment of PTFE films is well established in the literature [20,25–27], and plasma treatment of other polymer powders are state of the art [28–32], so far there is no disclosed literature work regarding the plasma treatment of PTFE powders and the use thereof in different types of engineering thermoplastic matrixes.

The low-cost generic polymers such as polypropylene, polyethylene offer good friction properties on their own and addition of any fluorinated additives to improve their friction properties is not very common. However, for standard engineering semi-crystalline polymers such as nylons, polyacetals, aromatic polyesters, the addition of PTFE to improve their frictional and wear properties is quite common. For high temperature engineering polymers such as polysulfone, polyethersulfone and polyetheretherketone which are processed (300-350 °C) and indeed also used at elevated temperatures, the addition of PTFE requires special considerations as the additive will get molten during the processing. The initial work on reducing the wear and friction properties for thermoplastics involved high molecular weight PTFE which however suffered from fibrillation especially during the high shear processing above its glass transition temperature of 19 °C. To overcome this issue, PTFE which was processed by heating it above its melting temperature i.e. sintered PTFE was

observed to show ease of processability. However, this high temperature sintering was shown to degrade the tensile and impact strength of the PTFE and consequently the host matrix. Upon compounding of the fluorinated additives such as PTFE into the thermoplastic matrix, their low surface energy is also imparted to the compounded material. While the intention of the using a high-shear process such as compounding is to ensure a homogeneous distribution of PTFE into the matrix, the differences in the surface energy of the compounds can lead to preferential segregation of the lowest-surface energy compound to the surface of the compounded material [33,34]. While in some cases this could be desirable to create surfaces which are water, oil, stain repellent but also helps in its processing especially with melt processing techniques of extrusion and mould release during die injection moulding. However, for applications of polymer-PTFE compounds such as bearings in diesel pumps or gears in different motor actuators, the excessive diffusion to the surface presents a significant issue wherein the diffused PTFE can be removed easily leading to increase in the surface energy and reduction in the friction and wear properties in creating a friction film on the surface and therefore decreasing *cof* and wear rate.

Polyamide 66, also well known as Nylon, has found great attraction as an engineering polymer in the fields of tribology, due to the high stiffness and wear resistance. The ability to form van der Waals forces and hydrogen forces [35] within their molecular structure leads to superior characteristics. To improve nylons against stress concentration, impact modification with rubber is well known [36]. The Izod impact value of modified compounds is more than one order of magnitude greater than compared to standard nylon 66 [37]. Yu et al. reported, that the impact modification with rubber is also beneficial for the friction and wear behaviour of those compounds [38], as the modification already works as a surface lubricant.

Friction and wear behaviour of standard nylon can be enhanced in using fillers and modifications [5,39–41] or by blending with other polymers [42,43]. One of the predominant solid lubricants used in polyamide 66 is polytetrafluoroethylene (PTFE) [34]. It is well known as anti-adhesive material, due to its low coefficient of friction. Numerous works have been published with the influence of PTFE modification on polyamide and its compounds [6,44–46]. It was shown, that PTFE decreases the coefficient of friction and potentially also the wear rate, but also weakens the mechanical properties of the compounds.

In general amorphous polymers such as polyethersulfone offer good chemical resistance in combination with good mechanical properties. PESU further has very low water adsorption and exhibits high dimensional stability, but poor wear resistance. It is frequently used in automotive, electric and electronic applications and as membrane materials [47]. However, the tribological performance of neat PESU is poor. While the coefficient of friction (CoF) of 0.5 (at 4 N/mm²) for PESU [48] is on the same level with standard engineering thermoplastics such as Polyoxymethylene (POM; CoF = 0.4) or Polyamide (PA66; CoF = 0.5), the wear rate of polyethersulfone of $2083 \times 10^{-06} \text{ mm}^3/\text{Nm}$ is significantly higher than those of POM, $19 \times 10^{-06} \text{ mm}^3/\text{Nm}$ or PA66 of $12 \times 10^{-06} \text{ mm}^3/\text{Nm}$ [48]. Therefore, it is desirable to develop PESU composites with improved tribological properties to be utilized in applications where high temperature resistance and good tribological properties are required. Unlike other engineering polymers, there are only a few reports on the friction and wear behaviour of pristine PESU [49–51], reinforced PESU [52] or composites containing PESU with fabrics [53–55].

1.2 Aims of the research

In this work, PTFE micro-powders were plasma treated in a low-pressure 2.45 GHz microwave plasma rotating drum reactor. To chemically alter the PTFE surface, ammonia and hydrogen gases were used as the process gases and treatment carried out for various treatment durations to study the influence of treatment time. The PTFE powders were characterized and the samples with the highest change in the ratio of carbon to fluorine, revealed in the XPS measurement, are used as a lubricant in PESU and PA66i matrix polymers, in order to improve the wear resistance properties. Compounds containing standard (non-plasma treated) PTFE are usually processed as physical blends in a melt mixing process. Since PTFE and other matrix polymers are usually quite different in their surface energies and polarities, the melt mixing process often leads to poor distribution. Due to this inhomogeneous dispersion of the PTFE particles in the matrix, the friction properties are usually inconsistent. Furthermore, the presence of PTFE as a second phase weakens the mechanical properties of the compound. The modification of the PTFE backbone, with the incorporation of functional groups, changes the polarity of the polymer and therefore the surface energy and miscibility can be improved. Due to the incorporation of the functional groups, inter molecular bonds are formed, which result in improvement of the mechanical properties such as tensile, tribological and wear.

1.3 Research Objectives

The specific objectives of this research are:

- 1.2.1 Incorporation of polar functional groups onto non-polar PTFE micro-powders by means of low pressure microwave plasma treatment.

- 1.2.2. Study the effect of process gases used for plasma treatment and their impact on the incorporated functional groups.
- 1.2.3. Study the effect of plasma treatment duration on the incorporation of functional groups on PTFE surface.
- 1.2.4. Comparison of mechanical properties of polyethersulfone and α -olefin impact modified polyamide 66 compounds containing various plasma treated PTFE powders.
- 1.2.5. Tribological evaluation of polyethersulfone and α -olefin impact modified polyamide 66 compounds containing various plasma treated PTFE powders.

1.4 Accomplishment of material production and tests

This work was performed with the support of many institutions and individuals. To distinguish the support from the author's activities following table has been set up:

Experiment / Data acquisition	Performed by	Contribution of candidate
Plasma treatment of PTFE powder	Diener Electronic GmbH Mr. Diener	Initial proposal of idea, evaluation of parameter settings, participation during the treatment
Compounding of test material	Sitraplas GmbH Mr. Marcus Warzel	Setting up and evaluation of parameter settings with Sitraplas GmbH, participation during the compounding
Injection moulding of test specimen	Ticona GmbH	Injection moulding was performed by Harald Hunke and colleagues of Ticona GmbH
Fourier transform infrared spectroscopy (FTIR) analysis	University of Applied Science Northwestern Switzerland Dr. Pascual	Data acquired while Harald Hunke was present - results were analysed by Harald Hunke and discussed with Dr. Pascual

Experiment	Performed by	Contribution of candidate
Differential scanning calorimetry (DSC)	University of Applied Science Northwestern Switzerland Dr. Pascual	Measurements acquired by Harald Hunke alongside Dr Pascual - results were analysed by Harald Hunke and discussed with Dr. Pascual
X-ray photoelectron spectroscopy (XPS)	University of Newcastle National EPSRC XPS User's Service (NEXUS)	Measurement was performed by the University of Newcastle - results were analysed by Harald Hunke and discussed with Dr. Soin
Thermal stability of plasma induced functional groups	University of Bolton Anand Arcot Narasimulu (University of Bolton)	Measurement was performed by the University of Bolton - results were analysed by Harald Hunke and discussed with Dr. Soin
Contact angle measurement of PTFE powders	Dr MSL Karuna (IICT, Hyderabad, India)	Measurement was performed by Dr MSL Karuna - results were analysed by Harald Hunke and discussed with Dr. Soin
Tensile test	Ticona GmbH	Tensile test was performed by Harald Hunke and colleagues of Ticona GmbH - Results were analysed by Harald Hunke
Melt volume-flow Rate (MVR)	Ticona GmbH	Melt volume-flow Rate test was performed by Harald Hunke and colleagues of Ticona GmbH - Results were analysed by Harald Hunke
Charpy notched impact test	Ticona GmbH	Melt volume-flow Rate test was performed by Harald Hunke and colleagues of Ticona GmbH - results were analysed by Harald Hunke
Dart drop test	University of Applied Science Darmstadt Dr. Witan	Measurement was performed while Harald Hunke was present - results were analysed by Harald Hunke
Dynamic-mechanical thermal analysis (DMA)	University of Bolton	Measurement was performed by the University of Bolton - results were analysed by Harald Hunke and discussed with Dr. Soin
Tribological test: PIN on disc	KATZ, Aarau Mr. Fabian Meier, Regina Straessle	Initial discussions and setting up of parameters, measurement was performed at KATZ, while Harald Hunke was present - results were analysed by Harald Hunke

Experiment	Performed by	Contribution of candidate
Tribological test: Block on ring	Tribologic GmbH Mr. Gebhard	Initial discussions about parameters and measurement done by Mr. Gebhard and Harald Hunke. Measurements were done while Harald Hunke was partially present Results were analysed by Harald Hunke
Scanning Electron Microscopy (SEM)	University of Bolton	Measurement was performed by the University of Bolton - results were analysed by Harald Hunke and discussed with Dr. Soin

2 Tribology: Fundamentals

Tribology is the science and technology of interacting surfaces, in relative motion, encompassing interfacial phenomena such as adhesion, friction, lubrication, and wear as well as the technical applications of the tribological knowledge. The word tribology is derived from the Greek word “tribos” which means rubbing. The term was introduced and defined in 1966, in the Jost report, a study conducted in the United Kingdom [56]. Tribology, despite being one of the oldest engineering disciplines, is one of the least developed classical sciences to date. In 1800 BC Egypt, water was being used to lubricate large sledges, which were used to transport construction materials [57]. In relatively modern history, Leonardo da Vinci (1452 – 1519) is often attributed as the father of modern tribology. He studied many subtopics of tribology, such as friction, wear, bearing materials or plain bearings more than 150 years prior to Amontons. In fact, da Vinci first defined the relationship between the friction force and nominal load, which is essentially the coefficient of friction. Sir Isaac Newton, in 1687, described the properties of fluids, which affected the lubricated friction [58]. In 1699, Amontons [59] verified that the friction force is directly proportional to the nominal load and is independent of the contact area. This led to the definition of the first and second laws of friction [57]:

First law: The force of friction is directly proportional to the applied load.

Second law: The force of friction is independent of the apparent area contact.

In 1785, Charles Augustin Coulomb stated the third law, saying that the friction force is independent of velocity for ordinary sliding speeds. He experimentally underlined this law, which is frequently incorporated into that proposed by Amontons. The laws

postulated by Amontons and Coloumb are some of the most important contributions in history of friction and wear knowledge.

2.1 Economic aspects of tribology

In the 1960's the British government assigned a commission, headed by Peter Jost, to investigate the economic aspects of friction and wear, especially in the industrial sector. The so called "Jost report" estimated that nearly £515 million worth of wastage occurred, because of ignorance of mechanical surface interaction phenomena [56]. An American report published in 1977, suggested that over US\$ 16.25 billion could be saved by the correct use of tribological knowledge [57]. In 1990, Peter Jost concluded that potential savings of 1.3% - 1.6% of the total GDP of an industrialized nation could be made through the understanding and correct use of tribological knowledge [57]. In the United Kingdom, this would mean, for 2013, a potential saving of nearly US\$ 31 billion, taking 1.3% of GDP into consideration. These savings are both substantial and significant, and can be obtained without the development of large capital investment [60]. Nowadays, besides the financial savings, also CO₂ and fuel savings are desirable. Reducing fuel consumption of about 5% of an average European car, which emits 3 tons of CO₂ per year (assuming CO₂ emissions of 190 g/km and 16,000 km per year), would almost save 4 million tons of CO₂ per year for the UK (25 million cars) [61]. According to Holmberg et al., 33% of the energy release of a combustion engine goes to exhaust gases, mainly as heat, 29% goes to cooling and 38% is converted into mechanical power. This 38 % of mechanical power can be divided into 5% energy loss to overcome air drag and 33% to overcome friction in the car [62]. In order to decrease the weight of the car, polymers are frequently used in automotive components. In the Volkswagen Golf

VII model 142 kg of polymers are used [63], which is about 10% of the total weight [63]. This means not only lighter vehicles but also at the same time lower fuel consumption. Polymers are not only used in automotive applications for reduction in weight and thereby enhancing the fuel consumption, but are also used frequently in tribological applications. Polymers offer intrinsically good tribological properties and with the economically efficient processing they can be used in parts such as gears, cams, wheels, bearings or seals, The parts and applications made from polymers can offer function, ease of integration and can have very complex geometries. In fact, polymers are frequently used in tribo-system in combination with other materials. The reasonably accessible components, produced from polymers, are exchanged with new components shortly before the end of their life-time. In fact, the materials are not used as pure polymers, but rather as customized compounds containing tribological additives for lubrication and/or fibre reinforcements in order to enhance their mechanical properties.

2.2 The tribological system

Friction is a common phenomenon, occurring not only in industrial scenarios but also in daily life, and is governed by the processes prevailing on the surface layers of the sliding bodies [64]. In tribological discussions, the two term model is frequently used for its explanation and is based on the idea that there are two main components of friction, the adhesion component and the deformation component. The two term model itself is based on three elements, involved in friction: 1. Interfacial bonds and their type and strength, 2. Shearing and rupture of rubbing materials inside and around the contact region, and 3. The real contact area [65]. Technical surfaces, even those which are very smooth, have asperities with “hills” and “valleys” on a microscopic scale.

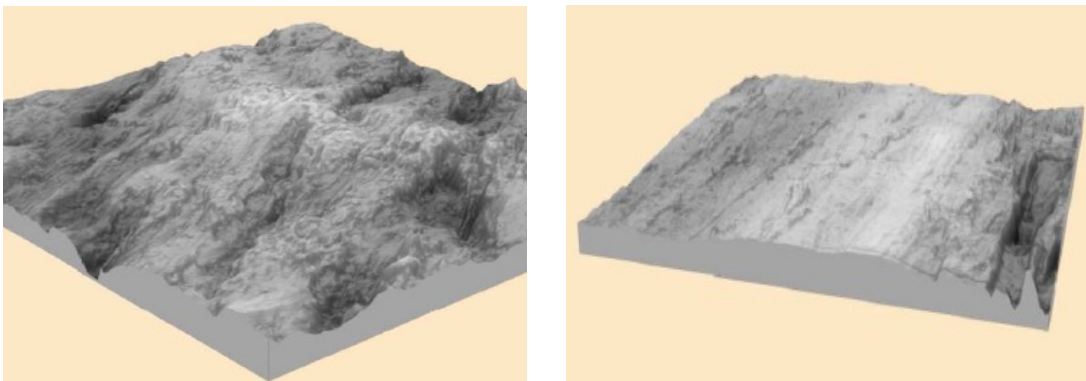


Figure 2.1 Real contact area of a Polyamide-PTFE sample 2-PA66-T2 before (left) and subsequent (right) to a ball on plate tribological test. AFM atomic force microscopy area: 30 μm x 30 μm

Figure 2.1 above (left) shows the surface of sample 2-PA66-T2 (polyamide 66 – PTFE), whereas figure 2.1 (right) shows the same material surface after a tribological pre-test in ball on plate test set up. The valleys and hills representing the different surface heights can clearly be seen. The right picture shows the sliding track with PTFE (brighter areas) on the surface. The “hills” from the picture on the left are

“grinded” flat. The contacts are limited to the highest asperities and are called the real contact areas. The real contact area is much smaller than the total area of the sliding partners. With increasing normal load, the number and sizes of asperities are increasing due to the elastic and/or plastic deformation. The specific load in the contact area reduces until the contact area can carry the load.

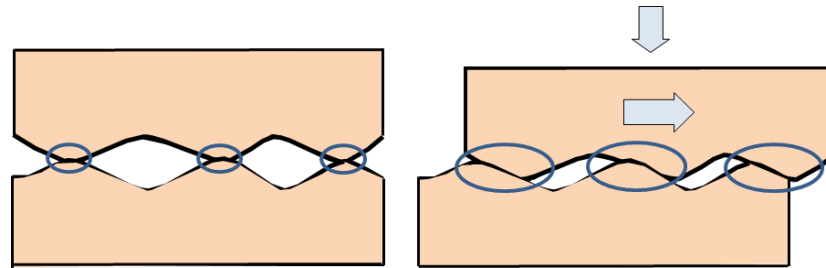


Figure 2.2 Schematic view of two surfaces in contact (left) and upon load and motion (right)

The friction and wear properties are related to the tribological system rather than the intrinsic material properties. Czichos invented 1978 the method of a system approach to investigate friction and wear in a particular application [66]. Therefore the whole component, e.g. a transmission, is divided into single individual tribo-systems such as two gear wheels working together. The two gear wheels in the transmission transfer an input rotational speed into an output rotational speed. In this single tribo-system the gear wheels, the lubricant and the surrounding air and temperature act as tribo elements. The gear wheels acting as one element of the tribologic system, with its two counter bodies sliding against each other, are governed by the volume, geometric and surface properties of the two sliding components. The interfacial medium can be considered as a solid, liquid or gas and is the second element. This element is also governed by the physical and chemical structure and its state. The temperature, the type of motion, and the load is seen as the third element, i.e. the external influences. Figure 2.3 show the system approach according Czichos based on the work of Uetz et. al. [67]. There are many publications underlining different

tribological values upon changes of different conditions of the elements. Tanaka et al. [68] and Chang et. al [69] report on different coefficient of friction and wear values upon different temperatures. Chang et al. report also on different friction and wear values in polymer on polymer combinations under oil-lubrication [41]. These examples show that the tribological systems are highly technical structures, with interacting surfaces in relative motion [70], which must be considered as a complete tribological entity. The tribological systems and their influences are summarised in Figures 2.3.

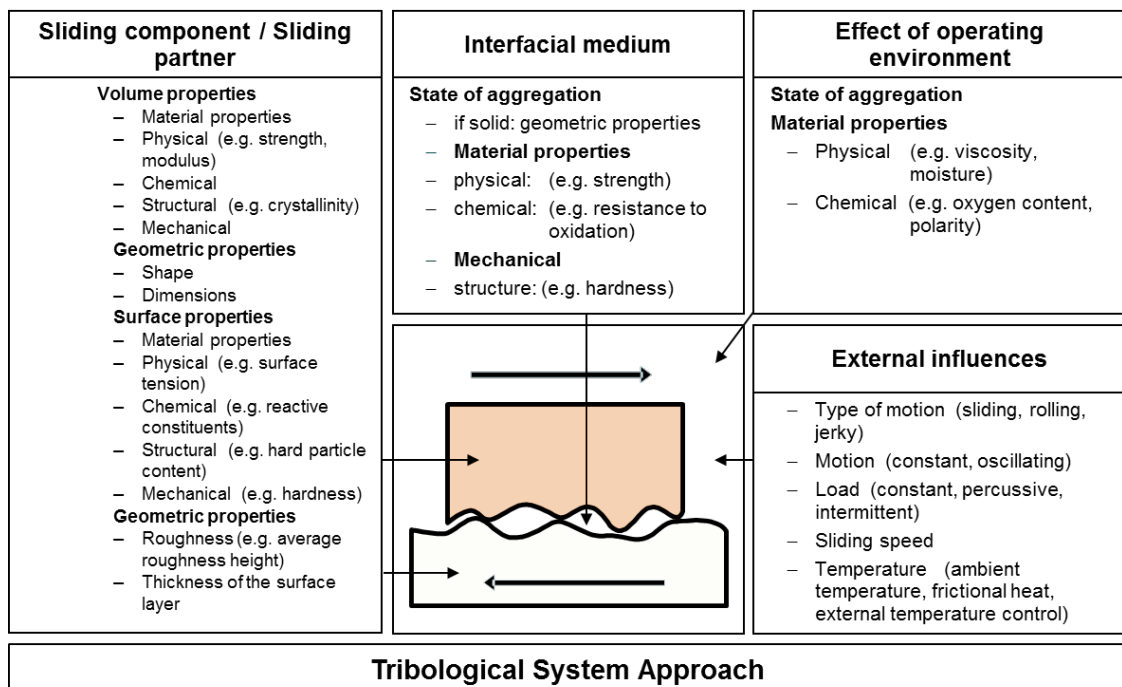


Figure 2.3 Tribological system and influences thereof based on: Uetz Wiedemeyer [67]

Friction is a complex process, which can be divided into three different stages [66]: Introduction of work, transformation of work and dissipation of energy.

In the introduction stage the asperities of the two friction partner come into contact and form the real contact area. The work is introduced into the system. Plastic and elastic deformation as well as adhesion transform the work into energy. The energy

can be stored or dissipated as heat. Due to the damage caused by the deformation, wear is generated.

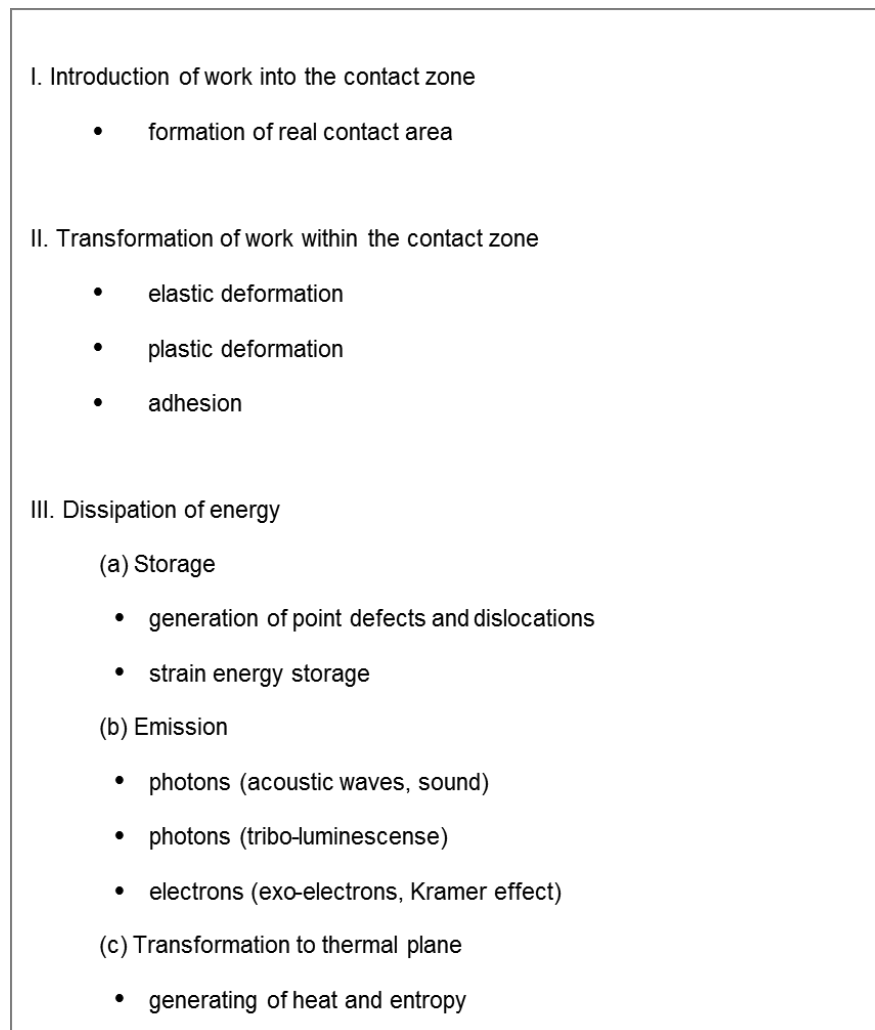


Figure 2.4 Phases of energy dissipation [66].

The loss values in technical systems, such as a transmission, between energy input and the resulting output can be friction, wear and the resulting heat energy thereof.

2.2.1 Theory of friction

Friction can be defined as the force resisting the start of relative motion (static friction) or the relative motion (dynamic friction) of two surfaces sliding against each other [70]. For any two given surfaces in contact, the number of micro-contacts in the real contact area increases linearly with the normal load with each of these micro-contacts acting as a resistance against the relative motion. Thus, the total number of micro contacts resisting against the relative motion is the friction force F_R .

According to the Amontons-Coloumb (1699, 1785) law, friction can be defined as:

$$F_r = \mu \cdot F_n = F_R/F_n \quad (1)$$

F_R : Friction force

F_n : Normal load

μ : Friction coefficient

The friction force is proportional to the normal load and is independent from the size of the contact area. The type of friction can be classified according the type of relative motion of the two counter bodies:

- Static friction
- Sliding friction
- Rolling friction

The Static friction is the frictional force that opposes any attempt to move a stationary object along a surface. When two solid surfaces are in contact and a force is applied to slide one object against the other, the type of friction is called sliding friction. A third kind of friction is, if one of the surfaces is a wheel or a bearing, the type of friction is then called rolling friction. Between the two sliding partners there

can also be a lubrication regime, like in a bearing system, where oil is acting between the surfaces of the acting counter faces. This system can then be classified according to the Stribeck curve. The Stribeck curve, depicts the variation of the friction coefficient versus the product of viscosity multiplied by sliding speed divided by the normal load (Figure 2.5). If viscosity and normal load is constant, then the x-axis is often plotted as the speed only. This regime can be divided into three parts: solid/boundary friction, mixed friction and fluid friction. Upon increasing speed, a lubricating film is generated in the boundary layer between the friction partners. In fact, in the solid friction phase (phase I), the material fatigue mechanism is predominant wherein both plastic and elastic deformation occurs, leading to the friction coefficient exhibiting a maxima. In phase II, mixed friction acts on the sliding partner. The lubricating film between the friction partner pushes the surface apart. The further the surfaces are pushed apart, the lower the friction. Hydrodynamic friction (phase III) occurs on the completely established friction film, when friction acts in the film between the sliding partners.

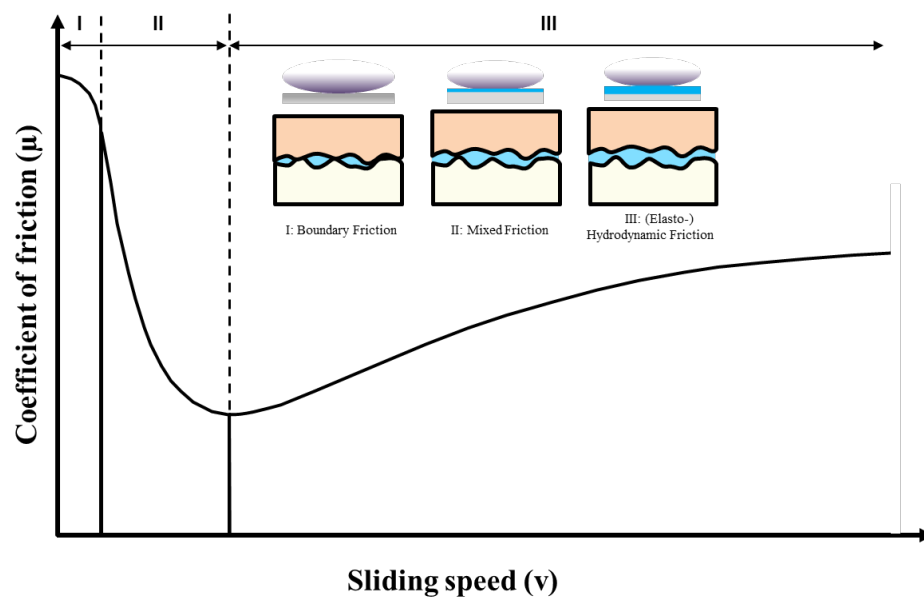


Figure 2.5 Stribeck curve with phase I.: solid friction, phase II.: mixed friction and phase III.: hydrodynamic friction

Lancaster mentioned four areas where dry lubrication of polymer bearing materials is beneficial [71]: 1). where the fluid lubricants are ineffective due to the hostile environment conditions, 2). where fluids cannot be tolerated because of contamination, 3). where is no opportunity of maintenance of the fluids and 4). where the fluids available are poor boundary lubricants for more conventional bearings. In these conditions, polymers are frequently used in dry sliding applications, with no external lubricant such as oil or grease. For these applications polymers with incorporated lubrication, such as PTFE, UHMWPE or silicone can be beneficial.

2.2.2 Friction mechanism

There are four basic friction mechanisms (Figure 2.6) in tribological systems of solid friction without lubrication:

- shear induced by adhesion
- plastic deformation
- ploughing induced by asperities and wear debris
- elastic hysteresis and damping

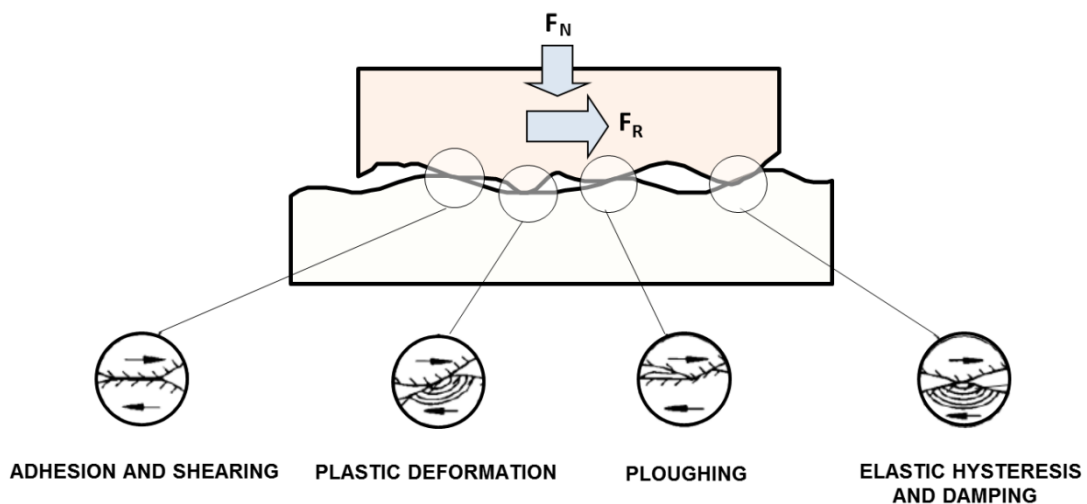


Figure 2.6 Schematic illustration of the basic friction mechanism [70]

Friction induced by adhesion plays a major role in polymer vs. polymer or polymer vs. steel friction combinations. The adhesion is based on the Van-der-Waals interactions, such as Dispersion forces, on dipole bonds, induction forces and hydrogen bonds. The adhesion is governed by the molecular structure of the friction partner and acts between them. The mechanism of deformation starts in the asperities of the two friction partners. The heights of the friction partners come into contact and start rubbing against each other. The harder friction partner will shear the heights of the softer. The real contact area is enlarging. The asperities of the harder friction

partner plough into the soft sliding partner and cause the ploughing friction mechanism. Elastic effects in the polymer counteract against the plastic deformation and thereby generate internal microscopic friction which leads to energy loss (hysteresis).

In tribo-systems, where the polymer is sliding against steel, the acting friction mechanism can be reduced to adhesion and deformation, as the elastic hysteresis can be neglected while the ploughing mechanism can be allocated to the deformation. Therefore, the friction force (F_R) can be divided into an adhesion component (F_{ad}) and a deformation component (F_{def}) [67,72]:

$$F_R = F_{ad} + F_{def} \quad (2)$$

Analogously, this applies to the friction coefficient:

$$f = f_{ad} + f_{def} \quad (3)$$

Adhesion itself is derived from the Latin word “adhaerere” (to adhere) and denotes the intermolecular interaction between two surfaces. The adhesive component and the deformation components vary as a function of different parameters such as load, contact area and roughness, but always occur in combination. The deformation component increases with roughness of the steel counterpart and increasing load; whereas the adhesive component increases upon increasing polarity of the sliding partner and increasing contact area. The adhesive component decreases with increasing contact pressure. An optimum surface roughness can often be determined for tribological systems, as the deformation and adhesion components depend upon the surface roughness (see Figure 2.7).

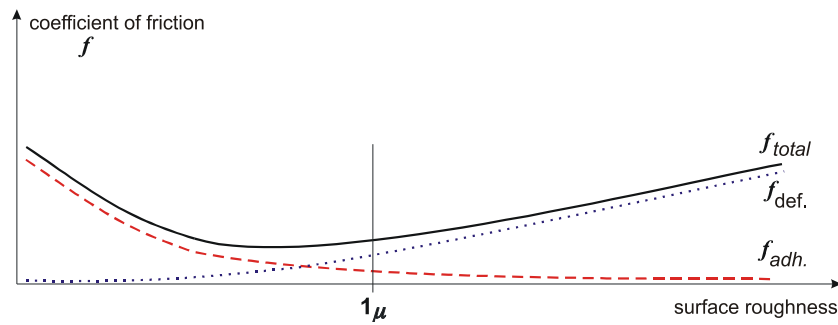


Figure 2.7 Influence of surface roughness [73]

The adhesive bonds are formed in two stages [64]. The first stage includes the orientation of the polymer on the counter body due to the load and temperature. The second stage includes the direct interaction of the atoms and molecules of the polymer and the counter body. Electrostatic interaction forms bonds between the real contact spots. Formation and rupture of junctions governs the adhesion component of friction [64,74]. A friction film can be created when the junctions are shared under a tangential force, because the adhesive bonds between the interacting surfaces are stronger than the cohesive bonds of the polymer. In polymers, Van-der-Waals forces, such as Keesom force, London dispersion force or Debye force, and hydrogen bonds are typical examples of the bonds involved. The adhesion component is determined by the molecular structure along with its surface tension. The surface tension itself is divided into polar and dispersive components as shown below [75].

$$\sigma = \sigma^d + \sigma^p \quad (4)$$

σ = surface tension

σ^d = disperse component

σ^p = polar component

The surface tension can be determined for solids by contact angle measurement or in the case of powders, by the capillary method. The interacting surfaces generate adhesion which can also be expressed as work of adhesion [76]:

$$W_{ad} = \sigma_S + \sigma_I - \sigma_{SI} \quad (5)$$

σ_S = surface tension of solid

σ_I = surface tension of liquid

σ_{SI} = interfacial tension

W_{ad} = work of adhesion

The deformation component acts on the surfaces of the sliding partners where small asperities of a certain height exist. Therefore the real contact area is smaller than the nominal geometrical contact area. The asperities of the harder sliding partner plough through the surface of the softer sliding partner. Thereby a kind of bow wave is created in front of the asperity, while the material “relaxes” behind the asperity. This alternating stress leads to the deformation of the material.

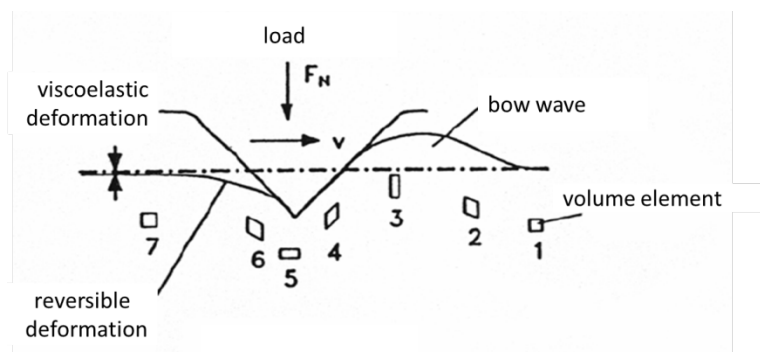


Figure 2.8 Model concept of deformation by tangential stress according to Erhard [77]

This deformation rate is dependent on the mechanical properties, the roughness and the contact stress of the sliding partner. The higher the Young's modulus of the polymer is, the lower is the deformation that is created. In tribological applications, both adhesion and deformation mechanisms acting together, so a classification is done for theoretical reason, only.

2.2.3 Stick-slip-phenomenon

In dry solid state tribological applications, notably where one or both sliding partners are polymers, a phenomenon called as “stick-slip” occurs, which is often accompanied by strong noise. It could be described as alternating motion and stopping [78] or jerking motion, where the friction coefficient is in-consistent during sliding [79]. Stick-slip phenomena occurs when the static friction coefficient is higher than the kinetic friction coefficient:

$$f_{\text{stat}} > f_{\text{kin}} \quad (6)$$

In the static “stick” phase, adhesion and interlocking asperities create a certain friction force. If the applied friction force of relative motion is larger than the static friction force, “slip” motion starts. If the static friction force is remarkably higher than the kinetic friction force, the tribo system can “stick” again. This jerking motion sets the sliding partner in vibration, which causes noise. According to Bowden and Tabor, stick-slip relates to the friction system [80]. The type of surface, the properties of the friction system and the velocity governing the stick-slip phenomenon [80]. In order to prevent the stick-slip phenomenon, the dynamic coefficient of friction needs to be adjusted closer to the static coefficient of friction. If changes to the general set-up of the tribo-system, like speed or load, cannot be changed, adjustments of the composition of the polymer, such as special lubricant additives, can help prevent the stick-slip behaviour [70].

2.2.4 Theory of wear

Wear is defined as the constant loss of material of two bodies in contact and in relative motion. Debris is produced, which can be removed from the contact area, depending on the contact geometry of the sliding partners [81]. According to Blau

[82], wear can be classified (Figure 2.9) according to the fundamentals of the motion causing the removal of the material:

- Sliding wear
- Impact wear
- Rolling contact wear

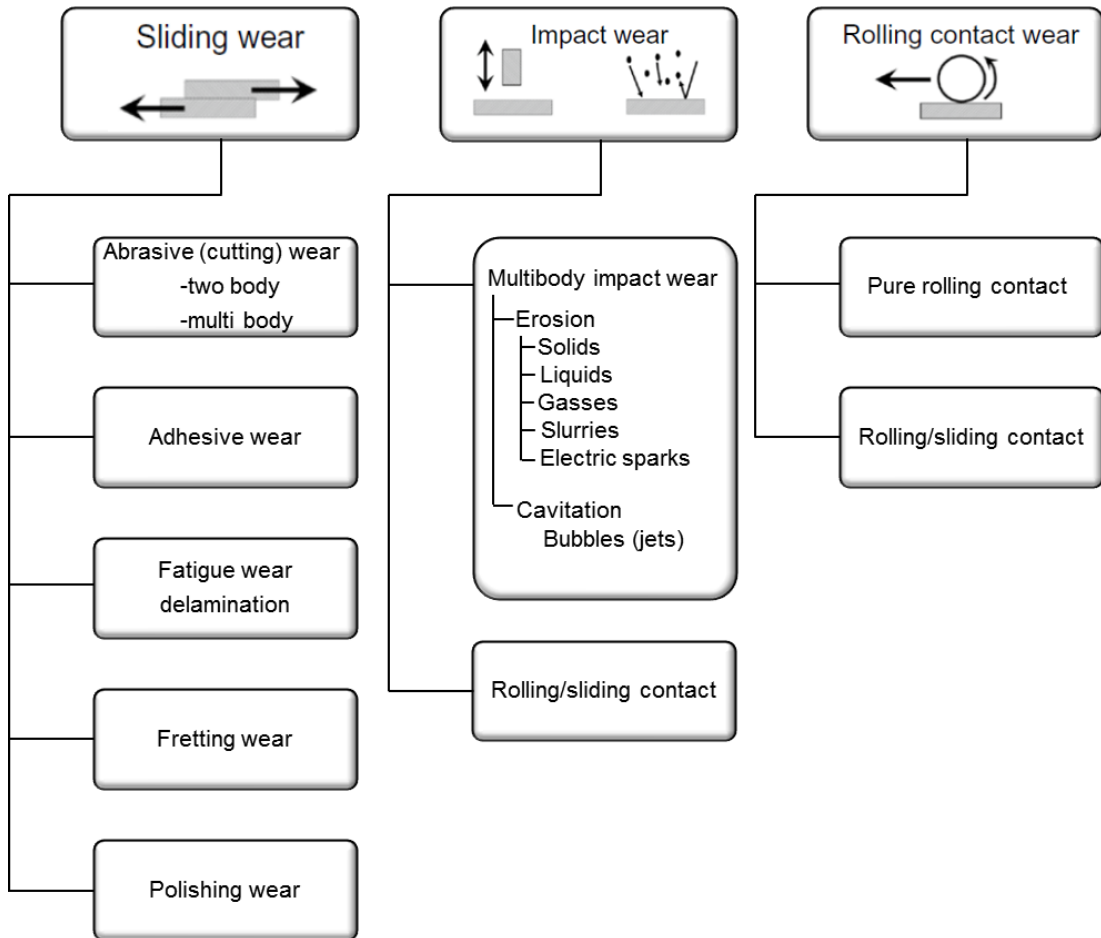


Figure 2.9 Categories of wear classified by the type of relative motion according to Blau [82]

In the real world scenario, wear is much more complicated as often more than one of the aforesaid processes occur [83]. Especially, as in the boundary layer, morphological changes are often accompanied by a local temperature increase, which occurs due to the physio-chemical processes involved. These morphological changes can influence the tribological behaviour [67].

2.2.5 Mechanism of Wear

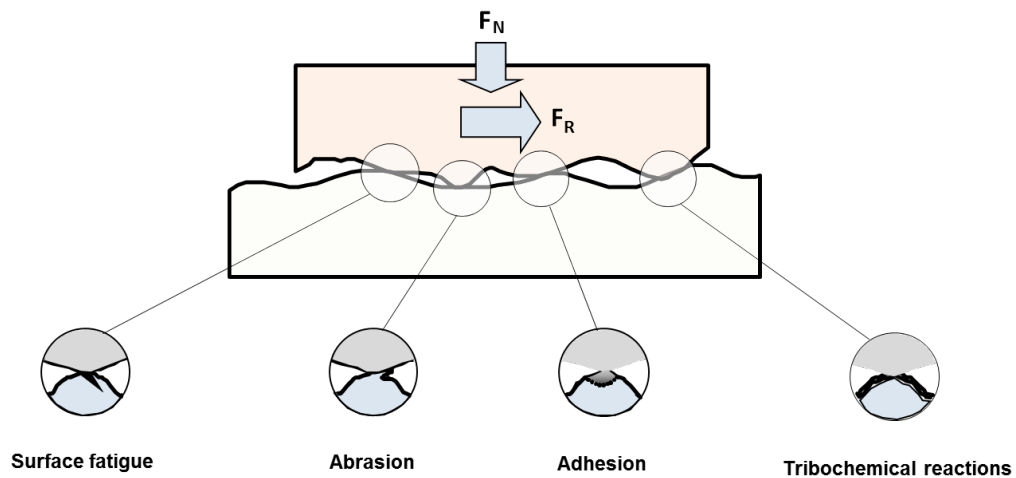


Figure 2.10 Wear mechanisms according to DIN 50320 [70]

According to the former standard (DIN 50320), the wear mechanism can be divided into four basic categories: Surface fatigue, abrasion, adhesion and tribo-chemical reactions (see Figure 2.10).

Surface fatigue is characterized by crack formation and crack growth accompanied by the generation of wear particles, which itself is caused by the alternating load on the surface of the sliding partner. The local material fatigue is caused on a microscopic scale by asperities and is mainly based on the action of the stresses in or below the surfaces, without needing a direct physical solid contact of the surfaces [84]. The surface fatigue is affected by yield stress, Young's modulus, Poisson's ratio and fracture toughness of the material.

The **abrasive wear mechanism** can occur in contact situation between the two sliding partners where the surface hardness is different. The asperities of the harder sliding partner interlock into the surface of the softer partner and displace wear particles from the softer material by combined effects of micro-ploughing, micro-

cutting and micro-cracking. Due to the great difference of surface hardness, the abrasive wear mechanism is of great importance in the sliding combination steel against polymer.

Adhesive wear mechanism is a result of micro-junctions formed between the opposing asperities of the surfaces of counter bodies. The asperities of the two surfaces form micro-joints and thereby create a micro welding of the counter bodies. The tendency to form micro-joints is subject to the physical and chemical structure of the materials. Polymers can, subject to their chemical composition, form Van-der-Waals bonds, electrostatic bonds and hydrogen bonds and interact with their counterpart. Polymers therefore can also interact with metals. If polymers are sliding against metals, a transfer film of polymer often covers the steel counter body in these tribological combinations [85].

Tribochemical reactions comprise, besides the two sliding partners, other substances from the environment of the tribo-system. Oxygen, water or oxides from a metal partner act against the polymer. Radicals are formed by the interaction of the sliding partner, the load and the heat in the boundary layer which can further react with other radicals or alter the polymer chains. The degradation of the polymer initiated by the radical leads to the formation of further radical species, enhancing the wear rate. Tribo-chemical wear is governed by the molecular structure of the sliding partner, the environment and the friction conditions (type of contact and the kind of relative motion). It is important to note that under some conditions several wear mechanism may operate simultaneously and, dependent on the magnitude of surface traction, the wear rate may change [86].

2.2.6 Measurement of wear

As wear is defined as the constant loss of material of two bodies in contact and relative motion, it can be measured by the thickness or volume loss of material or by weighting the sample before and after the wear process.

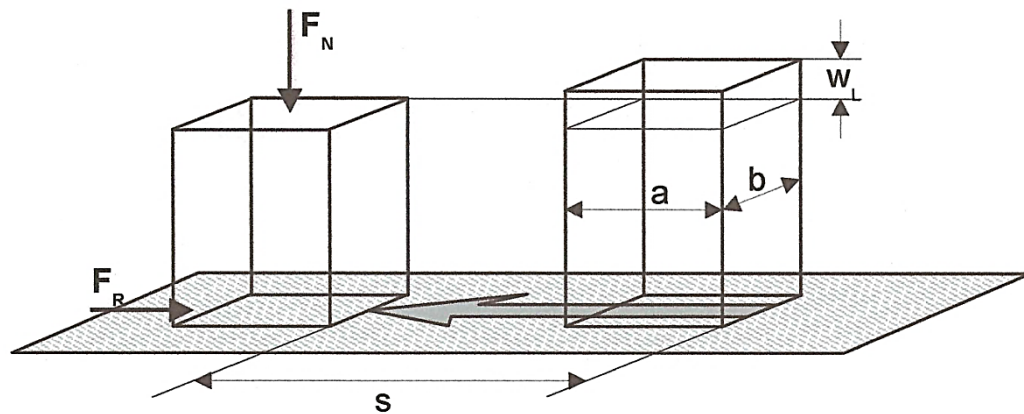


Figure 2.11 Measurement of wear [87]

F_N : normal load

W_L : linear wear

W_V : volumetric wear = $W_L \cdot a \cdot b$

s : sliding distance

The specific wear rate k , also known as wear factor, can be calculated according following equation:

$$k = \frac{W_V}{F_N \cdot s} \quad (7)$$

where W_V is the volume loss of material, s is the sliding distance and F_N the normal load. The measurement of wear is favourable by the measurement of wear loss in thickness, as weighing might not consider debris which are not removed from the friction body.

2.3 Classification of tribological tests

According to Uetz et al. [67] tribological tests can be classified into six categories from operational field test to simplified model test, as shown in Figure 2.12. Operational tests are carried out over a long time and under real operating conditions [88]. Bench tests are done in laboratories, under more simplified conditions. More simplified tests and therefore less cost effective, can be the subsystem test, where only the components are tested. The environment is substantially different from the bench or field test. In the component test, the subsystem is further reduced to the component and can be performed in the original or already miniaturized tests. The simplified component test is based on the simplified model test, but includes already operational demands, like exact loads or speeds or component shapes. Model tests are designed to study tribological basics of material pairs and simulate the tribological interactions of tribo systems. Model tests run over a short period and cannot be extrapolated by increased temperature or load as different wear mechanisms might occur [88].



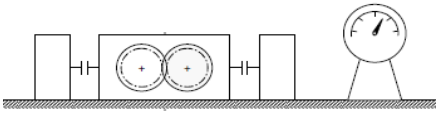
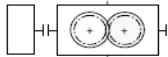


Category	Type of test		Example: system, component, model
I	operational trials	Operational field test	
II		Operational bench test	
III		Subsystem test	
IV	model trials	Component test original or miniaturized	
V		Simplified component test with operational demands	
VI		Simplified model test	

Figure 2.12 Classification of tribological tests according Uetz et al. [67]

The simplified model tests for basic tribological investigations can be done in different test set ups. DIN ISO 7148-2 defines different set ups for polymer materials as illustrated in Figure 2.13 [89].

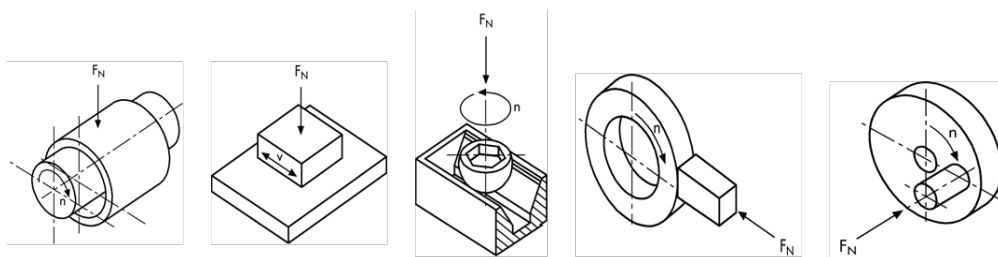


Figure 2.13 Simplified model tests according DIN ISO 7148-2 [89]

The geometry of the test specimen and thus the contact areas are different and cannot be compared, even if the load and test velocity are similar. For basic tribological tests in the fields of polymers, three different configurations have gained the most

acceptance which are: 1. Block-on-Ring test according ASTM G 137; 2. Ball-on-flat according ASTM G 77; and 3. Pin-on-disc according ASTM G 99.

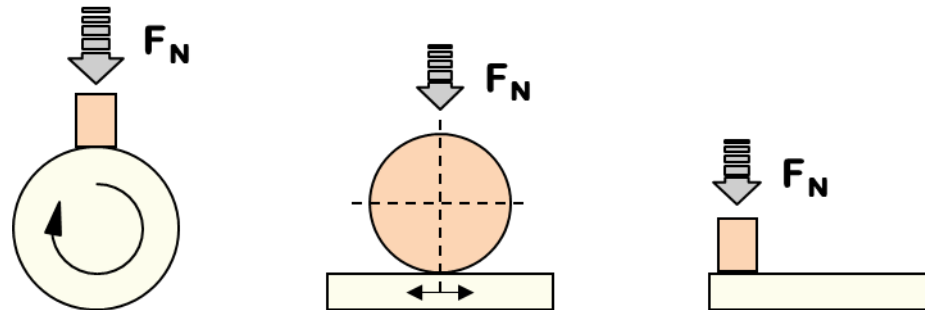


Figure 2.14 Simplified model tests for material evaluation: Block on ring (left), ball on flat (middle) and pin on disk (right)

Figure 2.14 (left) shows the block on ring test method. The block from the tested polymer material is pressed on a rotating steel shaft. Therefore the sliding surface of the polymer sliding partner is shaped from the steel shaft and changes the contact area. In the ball on plate test set up (Figure 2.14 middle) the ball can either be from the polymer material or a steel ball sliding on a polymer plate. The setup is often run in continuous sliding or in reciprocating motion. As the ball is in Hertzian contact pressure, perpendicular to the plate, the contact area changes according to material properties, load and speed. The pin on disc setup is shown in Figure 2.14 (right). The polymer pin is pressed onto a rotating steel disc under continuous sliding. The pin can be pressed from upwards onto the disc, or, to eliminate the influence of wear debris in the friction area, the pin can be pressed upwards under the steel disc. To generate basic knowledge of a tribological system, settings and counter materials must be the same for all trials in a series of different materials. There are two coefficients of friction that can be measured. The static coefficient of friction (f_{stat}) is found from the force that is just enough to start the block moving. Once the block is moving, it is possible to measure the dynamic coefficient of friction (F_{dyn}) from the

force that is just enough to keep the block moving [90]. In this work two test set-ups were used parallel to conduct measurements in order to save time. The PESU compounds were tested on a pin-on-disc tribometer in continuous sliding, where the pin is pressed from bottom upwards against the steel disc. The impact modified polyamide compounds were tested on a block on ring Atlas tribo tester, where the block-shaped test specimen is pressed against the outer circumference of a rotating bearing steel ring.

3 Materials in Tribology

Polymers are frequently used in tribological applications owing to their good strength to cost ratio, their low coefficient of friction and among further reasons, their ease of processing. Polymers can be classified on the basis of their molecular structure into amorphous and semi-crystalline polymers. The amorphous polymers have a randomly orientated molecular structure, which gradually soften with the increase in temperature and thus do not have a sharp melting point. The semi-crystalline polymers have a highly ordered molecular structure, which does not gradually soften with the increase in the temperature and instead remain solid until a given quantity of heat is absorbed and then rapidly change into a low-viscosity liquid. While the amorphous polymers lose their strength very rapidly above their glass transition temperature (T_g), the semi-crystalline materials retain useful levels of strength well beyond their T_g . Dependent on their structure, both the amorphous and semi-crystalline polymers offer certain mechanical properties, chemical resistance and sensitivity to heat. Therefore, it is important to select the most appropriate polymer for tribological applications. In mechanical and automotive engineering, semi-crystalline engineering thermoplastics, such as polyoxymethylene (POM), polyamide (PA) or polybutyleneterephthalate (PBT) are the most frequently used polymers. They offer good mechanical strength, chemical resistance and a continuous use temperature range up to 80°C (POM) or 100°C (PBT / PA66). Whenever the application requires higher continuous use temperatures or different chemical resistance, high performance polymers must be used. Figure 3.1 show a range of engineering plastics used in in tribological applications and their continuous service temperatures.

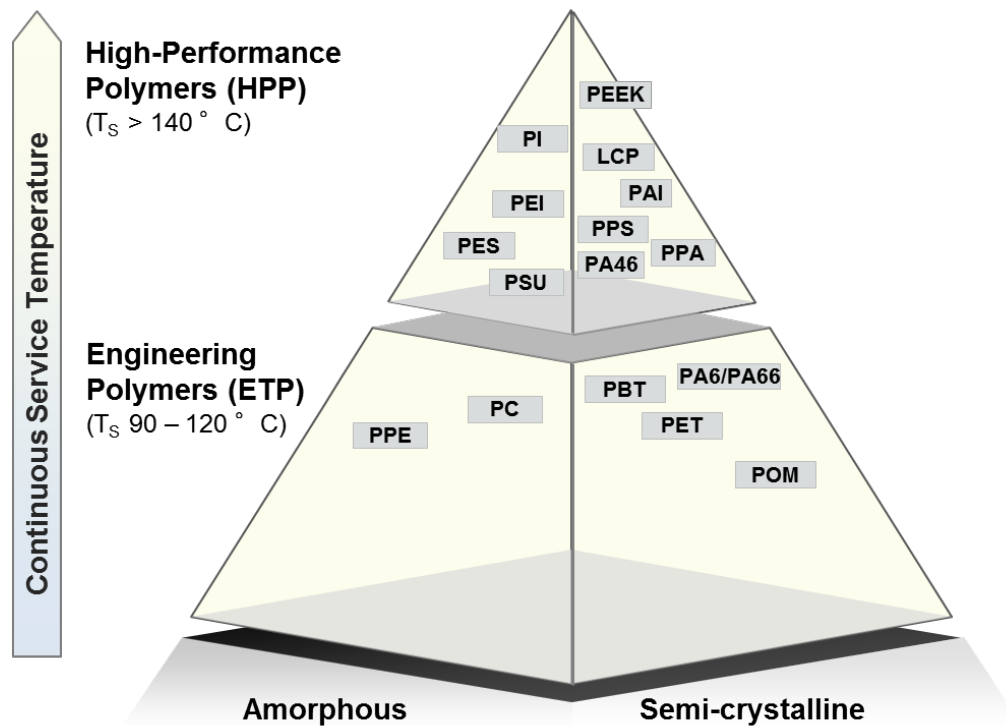


Figure 3.1 Engineering plastics in tribological applications and their continuous service temperature

High performance polymers (HPP) differ from engineering thermoplastics in their chemical structure, their chemical resistance and above all in their continuous use temperature [91]. According to Hergenrother, the most important virtues for HPP's are [91]:

- long term durability ($> 10,000 \text{ h}$) at 177°C
- thermal decomposition temperature $> 450^\circ\text{C}$
- heat deflection temperature $> 177^\circ\text{C}$
- glass transition temperature $T_g > 200^\circ\text{C}$
- high aromatic content and relatively rigid segments

The high stiffness and the specific interaction between the chain segments generate unique characteristics of the high performance polymers. Increased flexibility can be generated in these polymers by introducing aromatic rings, soft chain elements, such as sulfone-, ether-, ester-, amide-, or carbonyl groups [87].

3.1 Polymers in tribological applications

Polymers are frequently used in tribological applications as dry sliding materials due to their low density, and their potential of relatively easy and cheap processing compared to other bearing materials. In applications, elements made out of polymers are often maintenance free, noise-reduced and offer a high damping capacity. However, they also suffer from low resistance to creep, low heat conductivity and temperature dependent mechanical properties, especially as the thermal use of the polymers is limited by their softening point and indeed by thermal degradation temperatures. There are no applicable standards for the determination of short and long term use temperature of polymers in sliding applications, therefore empirical values have been obtained. The maximum surface temperatures in sliding applications according to Ehrenstein are shown in Table 3.1.

Table 3.1 Operating temperature (short term and long term) and sliding surface temperature [92]

Polymer	operating temperature [°C]		sliding surface temperature [°C]
	short term	long term	
POM	140	80	120
PA 66	160	100	100
PBT	160	100	120
PSU	185	150	140
PESU	210	180	140
PEI	190	170	210
PPS	300	200	240
PEEK	300	250	240

To improve the properties of polymers for tribological applications; fillers, such as minerals or graphite, reinforcements, like glass or carbon fibres, or lubricants can be incorporated in the polymer matrix. Reinforcements, such as carbon or glass fibres, improve the mechanical performance of polymers. In general the stiffness, hardness, tensile strength, dimensional stability as well as the density are enhanced with the

addition of carbon or glass fibres, whereas the elongation ductility, creep, shrinkage and heat expansion are lowered [93]. These mechanical changes have a positive influence on the wear characteristics of the compounds. Glass fibres are very abrasive so they can also counter-act, when worn glass particles between the sliding components increase the wear rate. The carbon fibre has also a lubricating effect. The graphite particles worn from the hexagonal structure of the fibre act as a lubricant in the boundary layer [94]. Due to the higher mechanical performance of compounds containing glass or carbon fibre compounds, the $p\nu$ value (product of pressure and velocity) is higher. The compounds are able to withstand higher pressures and/or higher velocities. In order to dissipate heat from the friction area, heat conducting additives, such as bronze powder, boron nitride or even carbon fibres are used. If the heat can be dissipated from the friction area, higher $p\nu$ values can be achieved. Their addition supports the wear resistance in dissipating the heat from the friction area [95], which prevents the polymer matrix from softening. The use of solid/liquid lubricants is a frequently used approach to reduce friction [83]. These lubricants, such as PTFE or ultra-high molecular weight polyethylene UHMW-PE, create thin, highly orientated friction films, which tend to reside between the sliding surfaces and fill the gaps between the asperities. The frictional forces can be reduced and the surface damage caused by asperities is minimised. Li et al reported on a higher coefficient of friction of PA6 GF15 modified with 5% UHMW-PE compared to a modification with 5% PTFE [96]. Highly viscous silicones can also act as lubricants in polymers. They have only limited compatibility with the polymer matrix and migrate slowly to the surface [83]. This so called blooming effect can also form a continuous lubricant film. In general the use of lubricating additives especially in unreinforced polymers can lower the mechanical properties of polymer compounds. As the silicones are dosed on a smaller scale, they do not substantially reduce the

mechanical properties of the polymer. As mentioned above the stick-slip phenomena occurs when the static friction coefficient is higher than the kinetic friction coefficient. The addition of PTFE, UHMW-PE or silicone lowers or eliminates the stick-slip effect due to the lowered adhesion between the friction partners. A further solid lubricant for polymers is molybdenum disulphide. It can form a friction film [2] between the sliding partner and therefore lowers the adhesion, which is beneficial for a low coefficient of friction. MoS₂ can also act in semi-crystalline polymers, such as polyamide, as a nucleating agent [97]: The enhanced fine crystalline structure yields higher mechanical properties and therefore improving the mechanical performance, which can be beneficial for lower wear values. Graphite, which is a crystalline form of carbon, is a temperature-resistant, low-cost filler and can help to improve the shrinkage isotropy and increase the compressive strength. Graphite particularly exhibits tribological advantages for applications in contact with water. Bijwe reported that, fillers that enhance the tribo-properties of a typical polymer, need not be equally useful for other polymers and wear situations [52]. In some formulations they are reported to have deteriorated tribo-performance [98,99]. Formulations of compounds used in tribological application must be carefully selected. The base polymer type, the filler or filler system as a combination thereof are depending on the counter body, the interfacial medium and the external influences of the tribo-system. Therefore, compounds in tribo applications need to be evaluated under selected test conditions in the tribological system approach before used in the field.

From temperature and chemical resistance standpoint high temperature resistant polymers are the first choice. Among the high performance polymers, PEEK offers one of the best tribo performances and can be improved even further with carbon fibre and/or PTFE [84,100,101]. However, the price level of PEEK-CF-PTFE compounds of approx. Eur 80 - 120 per kilogram prevents those compounds from

being used as a standard tribological material. Therefore, it is desirable to develop high performance polymer compounds with superior tribological properties on a competitive price level of around 20 Euro per kilogram. PESU as a high temperature polymer is an amorphous polymer and therefore dimensionally very stable. The price of about 15 €/kg is substantially less than PEEK. However, chemically it is not as resistant as PEEK. The friction and wear properties of neat PESU are rather weak compared to semi crystalline materials [52]. It would be desirable to combine the advantages of dimensional stability, mechanical properties and lower price with good tribological properties.

The majority of polymers used in tribological applications are semi-crystalline polymers, such as polyamides, polyoxymethylene, polybutyleneterephthalates, largely due to their superior mechanical strength. Lubrication with standard PTFE is commonly employed. For some polyamide 66 applications enhanced impact modification is required. Therefore, the polyamide can be modified with impact modifier [102]. In this work an impact modified polyamide 66 and an amorphous PESU are modified to enhance their tribological properties using plasma treated PTFE powders.

3.2 Polyamide 66 (PA66)

Polymers containing an amide group $-\text{CONH}-$ as a recurring part of the molecule are called polyamides (Figure 3.2). Polyamide 66 (IUPAC name: Poly[imino(1,6-dioxohexamethylene) imnohexamethylene]) was invented by Wallace Carothers in 1935 and was first commercialized in 1938 for the production of fibres. It was the first man-made fibre and became very popular in the US under the trade name of DuPont as Nylon [103]. In Europe, the pendant was called Perlon, invented by Paul Schlack from IG-Farben, which was based on polyamide 6 [104].

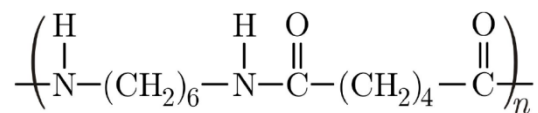


Figure 3.2 Structure of polyamide 66

PA66 is polymerized from hexamethylenediamine ($\text{NH}_2(\text{CH}_2)_6\text{NH}_2$) and adipic acid ($\text{HOOC}(\text{CH}_2)_4\text{COOH}$) through condensation polymerization. According to the IUPAC nomenclature, the digits in the nomenclature of polyamides stand for the carbon atoms in the monomers used for the polymerization of the polymer. For polyamide 66, the first digit stands for the number of carbon atoms in the diamine while the second digit stands for the number of carbon atoms in carboxyl monomer and hence the name polyamide 66. However, if the nomenclature has just a single number, like polyamide 6 or polyamide 12, the polyamide is polymerized from lactam rings, which are opened in a first reaction step and then polymerized to polyamide. The major manufacturers of polyamide 66 are DuPont, BASF and Rhodia with their respective tradenames of Zytel, Ultramide and Technyl.

Polyamide 66 exhibits a glass transition temperature (T_g) of 78 °C [105] with a crystalline melting point (T_m) of $\sim 265^\circ\text{C}$. Polyamide is largely used as an engineering thermoplastic due to its good mechanical properties and processability [106]. It is about 50% crystalline, dependent on the processing conditions, and therefore it offers high strength and high toughness, even at low temperatures (Table 3.2). It exhibits good resistance to heat and has a good creep behaviour. It also offers great rigidity, dimensional stability and resistance to chemicals.

Table 3.2 Mechanical properties of PA 66 according to [106]

Property	Unit	ASTM	Value
Density	$\text{g}\cdot\text{cm}^3$	D 792	1.13 – 1.15
Melt temperature	°C		265
Tensile strength	MPa	D 638	85
Elongation at break	%	D 638	5
Tensile modulus	Mpa	D 638	3,000
Flexural strength	MPa	D 790	100
Flexural modulus at 23 °C	MPa	D 790	2,800
Impact strength (Izod notched)	J/m	D 256	40 - 60

Polyamides tend to have an enhanced susceptibility to water/ moisture uptake which is largely defined by the number of amide groups [107] and therefore by the polarity [108]. The more the amide groups in the polymer chain, higher is the amount of water absorbed by the polymer. In the standard atmosphere, polyamide 66 absorbs between 2.5 % and 3.5 wt% water. At complete saturation, the absorption can be as high as up to 8%, however, the absorption process is completely reversible. The mechanical properties of polyamide are significantly affected by the level of moisture absorption. While some properties such as impact strength improve upon

water absorption, other properties like stiffness or electrical properties tend to deteriorate.

Much of the growth of the polyamide 66 market has been due the ease of its modification and optimisation, for dedicated engineering applications, with reinforcements such as glass or carbon fibres [107,109].

For tribological applications, polyamide is frequently modified with PTFE and/or other additives. Xing reported [39] that the modification with glass fibre and PTFE is beneficial for improved tribological performance. Basavaraj [5] compared PA66/graphite compounds with different PTFE filler contents. It is reported that the incorporation of PTFE and graphite improved the wear resistance.

In order to improve the interfacial interaction between the polyamide matrix and the PTFE, different researches have been carried out on the treatments of PTFE. Shojaei et al. treated the PTFE chemically with sodium naphthalene and achieved a breakdown of PTFE agglomerates, which led to a uniform dispersion of PTFE in the PA66 matrix [110]. The treatment led further to a lower wear loss rate. Franke et. al treated the PTFE with high energy radiation by electron beam irradiation [6]. It is stated that in polyamides the wear rate and the mechanical properties can be significantly improved by the treatment. Lehmann also reported a better wear resistance of polyamide compounds with altered PTFE modification by electron beam treatment [111].

While, polyamide is generally classified as an impact resistant polymer, PA66 shows low notched impact strength and to improve its properties against stress concentration, impact modification of PA66 with polyolefin rubbers/elastomers is well known [36]. Recently, polyolefin elastomers have been introduced as soft materials that can be used as efficient impact modifier materials [37,38,112]. The α -olefin-copolymer is a copolymer of ethylene and another α -olefin such as butane or

octane and is produced using metallocene catalysts with narrow molecular weight distribution. As α -olefin-copolymer is a non-polar polymer and has a weak miscibility with polar polymers such as polyamides, it is usually functionalised with low molecular weight polar groups on the polymer backbone. During the melt compounding of polyamide 66 and maleic anhydride grafted α -olefin-copolymer, the amine groups of the polyamide react with maleic anhydride to form a graft copolymer, which increases the interfacial adhesion between the two phases. This leads to a chemical coupling reaction across the interface with the amine end groups of the polyamides in the melt during the blending process, and resulting in the formation of small particles in the polyamide matrix [112,113]. In fact, the Izod impact values of these modified compounds are more than one order of magnitude higher than the pristine PA66 [37]. Yu et al. have reported that the impact modification with elastomer/rubber is also beneficial for the friction and wear behaviour of these compounds [38], as the modification works as a surface lubricant. However, Chen et al. reported that polyolefin modification in polyamide 66 compounds are only able to form a discontinuous patchy transfer film on the steel counter surface, which causes inconsistent friction and wear rates [114]. The α -olefin-copolymer impact modified polyamide 66 has to be considered as a two phase system of a hard phase (polyamide 66) and a soft phase (α -olefin copolymer). Table 3.3 shows the mechanical properties of the impact modified compound. For the work carried out in this thesis, the PA66i compound has a density of 1.07 g/cm^3 and a melt volume-flow rate of $3.84 \text{ cm}^3/10 \text{ min}$ ($275^\circ\text{C} / 5\text{kg}$).

Table 3.3 Mechanical properties of impact modified PA66 compound

Property	Unit	ISO	Value
Density	$\text{g}\cdot\text{cm}^3$	1183	1.07
Melt temperature	$^{\circ}\text{C}$		265
Tensile strength	MPa	527	35
Elongation at break	%	527	> 50
Tensile modulus	Mpa	527	1,700
Impact strength (Charpy notched)	KJ/m^2	179/2-1eA	90

3.3 Polyethersulfone (PESU)

Polyethersulfone (IUPAC name: Poly(oxy-1,4-phenylsulfonyl-1,4-phenyl) (PESU), is produced by polycondensation of aromatic dihalogen compounds and aromatic dihydroxy compounds in polar aprotic solvents in the presence of alkali metal carbonates [115]. The chemical structure of PESU is given in Figure3.3. PES is an amorphous engineering thermoplastic and due to its high thermal stability, with a glass transition temperature of 225°C and a continuous use temperature of up to 180°C , it belongs to the group of high performance polymers.

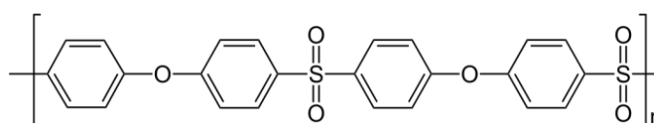


Figure 3.3 Structure of PESU with aromatic rings linked via sulfone group with ether linkages

Polyethersulfone has a brownish amber shade. It offers excellent dimensional stability, resistance to hydrolysis and it has excellent mechanical properties [116]. PES was first commercialized in 1965 by BASF. The polymer's high temperature resistance is due to its structure, which consists of aromatic rings containing sulfone

groups with ether linkages [50]. Polyethersulfone offers high stiffness and toughness and good dimensional stability. It is inherently flame retardant (V0 according the UL standard 94) and offers good dielectric properties [117]. Due to its amorphous structure and the low coefficient of thermal expansion, PESU has high dimensional stability. It is hydrolysis resistant in hot water and steam at temperatures up to 150°C and also offer high chemical resistance to acidic and salt solutions, and good resistance to detergents [118]. The main drawbacks of PESU are its susceptibility to stress cracking in certain solvents and poor weathering properties. Moreover, the tribological properties are quite poor due to its high coefficient of friction and high wear rate [48,50,119]. Bijwe reported that neat PESU showed a poor wear performance, which could be enhanced up to two times on the modification with glass fibres and PTFE [52]. Tanaka stated that over a wide range of temperatures, the coefficients of friction of PESU/PTFE compounds are little dependent on the temperature [68]. It was further found that the addition of PTFE powder to PESU matrix was effective in reducing its wear at high temperatures. Bijwe and Sharma investigated PESU composites with carbon fibre and PTFE [55]. It was reported that the plasma treatment of carbon fibre was beneficial for the mechanical properties due to enhanced fibre matrix adhesion. The addition of PTFE to the composite lowered the coefficient of friction by about 40%, which was dependent on different level of PTFE loading. Together with polysulfone, polyethersulfone belongs to the group of polyarylsulphones. PESU is superior to PSU in chemical resistance and impact strength [120]. PESU is produced by Solvay, BASF and Sumitomo under the trade names Veradel, Ultrason E and Sumikaexcel, respectively.

Table 3.4 Properties of PESU according [121]

Property	Unit	ASTM	Value
Density	$\text{g}\cdot\text{cm}^3$	ISO 1183	1.37
Glass transition temperature	$^{\circ}\text{C}$		225
Tensile strength	MPa	ISO 527-2	80
Elongation at break	%	ISO 527-2	6
Tensile modulus	Mpa	ISO 527-2	2,700
Flexural strength	MPa	-	-
Flexural modulus at 23 $^{\circ}\text{C}$	MPa	-	-
Impact strength (Izod notched)	Kj/m^2	ISO 180/A	6.5

In this work polyethersulfone (PESU) Ultrason E2010 (BASF SE, Ludwigshafen) was used as the base polymer for the matrix. PESU Ultrason E 2010 used in this study has density of 1.37 g/cm^3 and melt volume-flow rate (MVR) of $70 \text{ cm}^3/10\text{min}$ ($360^{\circ}\text{C} / 10 \text{ kg}$).

3.4 Polytetrafluorethylene (PTFE)

Polytetrafluoroethylene (PTFE) (IUPAC name: poly(1,1,2,2-tetrafluoroethylene)) is a unique polymer as it offers a mixture of chemical, electrical and thermal performance that is superior to all the other engineering thermoplastics. It was developed by Roy Plunkett (DuPont) in 1938 during his research for chlorofluorocarbon refrigerants [122]. He discovered in a storage cylinder a substance, tetrafluoroethylene, which could be molten, but was chemically so inert that it was not dissolvable. Five years later, it was used for the first-time in the nuclear energy sector. The polymer of tetrafluoroethylene (polytetrafluoroethylene), due to its high chemical resistance, was the only material that was able to resist the corrosive action of uranium hexafluoride (UF_6), an intermediate for the production of highly enriched uranium. In the following years, due to its chemical inertness, the high thermal stability and the

extremely low coefficient of friction, DuPont registered the trade mark under the name Teflon in 1944 [123]. Teflon has been commercially produced since 1947. The first commercial plant for the production of PTFE was established by DuPont in Parkersburg, West Virginia, USA. The chemical structure of PTFE is given in Figure 4.6.

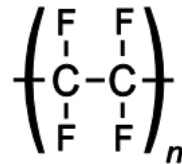


Figure 3.4 Structure of polytetrafluoroethylene PTFE

PTFE is produced from the monomer tetrafluoroethylene by suspension polymerization or emulsion polymerization. While suspension polymerization produces granular resin, emulsion polymerization produces aqueous PTFE dispersion and fine powders [124]. The linear chain of PTFE consists of 20,000 to 200,000 repeating units of tetrafluoroethylene [125]. PTFE is a highly crystalline polymer, which has very high resistance to almost all chemicals and solvents within its continuous operating temperature. It offers also very good thermal resistance for continuous use up to 260 °C and it is also hydrophobic and has a very low coefficient of friction. As the static and dynamic coefficient of friction is almost the same, there is virtually no stick-slip effect. The high bond energy (485 kJ/mol) between the carbon and fluorine atoms and the sheath of the fluorine atoms around the carbon back-bone provides the chemical inertness and offers the low chemical surface energy. The major PTFE producers are DuPont, Daikin, Solvay, Dyneon and Asahi and is produced under the trade names Teflon, Polyflon, Algoflon Dyneon PTFE and Fluon, respectively.

Table 3.5 Bond energies in polymers according to [122]

Carbon bond energies	
Bond Bond	Energy, kJ/mol
C – F	485
C – H	403
C – O	342
C – C	338
C – Cl	312
C – Br	269
C – I	232

The structure of PTFE macromolecule is a twisted helix (Figure 3.5), comprising of 13 (CF)₂ groups every 180° turn [122]. PTFE is chemically so resistant due to the strong bond energies of C-F bond (485kJ/mol) and C-C bond (338 kJ/mol) and due to the size of fluorine atoms in relation to the carbon atoms. Hence, PTFE exhibits a uniform formation of continuous covering of fluorine atoms around the carbon-carbon bonds. This conformation protects the PTFE molecule from attack and makes the molecule chemical resistance and stable. The thermodynamically favoured configuration exhibits the mutual repulsion of fluorine atoms. Due to the repulsion of the fluorine atoms and the bending of fluorine around the carbon backbone, PTFE exhibits low surface energy of 18 dynes/cm [126]. As fluorine is so electronegative, it tends to hold the electrons in the carbon-fluorine bonds closely to itself and therefore demonstrates mitigated London dispersive forces [55]. PTFE has therefore a very low coefficient of friction of 0.08 (static) and 0.01 (dynamic) over a wide temperature range between -260°C to +260°C [127]. The low surface energy leads to immiscibility with other polymers [128] although PTFE powders are employed as additives in polymer compounds.

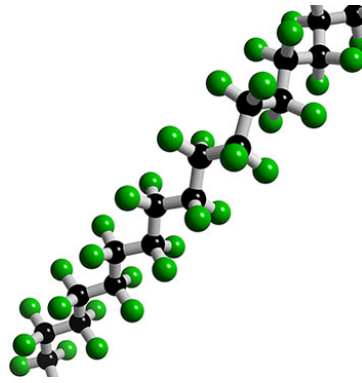


Figure 3.5 Helix structure of PTFE molecule [129]

The mechanical properties of PTFE at room temperature are similar to the medium density polyethylene. Therefore, the mechanical properties of the polymer are relatively poor compared to the engineering thermoplastics [122] and also the permeability to gases is high. PTFE under sustained load tend to exhibit strong creep behaviour, which can be reduced by adding fillers such as glass fibres and graphite. Due to the more expensive monomers and the more critical production process, PTFE is relatively an expensive polymer.

Table 3.6 Mechanical properties of PTFE according to [123,127]

Property	Unit	ASTM	Value
Density	$\text{g}\cdot\text{cm}^3$	D 792	2.1 – 2.3
Melt temperature	$^{\circ}\text{C}$		327
Tensile strength	MPa	D 638	20-35
Elongation at break	%	D 638	300-550
Tensile modulus	Mpa	D 638	550
Flexural strength	MPa	D 790	No break
Flexural modulus at 23 $^{\circ}\text{C}$	MPa	D 790	340-620
Impact strength (Izod notched)	J/m	D 256	188

3.4.1 Tribological aspects of PTFE as a solid lubricant

Much research has been carried out on the use of PTFE as a solid lubricant in tribological applications [5,84,130–133]. The long chains of PTFE can form a smooth and cylindrical surface against which the counterpart can slide [55]. The PTFE forms a thin and coherent transfer film on the sliding partner. The adhesion between the sliding partner decreases and therefore the friction coefficient is lower. The friction film can also prevent the asperities of the harder friction partner to interlock into the softer surface and hence prevent from higher wear rates. Now, the effect of particle size i.e. the molecular weight plays an important role in the friction and wear properties of the PTFE based compounds. It was recognized during some of the earliest studies that the high molecular weight PTFE has a low coefficient of friction (CoF of the order of 0.07-0.15) but rather a high wear rate of the order of 10^{-3} mm³/Nm. Moreover, it has been reported by Hu et al that both the friction and wear rates in the case of high molecular weight PTFE are a function of its molecular weight and crystallinity [134]. In their work, PTFE specimens produced from PTFE resin of molecular weight of $\sim 10^6$ and cooled at quenching rates of 100-0.5 °C per minute, the crystallinity was enhanced from 30 to 67%. Using pin-on-disc measurements, it was concluded that both the wear rate and the coefficient of friction decreased as following: (1) with increasing crystallinity for specimens of the same molecular weight and (2) with increasing molecular weight for specimens of similar crystallinity. The similar effect of the molecular weight on the wear rates of polymers which have different morphologies of fine structure suggests that the molecular mechanism of the wear of polymers should be considered. While the low CoF can be attributed to the oriented transfer film developed on the counterface surface, however due to the poor cohesive strength ensues that the transfer film can be removed rather easily thus contributing to the high wear rate. The tendency of the

high molecular weight PTFE to cold-draw (below its glass transition temperature) into fibril structure is also the underlying reason why high loading (> 5wt%) of high molecular weight PTFE is very difficult for thermoplastics.

However, upon a reduction in the molecular weight, the irradiated PTFE loses its ability to cold draw and thus does not present any fibrillation effects and thus can be compounded at higher loadings (5-20 wt%) into the thermoplastics. Interestingly, it has been reported that the low molecular weight PTFE shows a slightly higher CoF as compared to high molecular weight PTFE, however the wear rates show an opposite trend. Higher loadings of the PTFE additives are preferred and desired for many applications such as bearings with the sole motive of reducing the wear and frictional properties of the thermoplastic compounds. It should be noted that while there is a significant difference in the molecular weight of the PTFE upon irradiation, the molecular weight is still kept ``high-enough``. For very low molecular weight PTFE, the irradiated materials have a significant quantity of end functional groups (discussed in detail further in the section 4.1) such as -COOH which are highly unstable above 200 °C, which act as volatiles leading to frequent breakage during the compounding process. Moreover, if the host polymer is sensitive to acids, then for high temperature polymers such as polyacetal etc., the acidic HF groups pose a problem. One of the first works to use low molecular weight PTFE was disclosed by Allied Chemical Corporation (USA), where a composition of Nylon-6 and 5-25% fine particle size irradiated low molecular weight PTFE was utilised alongside small percentage of inorganic salts as nucleating agents for the α -crystallisation of the Nylon 6. The said composition was then further utilised as a sleeve bearing for steel cable owing to its low friction and high wear resistance against such cable and the ease of extruding it from the melt to produce a flexible tube [135]. Further work on

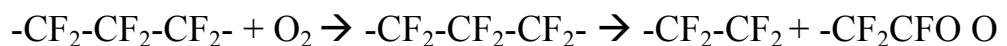
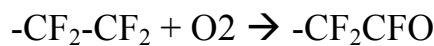
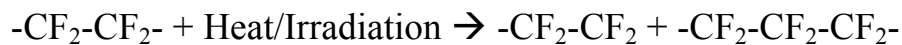
the high loading of PTFE was then largely exclusive to the use of low molecular weight irradiated PTFE. In the patent assigned to Crosby et al, ICI America, the use of irradiated PTFE and polyolefin blend in a glass-reinforced PA66, provided superior tribological (CoF and wear) properties with enhanced resistance to surface wear against a cold-rolled steel counterface [136]. When used against as

3.4.2 PTFE micro powder

Fluorinated polymers, in particular PTFE, are used as additives in thermoplastic resins for improving the wear and abrasion resistance and reducing the coefficient of friction. It increases the melt tension and strengthens and improves the processability in combination with an improved mould release behaviour [34]. In 1960, the first patent was issued for the use of PTFE in a polyamide 66 matrix to improve the tribological properties of the polymer [137]. Nowadays, PTFE is widely used in the form of micro powder. Micro powders are mainly intended for use as a minor part in the formulation of mixtures with other solids or liquids [34]. However, the standard PTFE powders cannot be reduced below a particle size of ~20-25 μm owing to their high molecular weight. In order to make the PTFE micropowder suitable for tribological applications, the particle size needs to be reduced via a reduction in its molecular weight. The reduction in particle size is especially required as during the compounding process where high-shear rates are encountered above the crystalline transition temperature, can cause fibrillation of PTFE. For the production of low molecular weight PTFE, a couple of processes exist in the literature including thermal cracking and irradiation. In the thermal process, the long chain PTFE molecules are heated beyond its degradation temperature, typically 400-500 $^{\circ}\text{C}$, in an inert atmosphere such as N_2 , which leads to the chain's cleavage leading to smaller chain lengths. Typically, the molecular weight reduces from 1-10 million to 2-200

thousand, providing products which are so brittle they can be pulverised by a mortar and pestle, however, the yield of the process is rather poor ranging from 10-60 %.

The reduction in the molecular weight can also be carried out by electron beam irradiation or gamma irradiation [138]. In this process, the PTFE resin is dispersed on a conveyor belt at a specific thickness and passed under the electron beam at a regulated speed corresponding to the desired dose. The irradiation dose is typically from 50 kGy up to 1000 kGy with the typical values required for degradation required of above 500 kGy. It is well-established that the electron beam or gamma radiation causes a rupture of the carbon-carbon backbone wherein this cleavage produces highly stable radicals which further combine with the oxygen to produce small molecular weight PTFE with functional end groups via the following reactions:



The end group of the e-beam exposed PTFE is acyl fluoride (-CFO) which reacts with water to form carboxylic acid (-COOH) to further evolve HF. Thus, the e-beam irradiation causes chain scission and therefore the PTFE becomes more brittle and then can be ground to smaller particles. The higher the irradiation dose employed, smaller are the PTFE particles obtained [138].

Now, the parameter selection for the e-beam accelerator is a multi-variable optimisation problem including input factors such as width, speed, loading i.e. thickness of the PTFE layer on the conveyor belt and indeed the final desired

application of the PTFE. The initial high cost of the accelerator demands that the process be optimised to produce high-quality material at lowest possible cost. Even after optimisation, it should be noted that the cost of irradiation adds nearly 10-30% to the cost of the polymer with increased dosage adding further cost. As mentioned earlier simple grinding can produce only larger PTFE particles, while the thermal/radiation degradation reduces the molecular weight of PTFE, resulting in simultaneous reduction of the average particle size to less than 15 μm . As discussed in the literature by Dillon et al. [139], with the increase in the irradiation time from 2.5 sec to 10 sec. and the consequential dose from 5 Mrad to 20 Mrad, the average particle size for unsintered PTFE was reduced from approximately 11.1 μm to 1.5 μm . The fine powder particles tend to re-agglomerate to 500 μm agglomerates as the surface of PTFE material is smooth and slippery and is considered to exhibit a very low energy surface with $\gamma_c = 18.5 \text{ mN/m}$ [122]. In this work, Dyneon PTFE TF 9201Z, supplied by Sitraplas GmbH in Bünde, Germany, was used for the plasma treatment and the subsequent compounding to obtain PA66i-PTFE and PESU-PTFE composites. The main properties of the starting PTFE micropowder are provided in Table 4.7.

Table 3.7 Properties of Dyneon PTFE TF 9201Z

Product	Particle size in μm	Bulk Density, g/l	MFI, g/10 cm^3	Specific Surface Area, m^2/g	Melting Point, $^\circ\text{C}$
TF9201Z	6	350	<2	10	330

One of the most significant issues around the use of low-molecular weight irradiated PTFE for compounding with high temperature polymers is that the functional groups such as (-COOH, -CFO) present are highly unstable above 200 $^\circ\text{C}$. For engineering polymers such as PA, PESU, PEEK etc., the compounding temperatures are in the

range of 260-350 °C. As the twin screw melt compounding process is carried out near/above the melting temperatures of the PTFE (~320 °C) and the polar groups on PTFE surfaces being mobile and adhesion to the surface low; further polar functional groups are required on the PTFE surface which are not only thermally stable but can also interact with the host polymer to provide other desirable properties such as low wear rate, low CoF and higher toughness, tensile strength etc. To this effect, the thesis focuses on the NH₃, H₂ microwave plasma treatment of PTFE micropowders and their subsequent use in PA66i and PESU host matrices to enhance their tribological and mechanical properties. These processes are discussed in detail in the following chapters.

4 Plasma modification of polymers

Plasma is considered as the fourth state of the matter and can be defined as partially ionized, macroscopically neutral gas, in which the reactive species (negatively charged electrons and positively charged ions, radicals) exhibit collective interaction behaviour [140]. Plasma can be classified into “hot”, equilibrium plasma, such as arcs, and “cold”, non-equilibrium plasma [141]. The cold plasma, wherein the temperature of the electrons is much higher than the temperature of the gas molecules (non-equilibrium state), is the most frequently used plasma technique in industrial engineering [142]. Thus, it is suitable for treatment of inorganic as well as organic materials (polymers). The plasma techniques for the treatment of polymers has been used since the 1960s [142]. It is an environmentally friendly technique, as it does not release toxic organic components to the environment. Plasma treatments can be performed at room temperature, and the process is easy to control [143] and is relatively low in cost [18]. Non-equilibrium plasma can be generated by low-frequency discharges in the frequency range between 40-450 kHz, radio-frequency (RF) discharges (13.56 or 27.12 MHz), and microwave discharges (915 MHz or 2.45 GHz). A vast amount of literature is now available concerning the plasma treatment of polymers by low-frequency discharges [25,144–146], radio-frequency discharges [9,15,26,27,147–153] and microwave discharges [20,32,154–156].

4.1 The plasma process

The ionisation in the plasma chamber starts with the collision of electrons (negatively charged particles) with molecules of the process gas. Further electrons are shot from the molecule. The molecules become positively charged ions and move

towards the cathode. The electrons move towards the anode and hit further molecules. The accelerated cations release numerous electrons from the cathode. This process continues until the gas is completely ionised. The collisions lead to visible light emission. This electrical gas discharge remains as long as there is an energy source.

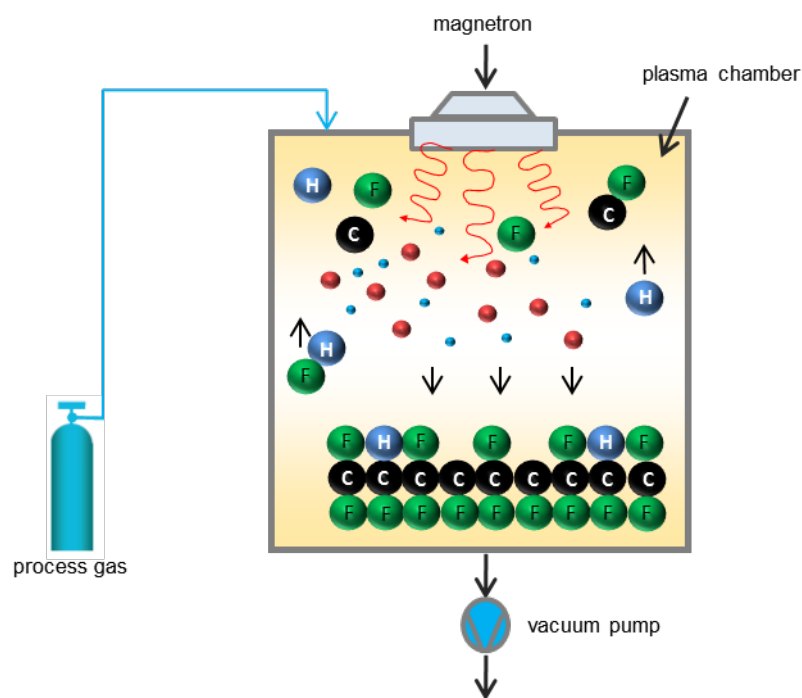


Figure 4.1 Microwave (MW) plasma treatment of PTFE with hydrogen as process gas

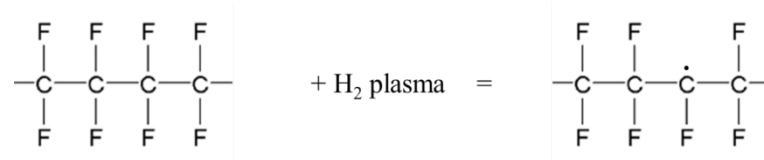
As process gas, either noble gases (Ar, He, Ne) or reactive gases or a mixture of these (e.g. O₂, N₂, H₂, NH₃) can be used. The desired result of the plasma treatment, e.g. cleaning, activation or etching of substrates, or like in this work, incorporation of functional groups, determines the process gas used. Noble gases typically do not incorporate any reactive functional groups onto the polymer surface but can induce radical formation through ion bombardment and ultra-violet radiation [157]. Inagaki reported that hydrogen is an effective gas for defluorination of PTFE [158]. H₂ plasma contains many reactive species such as H₂⁺ and H⁺ ions and H atoms (radicals). Wilson reported that ammonia (NH₃) plasma treatment can also be an

effective treatment for the incorporation of functional groups into PTFE [159]. Nitrogen, oxygen (coming from the air subsequent to the treatment) as well as hydrogen can be incorporated. Upon both treatments chain breakage occurs and thus cross linking can happen. Hansen used the expression “CASING” for the cross linking of polymer chains generated by reactive species [160]. Oxygen can also be typically observed on the functionalised surface upon plasma treatment with noble gases, if the radicals present on the surface react subsequently with the ambient oxygen from the air. In the plasma treatment with reactive gases, such as H₂, N₂, NH₃ or their mixtures, ion bombardment and incorporation of functionalities occur on the polymer surface. Typically, it produces various functional groups on the polymer surface with a functionalization depth of about 100 Å [161], while the deeper areas of the PTFE remain untreated. Yasuda et al. showed that functional groups can be incorporated by plasma treatment with different process gasses such as argon, nitrogen, ammonia, or hydrogen [24]. Various species can be incorporated depending on the process gas used (shown in Table 4.1).

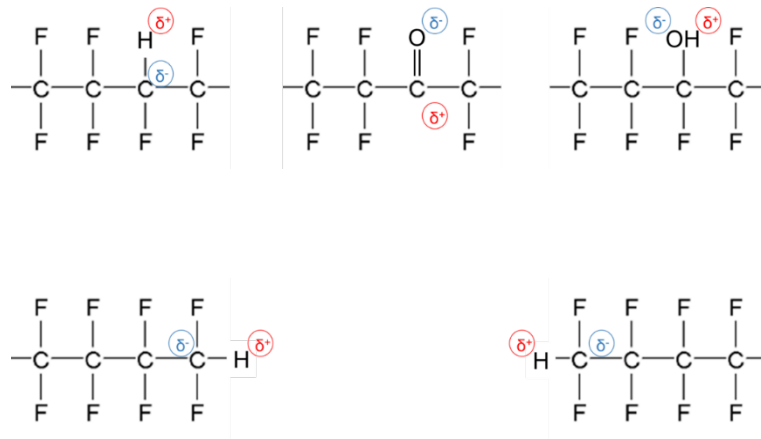
Table 4.1 Chemical assignments of C1s peak positions on PTFE treatment with hydrogen and ammonia

Configuration	C 1s peak (eV)	Literature
C-H _x	285	[162–164]
CF ₂	291.8	[165,166]
CH-CF _n , O=C-CF _n , CHF-CF _n	289.8	[9,151,167]
C-N, C=N, C≡N	286	[165,168,169]
C-O	286.5	[165,169,170]
C=O, O-C-O,	287.3, 289.2	[164,165,171]

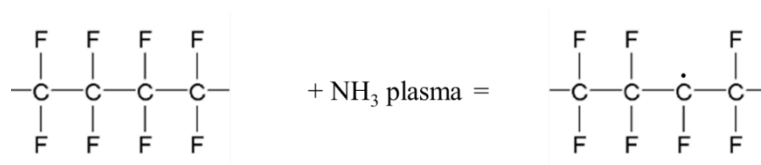
The surface modification process initiated by plasma involves essentially three chemical reactions [158]. The fluorine atoms of the PTFE are abstracted from the polymer chain and carbon radicals in the chain are generated.



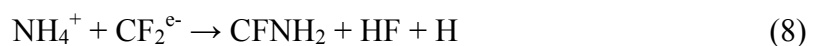
The hydrogen plasma treatment leads to degradation reactions as well as defluorination and oxidation on PTFE surfaces [9]. Various species of radicals are formed from the process gas and the abstracted fluorine. The carbon radicals in the chain or at the end of the chain, are terminated with the various species created by the process gas and the fluorine to create functional groups [158]. This process is dynamic in nature and the functional groups can again be modified. Therefore, the modification process by plasma is a balance between grafting reactions of functional groups on the PTFE surface and modification reactions of grafted functional groups [158]. As long as the supply of MW power to the system continues, the production and dissipation of hydrogen radicals and ions are in equilibrium [10]. If polymer substrate to be modified, is separated from the hydrogen plasma; radicals, rather than electrons and ions, will attack predominantly the polymer surface, and surface modification will occur without etching reactions [9]. The carbon radicals reacts with oxygen and nitrogen from the air to form different functional groups. Incorporated hydrogen and oxygen, as well as OH groups can be determined on the surface. The functional groups exhibit different partial charges, depending on the incorporated functionalities:



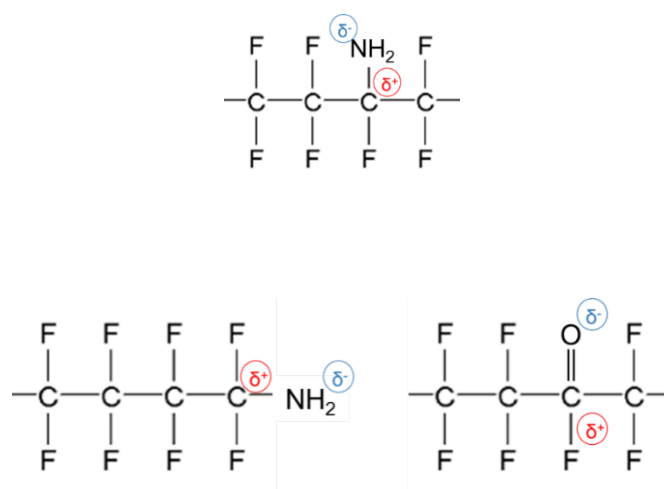
D'Agostino *et al.* have reported that the main species in a radio frequency plasma with ammonia as process gas are H_2 as well as N_2 [172]. Assuming a similar decomposition process in microwave plasma for ammonia as well as for hydrogen as process gas, Badey postulated that the first step of modification with both process gasses is similar, and starts with the formation of hydrogen radicals and excited species [151] which abstract the fluorine from the polymer chain:



Pringle reported that carbon radicals and NH_3^+ and NH_4^+ ions form functional groups of NH_2 according following equation [10]:



The NH_2 functionalities can be found in the middle of the polymer chain and also at the ends of the polymer chains as shown below:



Badey reported [151] that the results of ammonia and hydrogen plasma treatment of PTFE in a microwave frequency reactor are totally in agreement with the mechanism proposed by Clark and Hutton [173], which states that for both, the H_2 and the NH_3 plasmas, the first step of modification is the abstraction of fluorine from the CF bonds by hydrogen radicals. Subsequently hydrogen is incorporated. It was further found out that both H_2 and NH_3 plasma treatments lead to defluorination as well as single and double CC bond formation. Side reactions, such as oxygen uptake, can occur, due to the interaction of residuals of oxygen-containing species and the recombination of radicals respectively [173]. Similar results have been observed in this work in the XPS analysis, so we can safely assume that the reaction mechanism is similar.

The incorporation of various radicals and partially in combination with the very strong electronegative fluorine atoms on the opposing side of the carbon atom, enable different formations of electro negatively or positively charged functional groups. Positively charged hydrogen atoms in the functional group of the PTFE can create an intermolecular bond to the double bonded oxygen atom in the polyamide 66

structure (Figure 4.2 left) and to the double bonded oxygen atom in the ether bridge of the polyethersulfone (Figure 4.2 right).

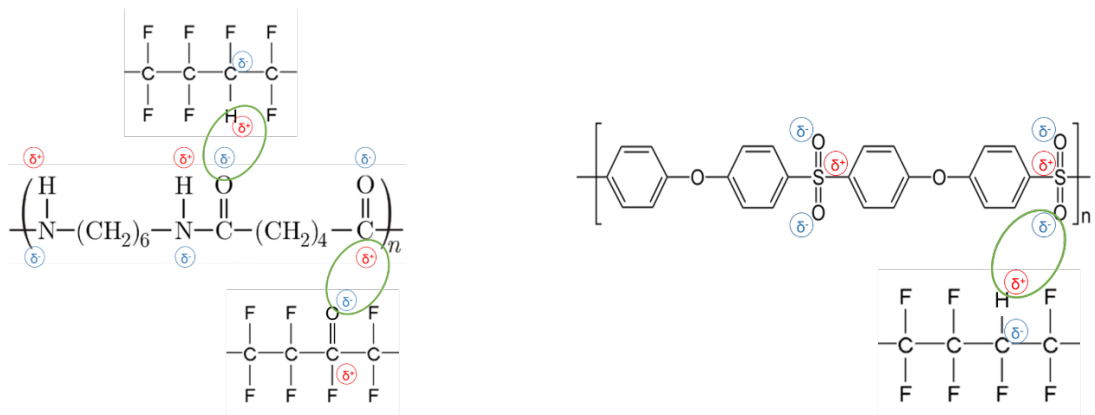


Figure 4.2 Inter molecular interaction between functionalised PTFE and polyamide 66 (left) and PESU (right)

Oxygen atoms which are covalently bonded to the carbon atom in the PTFE exhibit a negatively partial load. Therefore they can form an intra molecular bond to the positively charged carbon atom in the amide group of the polyamide 66 as shown in Figure 4.3 left.

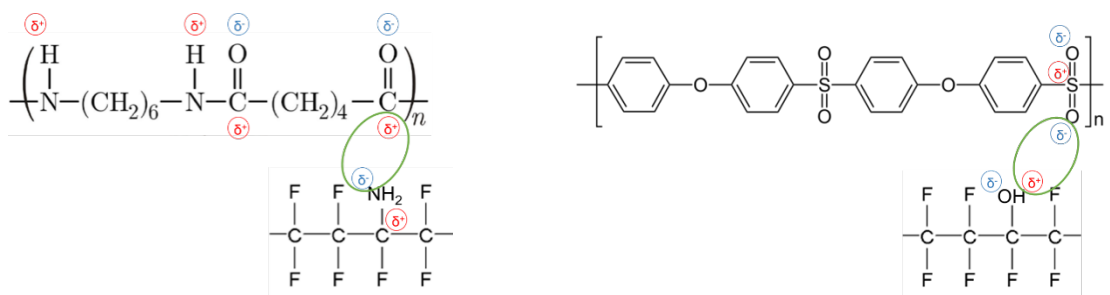


Figure 4.3 Inter molecular interaction between functionalised PTFE and polyamide 66 (left) and PESU (right)

NH₂ functionalities, which are created by the ammonia plasma treatment, can create an intermolecular bond to the negatively charged carbon atom in the amide group. The incorporated OH group is capable to interact with the negatively charged oxygen

in the ether group of the polyethersulfone. The interfacial interaction between the PTFE and the matrix polymer, by incorporation of functional groups, has a great influence on the mechanical performance of the compound and the dispersion of PTFE particles in the matrix [174].

4.1.1 Plasma treatment of polymer powders

Many publications on the plasma treatment of polymer powders such as polypropylene, polyethylene and ultrahigh molecular weight polyethylene (UHMWPE), polyamide (PA), and polyoxymethylene (POM) have been reported [28–31,147,175–177], but so far, to the best of our knowledge, there is no publication about the plasma treatment of PTFE powder. The reactor is the core of a plasma processing system. It is designed to couple the electrical energy into the plasma and contains the material for processing [178] taking into account the polymer particle's size, shape and chemical nature. In fact, the reactor design has to allow for uniform treatment of the polymer powder, homogeneity of the treated surface and reproducibility of the process. For this, the optimal contact between the gas-phase plasma species and the polymer powder surface is very important as the heat and mass transfer coefficients scale proportionally to the surface area of the powders exposed to the plasma. There are several concepts of plasma reactors for the treatment of polymer powders as illustrated in Figure 4.4. These include plasma downer reactors, plasma-fluidised bed reactors or plasma batch reactors [28,30,32,149,156,179–181]. According to Arpagaus, the most common plasma reactor for powder treatment is the plasma fluidized-bed reactor (PFBR) [182]. In the PFBR the process gas carries a small portion of the polymer particles from the bubbling fluidized bulk of the polymer powders into the plasma gas phase wherein

surface modification then takes place. While the PFBR offers high homogeneity of the surface modification owing to the intense mixing of the small quantity of powder with the plasma species, but these systems are not suited for large quantities [182]. Similarly, plasma batch reactors have been developed in which the particles are physically stirred in the reactor while plasma is ignited simultaneously. However, the system suffers from the drawbacks of non-uniform treatment and thus requires long treatment times. Another type of plasma reactor called as plasma circulating fluidized bed reactor (PCFBR) have also been developed which circulates the entire polymer powder through the plasma using a tube leading to intense contact between the plasma species and the polymer powders. With these systems, difficulties arise when the polymer powder has a range of particle sizes and owing to the process it is difficult to keep the larger particles suspended, while preventing the loss of smaller particles. Similar to the fluidized bed reactors, these systems are unsuitable for processing large quantities of polymers and also require multiple passes to provide a statistically uniform coating. To overcome the issues around PFBR and plasma batch reactors, agitating rotary drum reactors have been developed. The plasma rotating drum reactor (PRDR) offers the advantages of having high powder loads and throughputs. However, to compensate for the high loadings high levels of physical mixing alongside long treatment times are required, of the order of hours as the polymer particles in the bulk get less exposed to the plasma as compared to the top surface. It should be mentioned that among all the powder plasma modification systems, only the PRDR are the only commercially available systems which are capable of treating bulk quantities of powders (upto 75kg) in nearly 30 minutes as discussed by Berger et al in their disclosure [183] and Arpagaus [29].

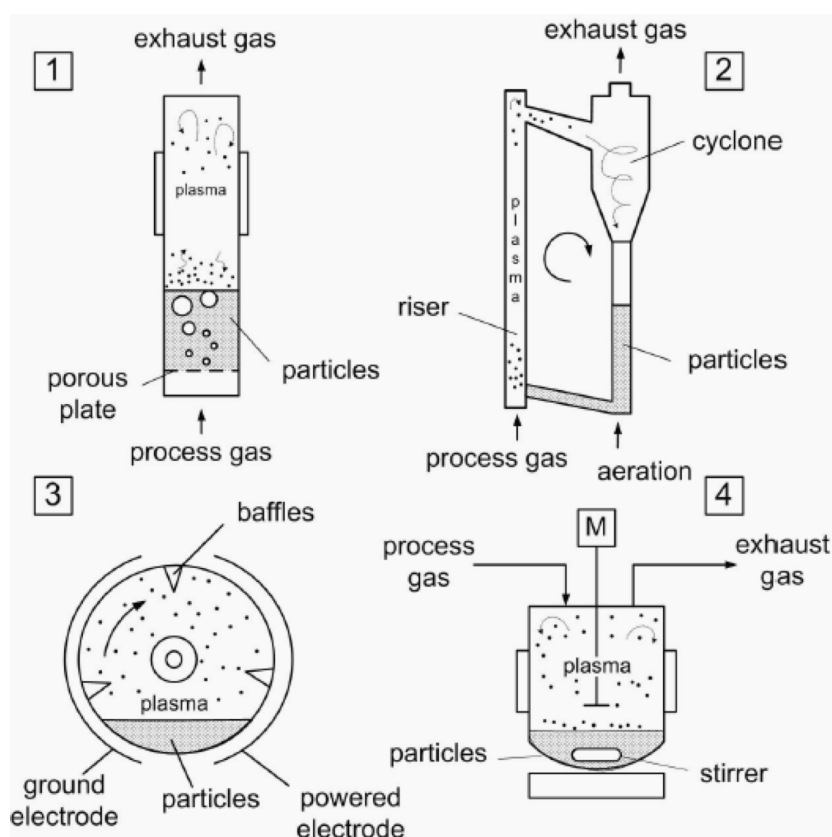


Figure 4.4 Reactor configurations for plasma treatments of polymer powders according to [181]. 1.) Fluidized bed reactor 2.) Circulating fluidized bed 3.) Rotating drum reactor 4.) Batch reactor

These PRDR reactors were initially used for the surface functionalisation of diozine blue and phthalocyanine blue to improve their gloss and flow properties using O_2 plasma [184]. In their study Godfrey et al used a rotary type plasma reactor to modify the surface of polystyrene beads ranging from 30 -800 μm using a non-isothermal CF_4 plasma. It was shown that different functionalisation depths could be achieved by varying the polymer pore architecture and further confirmed through a variety of techniques including XPS, FTIR, NMR and ToF-SIMS [185]. For this work, a plasma rotating-drum reactor (PRDR), with a high power output and the ability to treat large quantities of powders was chosen. Plasma systems can be distinguished between low-pressure and atmospheric plasma systems. In the low-

pressure plasma technology, the gas is excited in a vacuum chamber. This results in energetic ions and electrons, as well as other reactive particles, which constitute the plasma. The atmospheric plasma technology uses process gas, which is excited by means of a high voltage under atmospheric pressure. Laroche reported that functional groups could be incorporated into PTFE surfaces of flat sheets by applying hydrogen and nitrogen as process gas in a radio-frequency glow discharge reactor by using a low-pressure plasma [186]. Badey et al. stated that besides chemical treatment, many papers has been published applying the radio frequency plasma [187]. It was found out, that applying microwave frequency can realize a superficial physico-chemical modification of the polymer without spoiling its bulk properties [187]. Therefore, in this work, a low-pressure microwave (MW) plasma rotating drum reactor from Diener electronic GmbH was used and is described further in the next section.

5 Experimental set-up

5.1 Plasma Treatment of PTFE Powder

PTFE powders (Dyneon TF 9201Z), with an average particle size of 200 nm and 6 μm were treated at company Diener Electronic GmbH in Ebhausen, Germany in a “Nano” plasma device. This low-pressure microwave (MW) rotating drum plasma reactor has a maximum power output of 300 W and a maximum vacuum pump capacity of 8 m^3 per hour. The plasma chamber has a volume of 22 litre and is equipped with a rotary drum made of glass (see Figure 5.1 a, b), which has a volume of 18 litres. The treatment quantity of 3 kg was chosen to guarantee a uniform and homogenous treatment. The plasma device is computer controlled, which enables a continuous regulation and documentation of all process parameters. As discussed in the previous chapter, the PRDR based reactors are the only commercially available systems, which are capable of treating bulk quantities of powders. In order to account for the large sample size and to ensure homogeneity, the processing times are significantly higher than used for fluidized bed reactor based systems (see Table 5.1).



Figure 5.1 (a) Photograph of Microwave plasma device used during the study, (b) glass drum with the excited microwave plasma.

Hydrogen (H_2) and ammonia (NH_3) were used as the process gases. After the PTFE powders were placed into the glass drum, the treatment vacuum between 0.4 mbar

and 0.8 mbar, (see Table 5.1 for operational parameters) was created using a rotary vacuum pump. Once the required base pressure was achieved, the process gas (H_2 or NH_3) was fed into the drum. The plasma is excited between the electrodes in the glass drum by applying a voltage of 230 VAC at a working pressure of approximately 0.8 mbar. The low-pressure microwave (MW) plasma batch reactor process can be divided into the following five steps:

- 1. Pumping out:** Chamber is evacuated
- 2. Gas stabilising time:** Gas is let in the reactor and pressure stabilised
- 3. Process time:** MW generator is switched on
- 4. Flushing time:** Pump runs and process gas flows in. Potentially harmful process gases are purged out of the chamber.
- 5. Venting:** The chamber is back filled with air.

The process was operated at a microwave frequency of 2.45 GHz and a power output of 270 W. Due to the rotation of the glass drum, the powder particles pass through the plasma area between the electrodes. The rotation and the gas flow rate was held constant, to ensure uniform treatment of the powders. Fresh gas was continuously fed into the drum and, contaminated gas was evacuated while maintaining the chamber pressure. In order to determine the influence of exposure time, the treatment with ammonia as the process gas was conducted with different treatment times. Sample PTFE $NH_3/2.5h$ was treated for two and a half hours, sample PTFE $NH_3/10h$ was treated for ten hours, while all the hydrogen plasma treated samples were exposed for 10h to the plasma. The rather long treatment time of 10 hours was chosen primarily based on the previous experience and is based on the assumption that the treatment

time required for fluoropolymers needs to be a significantly higher than that of simple polyolefins. The strong carbon – fluorine bond of 485 kJ/mol and the twisted structure of the PTFE molecule compared to C-H bonds strength of 403 kJ/mol in polyethylene (see section 3, Table 3.5) necessitates a significantly longer treatment time for PTFE. Sample PTFE H2/10h/2011 was treated with hydrogen for ten hours. Subsequent to the treatment, the sample was stored in an airtight and uv-protected container for 12 months at room temperature in order to investigate the degradation of the plasma treated PTFE and the effect of ageing on the powder. To scale-up the powder quantity for potential commercial use, sample PTFE MAX H2/10h was treated with hydrogen as a process gas for ten hours in a larger reactor. The low-pressure microwave (MW) plasma rotating drum reactor called “Tetra 2400” has a maximum power output of 1200 W and a maximum voltage of 400 VAC. The treatment chamber offers a volume of 2400 litres and thereby enables treatment quantities up to 25 kg of polymer powders. The plasma process was again operated at a microwave frequency of 2.45 GHz; however, a power output of 900 W and a pressure of 0.4 mbar were applied to adjust settings to account for the treatment of the larger sample size.

Table 5.1 Parameters for Plasma treatment of PTFE samples

Material name	Process gas	Effective power [W]	Pressure [mbar]	Treatment time [h]
PTFE NH ₃ /2.5h	Ammonia	270	0.8	2.5
PTFE NH ₃ /10h	Ammonia	270	0.8	10
PTFE H ₂ /10h/2012	Hydrogen	270	0.8	10
PTFE H ₂ /10h/2011	Hydrogen	270	0.8	10
PTFE MAX H ₂ /10h	Hydrogen	900	0.4	10

5.2 Composition and compounding of samples

The PTFE micropowders can be considered as particulate additives for thermoplastics and to obtain a good distribution of the PTFE micropowders in the host polymer matrix (PA66i, PESU), melt mixers or compounders are necessary. The compounding of polymer materials is normally carried out on continuous processing extrusion/compounding lines with the extruders themselves being classified as single or twin screw extruders. The compounders themselves are classified as “single-screw” or “twin-screw”, wherein the twin-screw compounders are preferred especially for higher loadings of 5-10 wt%. As such the twin-screw compounders improve both the “dispersive” and “distributive” mixing. While the dispersive mixing breaks down the particulate agglomerates, the distributive mixing allows for a better distribution of particles in the host matrix. The high shear rates during melt processing are highly favorable to obtain breakdown of the agglomerated PTFE micropowder especially of highly immiscible polymer blends. The rotation of the twin screw extruders can be similar or counter-rotating. The polymer pellets are fed into the extruder and are melted by the heated barrel and the shear of the polymer, induced by the rotating screws. The additives or modifiers, such as glass fibres, glass beads, impact modifiers or lubricants, are fed from top mounted hoppers into the molten polymer and mixed directly into the melt.

The PTFE micropowders used in the current work being low molecular weight do not present the significant issues around fibrillation which high molecular weight PTFE displays during compounding processes above its crystalline transition temperature. Thus, dispersive mixing is easier for low molecular weight PTFE but owing to the high loadings, this advantage is negated. Apart from the compounding process, in the literature, Franke et al., have demonstrated the use of reactive extrusion to obtain PTFE-polyamide compounds. In their work, commercially

available e⁻-beam treated PTFE micropowder (ZONYL) with surface carboxylic acid groups produced as a result of e-/gamma irradiation of PTFE in the presence of oxygen, were extruded at 20 wt% content with PA6 [45]. Under polyamide melting conditions, the carboxylic acid groups present on the surface of PTFE exhibit high chemical reactivity for the formation of block copolymer in the polyamide melt. It was reported that the mechanical strength of these reactive-extrusion compounds was higher than as compared to the conventional PTFE-PA compounds and significant improvement in the friction and wear properties under unlubricated conditions was observed. However, as mentioned earlier in section 1.1, the e-beam process is quite capital intensive, difficult to control and the subsequent cost of the product is significantly higher (Eur 50-80/kg) to warrant use in low-cost high volume applications.

The changes in the fluorine to carbon ratio obtained in the XPS measurement of the plasma treated micro powders (see section 6.4.3), show that samples PTFE NH3/10h and PTFE H2/10h/2012 were treated most effectively and therefore these were thus chosen to be compounded with the polymer matrices of PESU and PA66i. As the requirements for PTFE modified high-performance thermoplastics are constantly increasing, therefore, it is necessary not only to optimise the matrices and the functionalization of the PTFE, but also it is important to ensure that the additives are optimally distributed in the matrix. However, as most lubricants such as PTFE tend to agglomerate, the compounding must ensure de-agglomeration as well as a homogeneous particle distribution in the polymer matrix. In this work, the incorporation of the PTFE in the matrix was done on a Coperion ZSK 26 MCC compounder at the facility of Sitraplas GmbH in Buende, Germany. The extruder used is a three zone extruder with co-rotating twin screws exhibiting an L/D ratio of 25 D. The set-up of the screw elements ensures minimal thermal degradation of the

polymer owing to the short residence time and prevention of the attachment of residues to the screw. The screw was configured with kneading, conveying and toothed elements. The kneading and tooth elements de-agglomerate and disperse the PTFE in the matrix material [188]. The co-rotating twin screw extruder and kneading and conveying elements are illustrated in Figure 5.2.

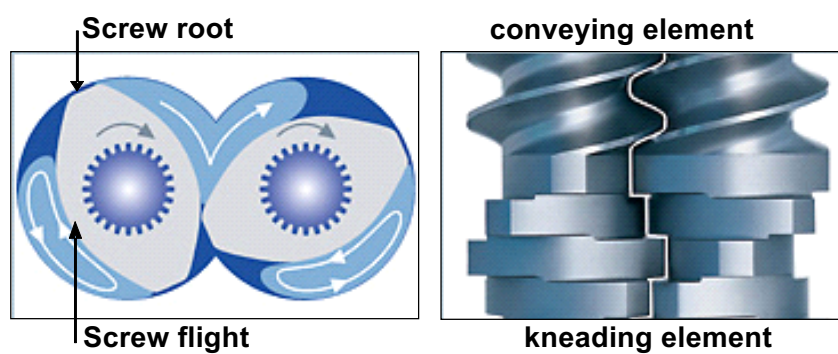


Figure 5.2 Schematic view of a co-rotating twin screw extruder (left) and kneading and conveying element (right)

In the first zone, called the feed zone, the polymer is fed onto the rotating screws and heated up by the barrel and the shear of the polymer (Figure 5.3). In the second melting zone, the channel depth of the screw gets progressively smaller and the polymer is completely melted. In the final metering zone, further components are dosed into the polymer and mixed uniformly [189]. If necessary, trapped gasses, such as moisture, air, solvents, or reactants can be evacuated. The melt is then pressed through the die plate, which forms the polymer strands. The polymer strands are further quenched and cooled in a water bath, before they are chopped into pellets in the pelletizer.

Material

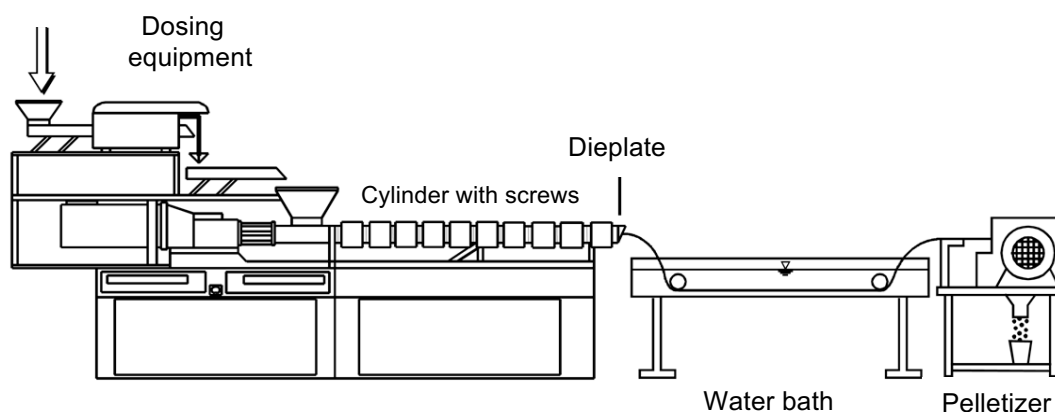


Figure 5.3 Schematic set up of the compounding line

The polyethersulfone was dried for four hours at 140°C and the polyamide 66 was dried for four hours at 80°C in a hot air dryer in order to remove any moisture taken up by the polymers. The temperature settings of the extrusion line for polyamide and polyethersulfone are shown in Table 5.2 and Table 5.3, respectively.

Table 5.2 Polyamide processing conditions

processing temperatures	barrel temperature [C°]							nozzle temp. [C°]
	1	2	3	4	5	6	7	
	185	270	275	275	280	280	285	290
processing parameters	p [bar]			screw speed [min ⁻¹]			output in [kg/h]	
	25			750			40	

Table 5.3 Polyethersulfone processing conditions

processing temperatures	barrel temperature [C°]							nozzle temp. [C°]
	1	2	3	4	5	6	7	
	220	330	340	340	350	350	360	350
processing parameters	p [bar]			screw speed [min ⁻¹]			output in [kg/h]	
	17			750			60	

The PTFE was dosed by means of gravimetric dosing equipment from Brabender, Germany, according to the compositions shown in Table 5.4 and Table 5.5 into the polymer. Subsequent to the production, the granules of the samples were placed in plastic bags and sealed to prevent moisture uptake. It should be mentioned that the

temperature conditions used during the compounding process are chosen based on the recommendations of the manufacturer. It has been observed that the agglomeration of the PTFE additives can be reduced if it is added to the downstream melt rather than using the pre-blends [190]. This has been attributed to the compaction of PTFE as it gets pressed against the unmelted plastic pellets at the hopper end of the extruder.

Table 5.4 Composition of polyamide 66 samples

Sample name	Composition
31-PA66	PA66 neat (for comparison purpose)
1-PA66-T0	PA66 impact = 80% polyamide 66 + 20% α -olephin-copolymer
2-PA66-T2	PA66 impact + 10%wt standard PTFE (no plasma treatment)
3-PA66-T4	PA66 impact + 20%wt standard PTFE (no plasma treatment)
6-PA66-H2	PA66 impact + 10%wt PTFE treated with hydrogen as process gas
28-PA66-NH3	PA66 impact + 10%wt PTFE treated with ammonia as process gas

Table 5.5 Composition of polyethersulfone samples

Sample name	Composition
14-PESU-T0	PESU containing no PTFE
15-PESU-T2	PESU + 10%wt standard PTFE (no plasma treatment)
16-PESU-T4	PESU + 20%wt standard PTFE (no plasma treatment)
19-PESU-H2	PESU + 10%wt H ₂ plasma treated PTFE
30-PESU-NH3	PESU + 10%wt NH ₃ plasma treated PTFE

5.3 Injection moulding of test specimens

For the injection moulding of the test specimens a Krauss-Maffei KM 125-390 injection moulding machine, equipped with a standard screw having a diameter of 30 mm, was used. Standard test bars with dimensions of 80 mm x 10 mm x 4 mm were moulded according DIN ISO 294 for the tensile tests and the milling of tribo pins.

Test plates with dimensions of 60 mm x 60 mm x 2 mm were moulded for the dart drop test. The injection moulding settings (Tables 5.6 and 5.7) used were those recommended by the producers of the resins (EMS Grivory for polyamide 66 and BASF for polyethersulfone).

Table 5.6 Injection moulding parameters and moulding times for polyamide 66

processing temperatures	barrel temperature [C°]					tool temp. [°C]
	1	2	3	4	Nozzle	
	260	265	270	275	275	75
processing parameters	Injection pressure [bar]			Holding pressure [bar]		
	1050			700		
processing time	Cooling time [sec.]			Cycle time [sec.]		
	15			45		

Table 5.7 Injection moulding parameters and moulding times for polyethersulfone samples

processing temperatures	barrel temperature [C°]					tool temp. [°C]
	1	2	3	4	Nozzle	
	340	350	360	360	360	160
processing parameters	Injection pressure [bar]			Holding pressure [bar]		
	900			650		
processing time	Cooling time [sec.]			Cycle time [sec.]		
	17			42		

6 Analytical Methods

6.1 Powder characterisation

Subsequent to the plasma treatments, the PTFE micropowders were placed in dark plastic bags and sealed, to prevent from contact with air and UV-radiation. The PTFE H2/10h/2011 sample was stored for twelve month under ambient room conditions to investigate the effects of degeneration of the functionalities from the PTFE surface over time. The PTFE micropowders were characterised using a variety of characterisation techniques including, Fourier transform infrared spectroscopy (FTIR), Differential Scanning Calorimetry (DSC), X-ray Photoelectron Spectroscopy (XPS) and contact angle measurements. These techniques are discussed in detail in the following sections:

6.1.1 Fourier transform infrared spectroscopy (FTIR)

Fourier transform infrared spectroscopy (FTIR) is a physical analysis to generate infrared spectra of solids, liquids or gases by means of absorbance or transmittance at specific frequencies. Therefore, it can be used to identify functional groups in molecules. The infrared wavelength range can be divided into the near infrared range (NIR 14,000 – 4,000 cm^{-1}), the mid-infrared range (MIR 4,000 - 400 cm^{-1}) and the far infrared range (FIR 400 - 4 cm^{-1}) [191]. Different absorption processes act in the three ranges and cause characteristic vibrations in the bonds of the molecules. The absorbance of the infrared waves corresponds to the frequencies of vibrations between the bonds of the atoms. The frequencies are then compared to a reference sample and calculated by means of the mathematical technique called the Fourier transformation. The obtained spectrum is a unique spectral fingerprint of a material.

To obtain the FTIR spectra, the PTFE samples were pressed into thin specimens and were then measured on a Centaurus IR microscope coupled to a Nexus IR spectrometer (Thermo Electron Corporation, Thermo Fisher Scientific, Dreieich, Germany) using an ATR-device with Ge crystal. The spectra were collected from 64 scans with the resolution set at $\pm 2 \text{ cm}^{-1}$.

6.1.2 Differential scanning calorimetry (DSC)

The differential scanning calorimetry (DSC) is a thermal analysis technique to determine the difference in heat flow between the measured sample and a reference sample. In the “heat flux” set up, the DSC converts the temperature difference between the sample and the reference into a measurement of the energy per unit mass associated with the phase change that cause the temperature difference to arise [192]. Both, the sample and the reference, are heated up and cooled down with the same temperature profile. The principle of the technique is that the polymer undergoes a physical transformation during the heating and cooling and therefore the required energy can be determined to measure melting point, crystallinity and glass transition temperature. Differences in the molecular structure can influence the melting behaviour of the samples during the thermal treatment and therefore DSC can be used to characterize and compare pristine and modified polymeric samples. The data acquired during the course of this work was generated using a DSCQ1000 (TA Instruments, Waters GmbH, Eschborn, Germany) wherein the PTFE samples were sealed in an aluminium pan and were heated from 0°C to 350°C at a rate of 10°Cmin^{-1} in the first heating cycle. Subsequently, the samples were cooled to 0°C (again at $10^\circ\text{C min}^{-1}$), and a second heating cycle was applied at temperatures up to 350°C

again. Both the measurements were performed in a dry nitrogen atmosphere at a flow rate of 50 ml/min⁻¹.

6.1.3 X-ray photoelectron spectroscopy (XPS)

X-ray Photoelectron Spectroscopy (XPS), also known as electron spectroscopy for chemical analysis (ESCA), is a surface chemical analysis technique to determine the elemental composition of a surface. As the surface of the sample interacts with the X-rays, electrons are emitted from the surface (with a maximum depth of 10 nm), with their emitted energy being used to identify the atoms from which they originated [193]. An XPS spectrum shows the electron count on the Y-axis versus the binding energy of the electrons of the detected components on the X-axis. Each component, such as a C=C, C-H_x, C-F bond produce a characteristic peak at specific binding energy. Thus, on comparison between the scans of the pristine and plasma modified polymer surfaces, the incorporation of functional groups can be determined and identified.

The XPS spectra were collected with an AXIS Nova Spectrometer (Kratos Analytical Ltd., UK) using a monochromated Al K α X-ray source (excitation energy of 1486.6 eV). The PTFE powder samples were press mounted on high-vacuum carbon tape using clean glass slides to provide a smooth surface for analysis. For energy calibration, the samples were energy calibrated to the (-CF₂)_n peak in the high-resolution C1s spectra at 292.8 eV or the F1s signal at 689 eV. To analyse the chemical bonding state of atoms, high-resolution C1s spectra were deconvoluted into Gaussian functions, fitting the experimental curves using a nonlinear, least-squares programme (Casa XPS).

6.1.4 Thermal stability of plasma induced functional groups

Owing to the fact that the twin screw melt compounding process is carried out near/above the melting temperatures of the PTFE and the polar groups on PTFE surfaces are mobile and their adhesion to the surface is low; the high temperature behaviour and stability of the polar groups on the surface of PTFE needs to be ascertained and investigated further [26,194]. Therefore, the temperature dependent XPS measurements were carried out to assess the stability of the functional groups on the function of temperature. The measurements were performed from 30°C to the melting point of PTFE at 325°C in order to investigate if the functional groups are stable enough to withstand the latter compounding process. For this, the PTFE powder samples were mounted on Beryllium Copper (BeCu) films wherein the low thickness of the BeCu films in conjunction with their high thermal conductivity ensures excellent heat transfer for thermal analysis. The thermocouple used to measure the sample temperature was mounted on top of the sample surface. The temperature dependent XPS measurement were carried out at temperatures of 30°C, 100°C, 200°C, 300°C and 325° C (melting point of the PTFE) by heating the samples inside the XPS chamber under ultra-high vacuum conditions. The XPS spectra were taken once the samples had cooled back down to the room temperature after the heating cycle.

6.1.5 Contact angle measurement of PTFE powders

The most apparent effect of plasma treatment of a polymer is the improved wettability of the surface [181]. The contact angle hereby reflects the quantitative measurement of the wetting of a solid by a liquid. A contact angle over 90° is hydrophobic. This condition reflects poor wetting, poor adhesion and low solid

surface free energy. A droplet with a small contact angle is hydrophilic. This condition reflects better wetting, better adhesiveness, and higher surface energy.

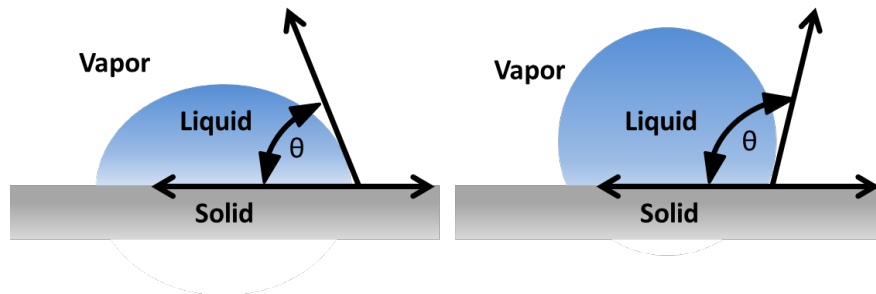


Figure 6.1 Hydrophilic (left) vs. hydrophobic droplet (right)

The contact angle, θ , is geometrically defined as the angle formed by a liquid at the three-phase boundary where a liquid, gas and solid intersect. Young described the balance at the three-phase contact of solid-liquid and gas in the equation [195]:

$$\gamma_{sv} = \gamma_{sl} + \gamma_{lv} \cos \theta_Y \quad (9)$$

θ = contact angle

γ_{sl} = solid / liquid interfacial free energy

γ_{sv} = solid / vapor interfacial free energy

γ_{lv} = liquid surface free energy

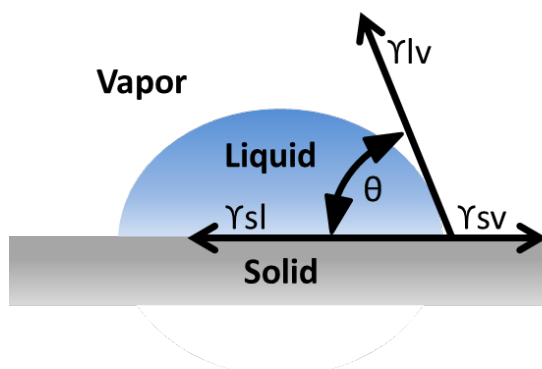


Figure 6.2 Balance of forces at liquid droplet on a surface (Young's equation)

Contact angle of powders cannot easily be measured as those of solids. Therefore, the Washburn method can be applied [196] using a KRUSS Tensiometer K100 from company KRUSS GmbH Hamburg, Germany. The PTFE powders (about 1 g) were properly packed into a cylindrical tube with a filter base and hooked on a balance to be weighed. A consistent packing of the powder is extremely important to obtain reproducible results. The vessel is then brought into contact with the liquid, which starts to wet the powder, hence the liquid rises inside the tube. The speed at which the liquid rises through the bulk powder is measured by recording the increase in weight as a function of time. Bulk powder through which a liquid flows, can be regarded as being a bundle of capillaries. This means that for the calculation of the advancing angle, which corresponds to the contact angle between the solid and the liquid, the following Washburn equation, applicable to capillaries, can be used:

$$m^2/t = c \cdot \rho^2 \cdot \sigma \cdot \cos\Phi / \eta \quad (10)$$

m = mass

t = flow time

σ = surface tension of the liquid

c = capillary constant of the powder

ρ = density of the liquid

θ = contact angle

η = viscosity of the liquid

The constant c includes the number of micro-capillaries and their mean radius, and it depends on the nature of the powder and also on that of the measuring tube. Plotting the square of the mass (m^2) against time (t) shows a linear region, the slope of which, for known liquid properties (σ , ρ and η), only contains the two unknowns c and θ . To determine the constant c , a measurement is carried out with an optimally wetting

(spreading) liquid, a non-polar liquid (e.g. n-hexane), with which the contact angle θ is 0 ($\cos \theta = 1$). The value of c is substituted in the equation in order to determine the contact angle θ with the help of other liquids. The contact angle measured in this way is an advancing angle, as it is measured in the course of wetting. As c depends on the bulk density, the powder packing must be consistent for all measurements on the same powder. Contact angles greater than 90° cannot be measured using this method, as no wetting of the powder takes place.

6.2 Compound characterisation

6.2.1 Tensile test

For the mechanical evaluation of the compounds, stress-strain-curves were recorded in a quasi-static tensile test according DIN 527-2 [197]. The trials were conducted on a Zwick universal tensile tester Z020 (Zwick GmbH & Co. KG, Ulm) at room temperature of 23°C and a relative humidity of approx. 50%. The measurement of elongation was carried out with an incremental sensor. The Young's modulus was measured at a cross head speed of 1mm/min between 0.05% and 0.25% strain. The determination of the other tensile properties was done at a cross head speed of 20 mm/min.

6.2.2 Melt volume-flow Rate (MVR)

The flow behaviour of the compounds was characterised by the Melt Volume-flow Rate (MVR) test according ISO 1133 [198]. The MVR is a measurement of flow of polymers. It determines the volume of polymer (in cm^3) flowing in 10 minutes through a capillary, which is of defined size and length. A specific load and temperature for each kind of polymer is applied. For the polyamide samples, a

temperature of 275°C and a load of 5kg was applied, while for the PESU samples the temperature was 360°C and the load was set at 10kg. Prior to MVR measurement, the samples were dried for four hours at 140°C (polyethersulfonesulfone) and at 80°C (polyamide 66). The Melt Volume-flow Rate is relatively easy to measure and is an indirect measurement of molecular weight, with high melt flow rate corresponding to low molecular weight.

6.2.3 Dart drop test

The instrumented dart drop test determines the multi axial impact behaviour of the compounds. The test was conducted according DIN EN ISO 6603-2 [199] on a high speed tester (Coesfeld GmbH, Dortmund). Therefore, injection moulded test plates, with the dimension 60 mm x 60 mm with a thickness of 2 mm, were tested at ambient temperature of 23°C. The plates were pneumatically clamped into the frame of the device. The dart with a weight of 20.33 kg falls perpendicular with a velocity of 4.4 m/sec. down the dart frame. The speed is additionally measured with a photoelectric sensor. The impact causes either plastic or elastic deformation (dependent on the material properties) and eventually leads to the fracture of the specimen. The attached load cell measures the maximum force (F_m) recorded during the impact, which is then used to calculate the correlated energy uptake [200].

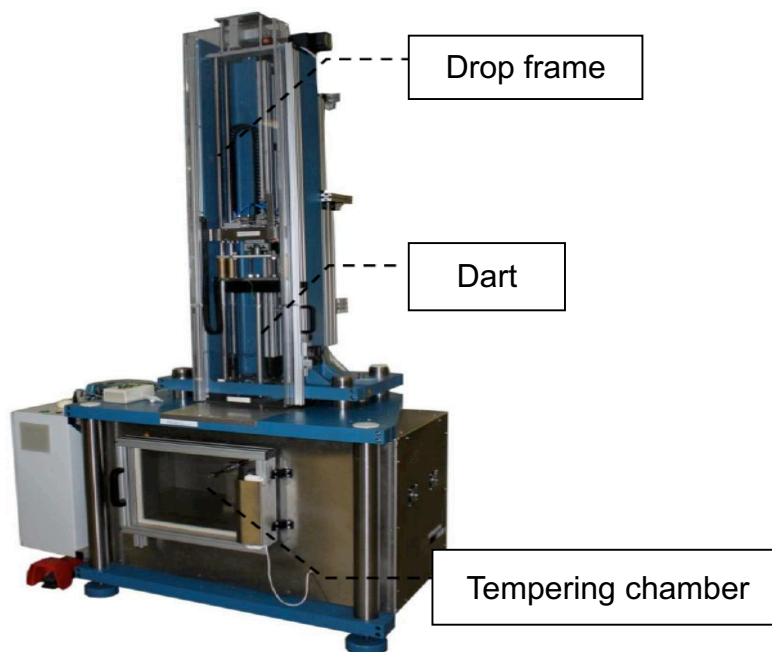


Figure 6.3 Dart drop test apparatus

The energy absorption is represented by the integral of the area under the force-displacement curve [201]. From the generated data, a force time diagram can be obtained and the maximum energy (E_m) can then be calculated.

6.2.4 Dynamic-mechanical thermal analysis (DMA)

Dynamic mechanical thermal analyses (DMTA) were carried out in tensile mode with a TA Instruments DMA 2980 at a frequency of 1 Hz, a heating rate of $10^{\circ}\text{C min}^{-1}$ and a temperature range from 30 to 200°C . The Dynamic-Mechanical Thermal Analysis (DMTA) records the temperature-dependent visco-elastic properties and determines the modulus of elasticity and the damping values. Therefore, an oscillating force is applied to the sample while the storage modulus curve is determined.

6.2.5 Scanning Electron Microscopy (SEM)

The SEM microscopy of the fractured tensile bars was conducted with a SEM microscope Hitachi S3200. The tensile test bars were fractured on the tensile tester (see 6.2.1.) and the fracture area were sputtered with thin film of gold prior to imaging using an excitation voltage of 1.5kV. The dispersion of the PTFE and size of the PTFE particles and the bonding to the polymer matrix can be studied from the SEM micrographs obtained

6.3 Tribological testing

The determination of the friction and wear values was done using two different test set-ups. The polyethersulfone compounds were tested in a pin on disc set-up (according to ASTM G99 standard) whereas the impact modified polyamide compounds were tested on a block on ring test set-up (according to ASTM G137 standard). In both the configurations, the polymer specimen is pressed against a rotating counter body. Although the counter body geometry is slightly different, the measurement principle is very similar and is explained below.

6.3.1 Pin-on-disc test

The pin on disc tribometer was used for measuring the friction and wear properties of PESU compounds sliding under load. The tests were conducted on a WAZAU tribometer TRM 1000 (Wazau GmbH, Berlin).

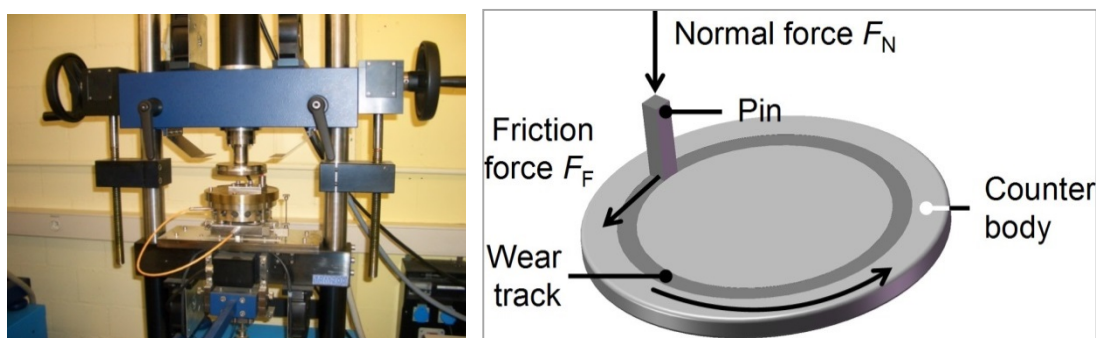


Figure 6.4 WAZAU tribometer (left); schematic of the pin-on-disc measurement (right)

The drive unit is a servomotor, which was adjusted to a sliding speed of 0.5 m/s for the sliding distance of 14,000 meters. The load was provided by the movement of the motor block via a motor spindle system and was adjusted to 27 N. During the testing the load, ambient temperature, sliding distance, rotational speed and friction torque

were continuously measured. The test pins for the measurements were milled from tensile test bars.

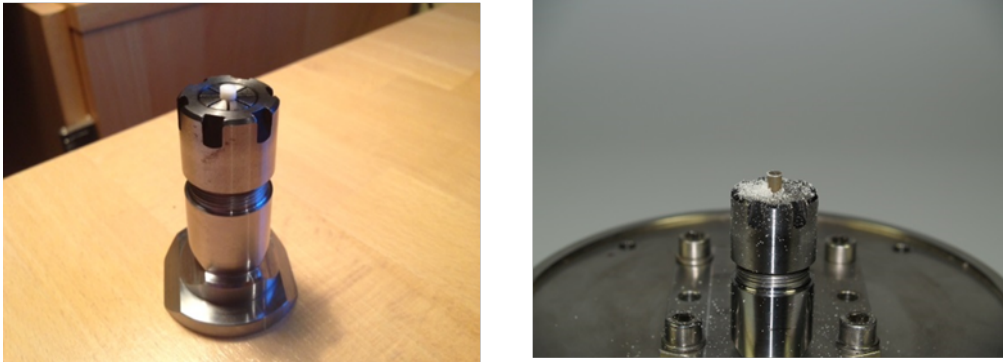


Figure 6.5 Tribo pins with carrier before test (left) and subsequent to the test (right)

A special carrier was necessary, which was specifically tailored for the pins. The carrier had a length of 10 mm and a radius of 1.7 mm, resulting in a contact area of 9 mm². With the applied load of 27N and contact area of 9 mm², the effective contact pressure was calculated to be 3 MPa. In order to examine the influence of the injection moulded surface, especially during the run in phase, the pins were cut from the end of the test bar, opposite to the injection gate, still exhibiting the injection moulding skin. All specimens were cleaned with ethanol before testing. The pins were then put in the carrier, which was pressed under the rotating steel disc of 100Cr6 steel, having a surface roughness of R_z 2. The parameters for the tribological tests are summarised in Table 6.2

Table 6.1 Parameter of tribological tests

Pin-on-disc test (plastic vs. steel)	
Pin	PESU and compounds thereof
Counterpart	100Cr6 steel
Contact pressure	3 MPa
Sliding velocity	0.5 m/s
Temperatures	Ambient
Sliding distance	14,000 meter
Kind of motion	Continuous - rotating sliding
Lubricant:	none, dry sliding
Friction radius	41 mm / 46 mm / 50 mm

The dynamic coefficient of friction was continuously calculated according to the following equation:

$$\mu = \frac{F_F}{F_N} \quad (11)$$

where F_F is the frictional force, F_N the normal load and μ is the coefficient of friction. The specific wear rate W_s was calculated according to the following equation:

$$w_s = \frac{V}{F_N s} \quad (12)$$

where ΔV is the volume loss of material calculated by the removed material. The removed material was computed by the vertical displacement of the pin carrier, measured in μm and multiplied by the area. F_N is the normal load and s the sliding distance. The pin-on-disc tests were performed in triplicates. Outlying observations were eliminated by standard procedures and arithmetic means, standard deviations and confidence intervals were computed from the outlier-free data samples.

6.3.2 Block-on-ring test

The tribological measurements of the friction and wear data of the impact modified polyamide 66 were carried out in a 4-station block on ring set-up on an Atlas TriboTester at Tribologic GmbH (Kaiserslautern, Germany) according to ASTM G137 [202]. The test generates friction and wear by pressing a block-shaped test specimen with rectangular cross section against the outer circumference of a rotating bearing steel (100Cr6, Mat. No. 1.3505) ring.

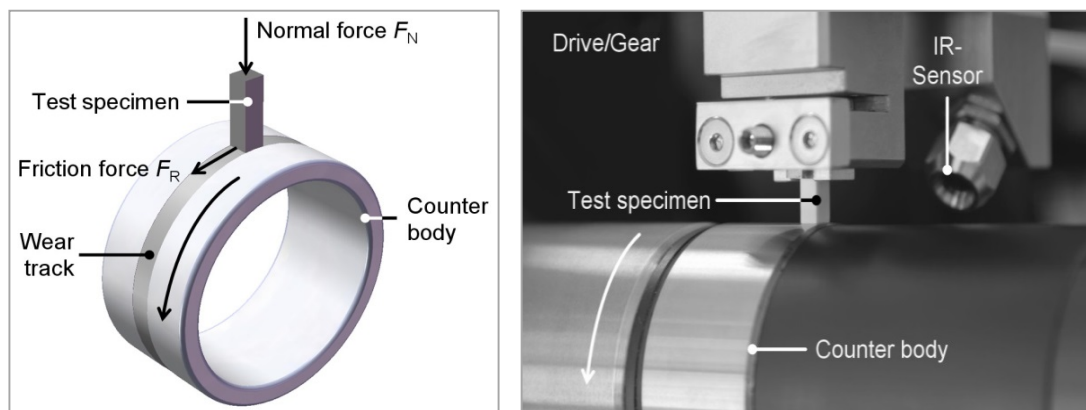


Figure 6.6 Schematic of the block on ring test (left); Atlas TT block on ring tester (right)

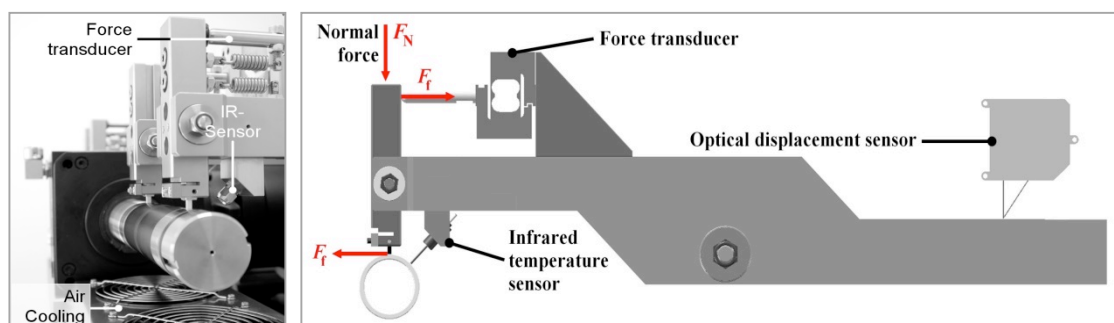


Figure 6.7 Side view of Atlas TT tester (left); schematic set-up of Atlas TT (right)

The steel ring was hardened to 60 HRC and ground to a surface roughness of $R_a = 0.1 - 0.2 \mu\text{m}$. During the CNC milling of the test bars, the moulding skin was removed from the inner section of tensile test bars in order to rule out effects that might originate from an uneven particle distribution in regions close to the surface of the test specimen precursors. The nominal contact area of the pins was 16 mm^2 . The parameters for the tribological tests are summarised in Table 6.3.

Table 6.2 Parameter of tribological tests

Block-on-ring test (plastic vs. steel)	
Pin	Impact modified polyamide and compounds thereof
Counterpart	100Cr6 steel
Loading	2 MPa
Sliding velocity	1 m/s, 1.5 m/s, 2 m/s, 2.5 m/s, 3 m/s
Temperatures	Ambient
Sliding distance	Variable, 21,600 meters on average
Kind of motion	Continuous - rotating sliding
Lubricant	none, dry sliding

Subsequent to the machining, all tribological test specimens were conditioned in a HPP 108 (Memmert GmbH, Germany) constant climate chamber according to ASTM D 618 [203] at $23 \text{ }^\circ\text{C}$ and 50 % relative humidity for at least 40 h. The polymer specimens as well as the steel counter bodies were thoroughly cleaned and degreased using petroleum ether before the testing. The contact area of the test specimen was treated with a thin strip of 1200 grit-sand paper subsequent to grinding in order to prevent a Hertzian contact between the initially planar test specimen and the curved steel ring. The sand paper was removed and both the plastic and the metal ring were cleaned again with petroleum ether. This procedure prevents the initial phase of the test to be influenced by the transition from line or Hertzian contact to

full conformal contact. The same is true for the wearing off of geometric errors like edge loading. Therefore, the breaking-in phase of the experiment is roughly limited to reaching a thermal equilibrium, forming a transfer film and changes in the surface topography. The contact pressure was set to 2 MPa (= 32 N absolute load). It is a well-known fact that materials may exhibit similar friction and wear at a given pv (where pv is the product of contact pressure p and sliding speed v) but start to yield different values for CoF and wear rate when the pv values are increased. In order to examine the different PTFE variants at variable pv -values, v was incrementally increased from 1 m/s to 3 m/s in steps of 0.5 m/s while keeping p at 2 MPa

The TriboTester is equipped with various sensors, which enable time resolved tracking of friction, wear and counter body temperature. The coefficient of friction μ was calculated by the measured friction force F_F and the applied normal force F_N according to equation 11. The test specimen's height loss h was also tracked in a time resolved manner, which gives direct access to the linear wear rate w :

$$w = \frac{h}{t} \quad (13)$$

The linear wear rate w was obtained in applying different sliding speeds of 1 m/s, 1.5 m/s, 2 m/s, 2.5 m/s, 3 m/s. Every sliding speed was seen as a single data set. Within the single data sets the first 50% of measured values were ignored. During this phase the test specimen height loss signal is distorted by the thermal expansion of the polymeric test specimen as well as of all other components of the test setup. Therefore, evaluation according to Eq. 13 was delayed until the friction and temperature have reached their new respective equilibrium values. As a general rule, this was simply done by ignoring the first 50 % of each sliding speed segment's data set. On the second 50 % of the data set, the volume loss data, which is computed

from the height loss data according to the utilized test specimen geometries, is approximated by a linear fit using the method of least squares. The linear wear rate is then computed from the slope of the resulting linear function. The specific wear rate w_s , was further calculated from w , using the applied contact pressure p and the sliding speed v , according to the following equation:

$$w_s = \frac{1}{\rho v} w \quad (14)$$

In order to ensure a reasonable statistical resolution of the test procedure, all friction and wear tests were done eight times per sample. Outlying observations were eliminated by standard procedures and arithmetic means. Standard deviations and confidence intervals were computed from the outlier-free data samples.

6.3.3 Statistical methods for result evaluation

When only a limited number of single measurements are available for the calculation of the mean values, the results need to be statistically validated. Therefore a calculation test on outliers according to Nalimov and an indication of the confidence interval is necessary.

6.3.3.1 Statistical outlier test according Nalimov

According to Grubbs, Nalimov or Dixon outlier tests can be applied to detect outliers in data sets. The methods can be used to check the reliability of data sets and if the methods of measurement are reliable. The Nalimov test calculates if a result is an outlier of a group of single results. Therefore the test requires minimum three valid results. A particular value x^* is considered to be an outlier, if a calculated test statistic r^* exceeds the critical threshold r for a given level of significance. The r^* comparison value is calculated according to the following equation:

$$r^* = \frac{|x^* - \bar{x}|}{s} \sqrt{\frac{n}{n-1}} \quad r^* \quad (15)$$

s : standard deviation of all values

\bar{x} : mean value of results (including the suspected value X^*)

n : number of values

r^* comparison value

The r^* value is compared with a nominal value r according to the table of Kaiser and Gottschalk (please see appendix), which is dependent on the significance level and the number of values n . Table 6-2 shows the r value ranges corresponding to the outlier classification.

Table 6.3 r values and corresponding outlier classification

Condition	Result
$r^* < r(95)$	no outlier
$r^* \geq r(95)$ and $r^* < r(99)$	potential outlier
$r^* \geq r(99)$ and $r^* < r(99,9)$	significant outlier
$r^* \geq r(99,9)$	highly significant outlier

If the r^* value exceeds the r value, the measurement value x^* must be considered as an outlier. Therefore, the value must be excluded from the measurements and the Nalimov test must be repeated with the remaining values, as the standard deviation and the mean value will be different without the outlier [204].

6.3.3.2 Standard deviation and confidence interval

The standard deviation is a measure that is used to quantify the variation of a set of data values. The reference point for the calculation is the arithmetic mean \bar{X} of the

single values. With the number of values n and the measured values x_i , the standard deviation s can be calculated according to the following equation:

$$s = \sqrt{\frac{1}{n+1} \sum_i (x_i - \bar{x})^2} \quad (16)$$

From the standard deviation the confidence interval was calculated according to:

$$\mu = \bar{x} \pm s \frac{t(\alpha, n)}{\sqrt{n}} \quad (17)$$

The confidence interval gives the estimated range of values that contains, with a specific probability, the estimated range from a given set of values. $t(\alpha, n)$ is student's t -distribution, which is a nominal value based on the significance level and number of results. The confidence interval of 95% indicates that when the same sample is generated multiple times, the arithmetic mean will be within the given interval in 95% of times. Due to the relatively high values of the student's t -distribution factor at small sample sizes, high standard deviations are particularly detrimental for the confidence level of the mean values. On the other hand, results with only small scattering of individual values indicate already reliable results, even with small number of samples. For a given standard deviation higher statistical surety can therefore only be achieved by more extensive sampling. The acceptance of a higher error probability would of course minimize the figure of the confidence interval, but this does not lead to a real increase in the confidence level of the estimated mean value.

6.3.4 Raw data analysis

All measurements were carried out in eight statistical valid measurements on each sample. If an outlier according chapter 6.3.3 occurs, a substitute measurement was carried out.

Table 6.4 Report of Atlas tribo tester for sample 1-PA66-T0 at 2 MPa and a sliding velocity of [m / s]

Hunke 1-PA66-T0 (1-PA66-T0) vs. IR 50x60x28 (GK-Ch 111), dry sliding
 $p = 2.0$ MPa, $v = 1.0 - 3.0$ m/s, $\vartheta_{cb} = \text{SAT}$ (23 °C)

2.5 m/s: individual tests numeric results

Wear test	Linear wear rate w_t [$\mu\text{m}/\text{h}$]	Specific wear rate w_s [10^{-6} mm ³ /Nm]	Coefficient of friction [1]	Counter body temperature ϑ_{cb} [°C]
339707	24	1.4	0.51	60
339728	29	1.6	0.52	78
339732	56*	3.1*	0.61	91*
348880	18	1.0	0.59	76
348881	22	1.2	0.57	71
348973	18	1.0	0.56	80
348974	24	1.3	0.60	69
348993	21	1.2	0.57	77
348994	32	1.8	0.61	61
$\bar{x} \pm \Delta x$	24 ± 4	1.3 ± 0.2	0.57 ± 0.03	71 ± 6
σ, n	5, 8	0.3, 8	0.04, 9	8, 8
$c = \sigma/\bar{x}$	0.213	0.213	0.063	0.106
$(\bar{x} \pm \Delta x)$	27 ± 9	1.5 ± 0.5	0.57 ± 0.03	73 ± 7
(σ, n)	12, 9	0.7, 9	0.04, 9	10, 9
$(c = \sigma/\bar{x})$	0.437	0.437	0.063	0.130

* = outlying observation, ** = invalid, () = parameter incl. outlying observations

According chapter 6.3.3 the third measurement of the sample with a linear wear rate of 56 $\mu\text{m}/\text{h}$ was considered as an outlier table 6.4). The mean value of linear wear rate including the outlier would have been 27 ± 9 . A substitute measurement with another sample was carried out and the outlier excluded, so the valid mean value of the linear wear rate is 24 ± 4 . In similar pattern tests with all materials has been performed and data were recorded. The individual wear rates as well as the coefficient of friction were calculated. On each sample, outlier tests were performed as mentioned

in chapter 6.3.3. and results of arithmetic mean values, the standard deviation and confidence intervals were calculated.

6.3.5 Number of tests

Various tests have been carried out in order to characterize the powder samples as well as the compound samples. In order to show the number of individual tests done, following table has been set up:

Table 6.5 Number of tests conducted and standards used

Experiment	Number of tests per sample	Standard if applicable
Fourier transform infrared spectroscopy (FTIR) analysis	1	
Differential scanning calorimetry (DSC)	2	
X-ray photoelectron spectroscopy (XPS)	3	
Thermal stability of plasma induced functional groups	1	
Contact angle measurement of PTFE powders	3	
Tensile test	10	DIN 527-2
Melt volume-flow Rate (MVR)	5	ISO 1133
Charpy notched impact test	10	DIN 179/1 eA
Dart drop test	10	DIN EN ISO 6603-2
Dynamic-mechanical thermal analysis (DMA)	1	
Tribological test: PIN on disc	3	ASTM G99
Tribological test: Block on ring	8	ASTM G137
Scanning Electron Microscopy (SEM)	1	

7 Experimental results and discussion

The first step in this study resulting in three papers was the plasma treatment of PTFE micro powders. This was done by plasma treatment in a low-pressure 2.45 GHz microwave plasma rotating drum reactor, as discussed in chapter 5.1. To chemically alter the PTFE surface by incorporation of functional groups, ammonia and hydrogen gases were used as process gases. The influence of treatment time was investigated by choosing different treatment durations. The effect of the plasma treatment was then analysed by Fourier transform infrared spectroscopy (FTIR), differential scanning calorimetry (DSC) and contact angle measurement of the PTFE powders. The results are described in the following chapter (7.1.1 – 7.1.5). As the plasma altered PTFE micro powders are intended to be used as dry lubricants in polymer compounds, the incorporated functional groups have to undergo the compounding process near/above the melting temperatures of the PTFE. Therefore, the high temperature behaviour and stability of the polar groups on the surface of PTFE has to be ascertained. The thermal stability of plasma induced functional groups was investigated and is proved in chapter 7.1.4.

7.1 Results of PTFE plasma treatment

7.1.1 Fourier transform infrared spectroscopy (FTIR)

The FTIR spectra of pristine and plasma treated samples are shown in Figure 7.1 (a,b) where the characteristic bands of CF_2 wagging, CF_2 stretching and CF_3 stretching could be observed at $620\text{--}640\text{ cm}^{-1}$ (not shown here), 1150 cm^{-1} and 1240 cm^{-1} , respectively [205]. The absorbance band observed at 1300 cm^{-1} in the spectra of the H_2 -treated sample (PTFE $\text{H}_2/10\text{ h}$) and NH_3 -treated sample (PTFE $\text{NH}_3/2.5$

h) indicated that slight changes occurred on the surface of the PTFE. In Figure 7.1 (a), the absorbance of hydrogen-treated PTFE (PTFE H2/10 h/2012) was located at 1210 cm^{-1} , which was higher than the bands of the other samples at 1205 cm^{-1} . The frequency and intensity shift of this band was assigned to the transformation of C–F bonds into C–H bonds and possibly C–CF₃ bonds. The bands of all of the other treated samples were on the same level as the bands of pristine PTFE. According to Heitz et al., for NH₃-treated sample, the band at approx. 1300 cm^{-1} can be attributed to the formation of ammonium fluoride [206]. As described by Dorschner et al., ammonium fluoride disappeared after post-treatment under vacuum at $100\text{ }^{\circ}\text{C}$ [17]. In addition, for NH₃ plasma treated samples, some weak and broad bands were observed in the range of 1550 and 1700 cm^{-1} , which were absent in the pristine samples, for which the band assignment is ambiguous. The adsorbed water molecules are known to be broadly centered at 1600 cm^{-1} , however they show a sharp spike which were not observed in our case. Alternatively, these peaks could indicate the presence of amide with absorptions of C=O at 1637 cm^{-1} and NH/CN at 1578 cm^{-1} , or attributed to N=O or C≡N, which are known to occur in this region [28]. In accordance, Shojaei reports on peaks in the region of 1700 cm^{-1} ascribed to oxygenated groups, which were observed on the surface of chemically treated PTFE [110].

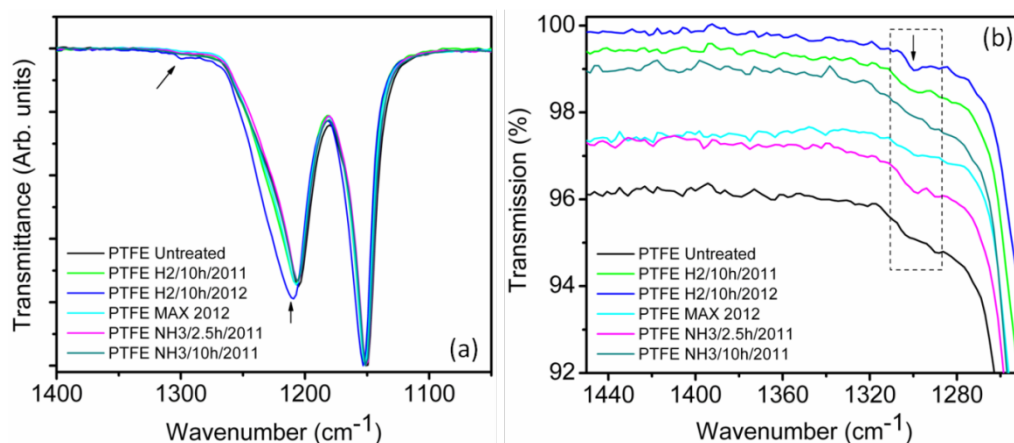


Figure 7.1 ATR FTIR spectrum of treated and pristine PTFE samples **(a)** In the region between 1250 cm⁻¹ and 1450 cm⁻¹ showing the slightly stronger reflection of the bands of PTFE H₂/10 h and PTFE NH₃/2.5 h in the vicinity of 1300 cm⁻¹. **(b)** in the region between 1050 cm⁻¹ and 1400 cm⁻¹ showing the shifted bands of PTFE H₂/10 h.

7.1.2 Differential scanning calorimetry (DSC)

The DSC values shown in Table 7.1, including the melting point or enthalpy of fusion, were identical in the first and second heating cycle for treated samples and pristine PTFE. As seen in Table 7.1, no considerable difference was obtained in the melting temperatures of the pristine and plasma treated PTFE powders; however, the melting enthalpy showed considerable differences upon plasma treatment. It should be noted that the values reported here for the melting point and melting enthalpy are quite similar to those reported by Dumitras and Odochian [207].

Table 7.1 Summary of various differential scanning calorimetric values of different PTFE samples

Sample		PTFE Pristine	PTFE H ₂ /10 h/New	PTFE MAX H ₂ /10 h	PTFE NH ₃ /10 h
1st heating cycle					
T _{m10}	[°C]	14	14	14	15
ΔH _{m10}	[J/g]	8	7	7	8
T _k	[°C]	–	116	133–167	–
ΔH _k	[J/g]	–	6	9	–
T _{m1}	[°C]	326	327	326	328
ΔH _{m1}	[J/g]	66	58	67	62
ΔX _c	[%]	80.5	70.7	81.7	75.6
2nd heating cycle					
T _{m20}	[°C]	19/28	18/28	18/28	19/30
ΔH _{m20}	[J/g]	11	8	11	8
T _{m2}	[°C]	327	326	327	328
ΔH _{m2}	[J/g]	65	57	67	54

The enthalpy calculated for pristine PTFE powders is ~66.0 J/g, giving a crystallinity value (ΔX_c) of nearly 80.5% (with ΔH_{m100} for 100% crystalline PTFE being 82.0 J/g). Upon H₂ plasma treatment, the ΔH_{m1} value reduces to 58.0 J/g providing a ΔX_c of 70.7% (Figure 7.2 a). Similarly, upon NH₃ plasma treatment the ΔH_{m1} value reduces to 62.0 J/g providing a ΔX_c of 75.6% (Figure 7.2 b). However, samples PTFE MAX H₂/10 h did not show any major changes in the ΔH_{m1} value and displayed a value quite close to that of pristine PTFE at 67 J/g providing a ΔX_c of 81.7% (Figure 7.2 c). Conte et al. report on lower wear values of compounds with PTFE as base polymer, when the crystallinity value is higher [208]. This is not in

accordance with the wear measurements in this work, as the PTFE has only a content of 10% in the final compound. However the compounds exhibiting better wear performance, contain the PTFE having a lower crystallinity. Khan reported that upon electron beam treatment of PTFE, which causes similar effects as plasma treatment, chain scission occurs. This leads to different PTFE molecule chain length. As a result the crystallization peak occurs at lower temperatures and the crystallization process continues till much lower temperatures in comparison to non-modified PTFE powder [209]. The DSC curve of PTFE H₂/10 h/2012 and PTFE MAX H₂/10 h showed signatures of post-crystallization in the range of 100–150 °C, which is again indicative of the changes in the chemical structure of treated polytetrafluoroethylene.

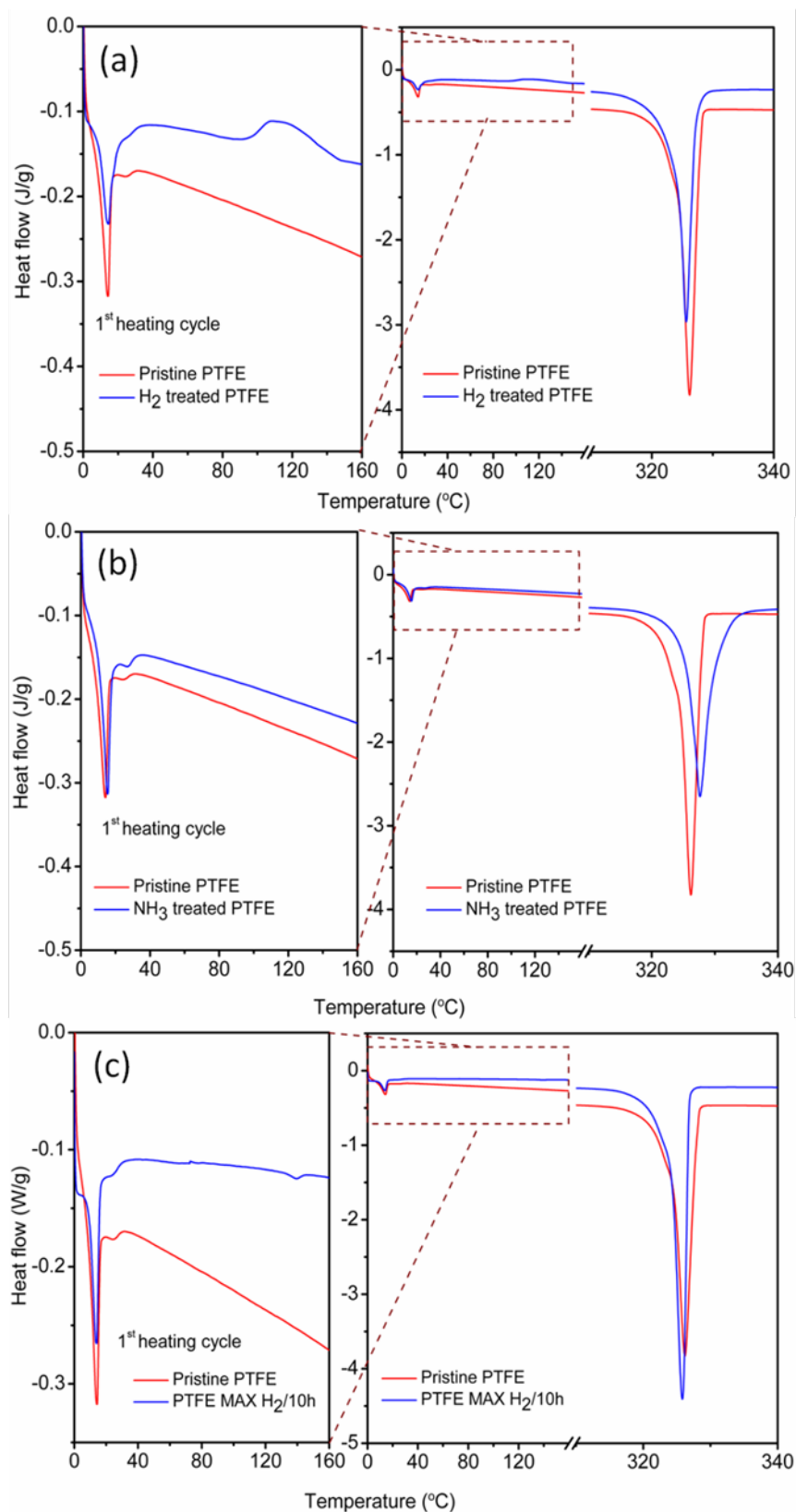


Figure 7.2 DSC curves of 1st heating cycles of (a) H₂ plasma treated PTFE sample. (b) NH₃ plasma treated PTFE sample. (c) MAX H₂ plasma treated PTFE powders. The expanded curves on the left show the post-crystallization peaks observed for the plasma treated samples.

7.1.3 X-ray photoelectron spectroscopy (XPS)

In the literature, the effects of NH₃ and H₂ plasmas on PTFE films have been studied extensively, and XPS results have demonstrated that these treatments lead to partial loss of fluorine (defluorination) accompanied by the production of hydrocarbons, cross-linking, chain scission and, depending on the feed gas used, incorporation of oxygen- and nitrogen-containing groups [8,30,196]. As shown in table 7.2, both the H₂ and NH₃ plasma treatments were successful in altering the surface of the PTFE with varying levels of defluorination. In fact, the lowest fluorine to carbon atomic ratio was observed on the sample treated for ten hours with NH₃ as a process gas (PTFE NH₃/10 h; F/C ratio: 1.13), followed by the sample treated for ten hours with H₂ (PTFE H₂/10 h/2012; ratio: 1.30) as compared to pristine PTFE (F/C ratio 1.86).

Table 7.2 Atomic percentages and associated elemental ratios of PTFE samples

Sample	Atomic Percentage [%]				Elemental Ratios		
	C	F	O	N	F/C	O/C	N/C
Pristine PTFE	34.94	65.06	--	--	1.86	--	--
PTFE NH ₃ /2.5h	39.48	58.35	0.92	1.24	1.48	0.02	0.03
PTFE NH ₃ /10 h	44.85	50.81	1.66	2.68	1.13	0.04	0.06
PTFE H ₂ /10 h/2011	36.74	62.20	0.45	0.61	1.69	0.01	0.02
PTFE H ₂ /10 h/2012	43.11	56.04	0.85	--	1.30	0.02	0.00
PTFE Max H ₂ /10 h	36.21	63.72	0.07	--	1.76	0.002	0.00

Figure 7.3 a,b shows the high-resolution C1s spectrum for the pristine PTFE powder samples. The core-level peak is quite symmetrical with a narrow full width at half-maxima (FWHM) of 1.45 eV and the binding energy (292.2 eV) consistent with the $(-\text{CF}_2)_n$ coordination. A broad discernible band at approx. 285 eV, ascribed to adventitious $-\text{C}-\text{H}_x-$ moieties is also observed [30,196]. The binding energy difference between the $(-\text{CF}_2)_n$ and the $-\text{C}-\text{H}_x-$ peaks of nearly 6.6 eV is quite similar to the values reported earlier in literature (6.5 eV) [159]. The high resolution

F1s spectrum (Suppl. Figure S2) at 689 eV presented a FWHM of 1.92 eV and was quite symmetrical in nature [30,159,196]. As shown in Table 1, the measured value of fluorine to carbon (F/C) ratio of 1.86, matched well with the values reported in the literature [30,159,196]. It must be noted that for pristine samples, the O1s signal was quite weak and no significant quantities of oxygen could be detected on the pristine PTFE surfaces.

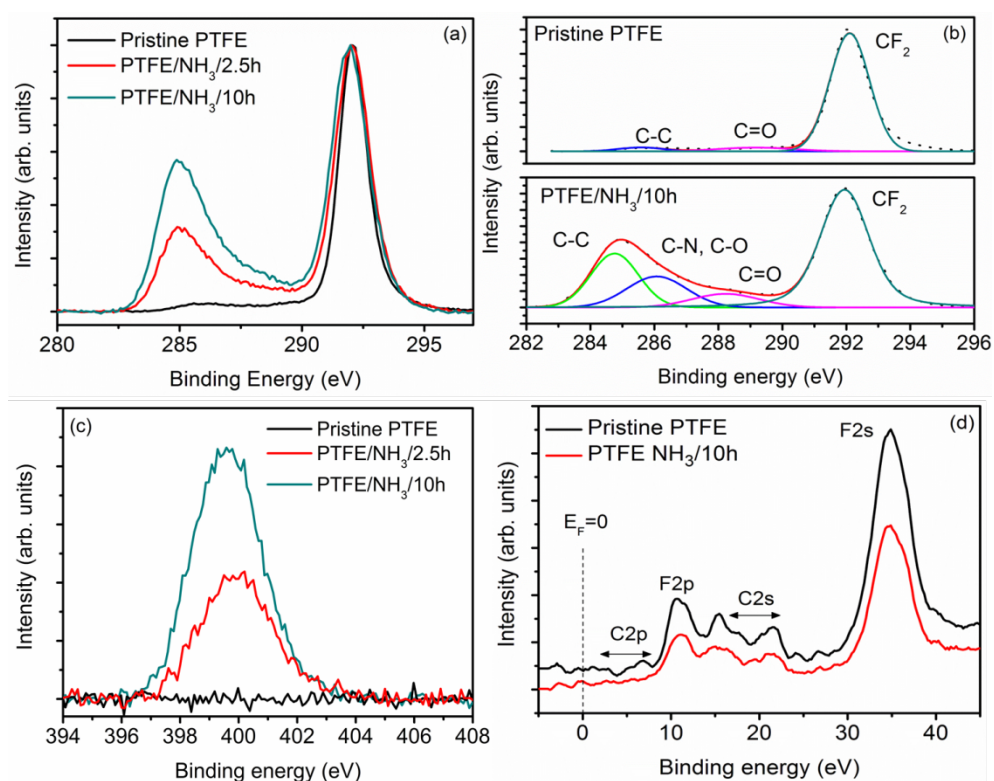


Figure 7.3 (a) High resolution C1s spectra of pristine and NH₃ plasma treated PTFE powders. (b) Deconvolution of C1s spectra of pristine and PTFE/NH₃/10 h samples. (c) Increase in the N1s signal intensity as a function of NH₃ plasma treatment time. (d) XPS valence band spectra of pristine and PTFE/NH₃/10 h samples.

The surface composition of NH₃ plasma treated PTFE powder samples, measured by XPS, is shown in Table 2. As compared to pristine PTFE, significant changes can be observed in the C1s envelope of NH₃ plasma treated samples, especially with regards to the increase in the peak intensities around 285 eV (Figure 7.3 a,b). In fact, an increase in the asymmetry and the width of the (-CF₂)_n peak with the increase in

the treatment time could also be observed clearly. The increase in the component at 285 eV has been attributed to the formation of $-C-C-$, $-C=C-$ and $-C-H_x$ moieties, although these groups cannot be resolved separately; while, the peaks located at 286.0, 288.2 and 291.9 eV can be ascribed to C-O/C-N and C=O, respectively [159]. It should be noted that the C-C bonds arise due to the strong surface defluorination and chain scission of the PTFE and have been reported earlier as well [205]. In view of the extensive loss of fluorine (65 at.% in pristine vs. 50.8 at.% for NH₃ treated samples), Wilson et al have ascribed the peaks in this region to $-C-CF$ and $-C-F$ formed by the reaction of CF₂ radical with liberated fluorine and oxygen in the plasma chamber [30,196]. For the NH₃ treated samples, the core F1s level increased in asymmetry and the FWHM increased to 2.25 eV vs. 1.92 eV for pristine samples (Suppl. Figure S2). In fact, with the increase in the treatment time from 2.5 h to 10 h, an incremental increase in defluorination was observed with the F/C ratio going down from 1.48 (for 2.5 h treatment time) to 1.13 (for 10 h treatment time) as compared to 1.86 for pristine samples. The defluorination effect itself is attributed to the physical sputtering of the PTFE surface upon nitrogen ion bombardment in plasma. Accordingly, the N content increased from 1.24 to 2.68 at.% along with an increase in the O content from 0.92 to 1.66 at.%, for 2.5 h and 10 h samples, respectively. This oxygen, which was detected at the surface after NH₃ plasma treatment, can occur due to O-grafting during or after the treatment. The incorporation of oxygen upon polymer surfaces in non-oxygen plasma treatments is quite common and occurs due to presence of free radicals that are created on a polymer surface during the plasma treatment. Upon exposure to the ambient environment, these unreacted free radicals interact with oxygen to create the oxygen functionalities on the polymer surface [30,196]. In addition, the possibility of leakage of air into the plasma chamber during plasma processing can lead to the formation of oxygen moieties. As

the leak rate of the chamber was quite low, we believe that the oxygen moieties were formed upon the exposure of the powder samples to the ambient environment only. However, further systematic studies are required to ascertain the effect of exposure time on the increase in the oxygen content, such as those performed by Werner et al [194] and Wilson et al. [166]. In Wilson's, it was observed that plasma treated PTFE sheets undergo further chemical changes as a function of time with the reaction kinetics dependent on the storage media as well as the gas used for plasma treatment [166]. Especially for samples stored in air, a steady state was reached within one month with the reaction attributed to the replacement of amines by either hydroxyl or amide groups [166]. Even though the increase in the treatment time nearly doubled the N content, the N1s core level signal did not show any changes in its shape, implying the nature of moieties attached to the surface remained similar (Figure 1c). The N1s signal was deconvoluted into two major components at 399.5 eV and 401.2 eV, corresponding to C-N and N-C-O configurations, respectively, with C-N being the dominant component [30,159,196]. The presence of these functional polar groups on PTFE molecule can lower its surface energy and improve the wettability. The valence-band spectrum for pristine and NH₃ treated PTFE is shown in Figure 1d. The two major peaks associated with C-F bonding appear at approx. 11 eV and 35 eV, corresponding to F2p and F2s, respectively [30]. The C2p shows up as low intensity peak between 5 eV to 12 eV and is indicative of C-H bonding [30]. The C2s peak gives rise to signals at 16 eV and 22 eV corresponding to C-C anti-bonding and bonding orbitals [22]. Upon NH₃ plasma treatment, a decrease in the intensity of F2p and F2s signals was observed along with a broadening of the C2p signal, representative of the formation of C-N groups upon NH₃ plasma treatment [30]. These results are in confirmation of the results previously reported on the NH₃ plasma treatment of PTFE sheets by various groups [30,196].

The surface composition of H₂ plasma treated PTFE powder samples, as measured by XPS, is shown in Table 7.2 and it can be clearly observed that the treatment led to the attachment of mainly hydrogen and oxygen moieties. For PTFE H₂/10 h/2012 samples, the F/C ratio is 1.30 which is much lower than that of pristine PTFE (F/C ratio of 1.86), accompanied by an increase in the oxygen content to 0.85 at.% (O/C ratio of 0.02 vs. no oxygen detected on pristine PTFE surfaces), indicative of the defluorination of PTFE powders by H₂ plasma treatment. This small increase in the O/C ratio to 0.02 upon plasma treatment means that some oxygen functional groups were formed simultaneously during/after the defluorination process. These oxygen functional groups correspond to the components at 287.7 and 290.0 eV, which are assigned to C-O and C=O bonds, respectively (Figure 7.4 a). Inagaki *et al.* have ascribed these peak positions in H₂ treated PTFE surfaces to O-CH-CF_n, CHF and O=C-CF_n, CHF-CF_n groups, respectively [8]. The defluorination mechanism in H₂ plasma treated powders can be explained using the following schematic. The formation of H• radicals in the H₂ plasma abstract fluorine atoms from the PTFE surface to form free carbon radicals [8]. These carbon radicals recombine with other hydrogen radicals in the hydrogen plasma to form C-H bonds which correspond to the defluorination mechanism [8]. However, similar to the NH₃ plasma treatment, not all the carbon radicals which are formed by hydrogen abstraction recombine with the other radicals. A part of these carbon radicals remain on the surface of the PTFE particles even after the plasma processing has been completed. When the chamber is opened and the powders exposed to the ambient environment, the remaining radicals come in contact with the air to form peroxide groups which then further modify into hydroxyl and carbonyl groups observed in the XPS analysis. The samples treated with H₂ plasma, PTFE H₂/10 h/2012 and PTFE H₂/10 h/2011 showed a small peak at

294 eV, which according to Vandencastele, can be attributed to CF_3 components produced via chain scission [143].

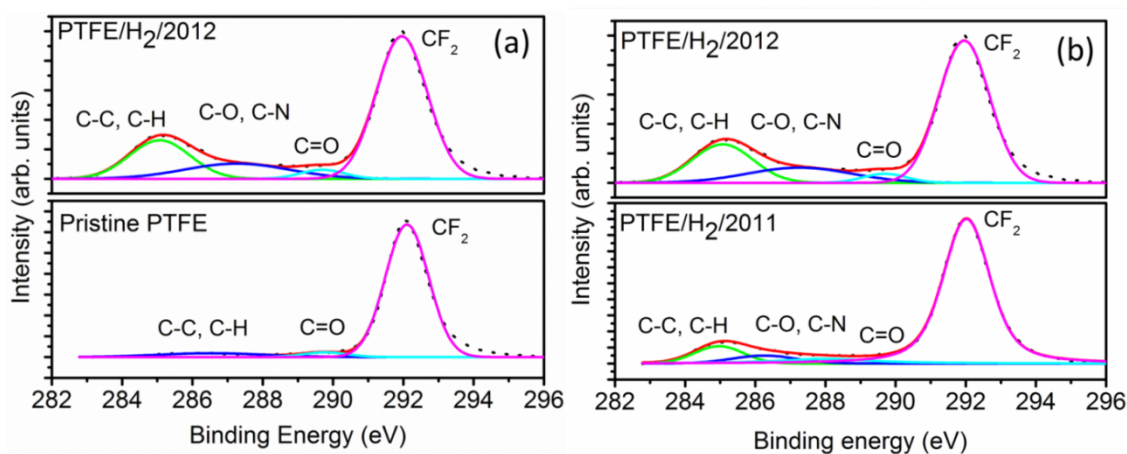


Figure 7.4 (a) High resolution C1s spectra of pristine and H₂ plasma treated PTFE powders showing the efficacy of the process. (b) High resolution C1s spectra of PTFE/H₂/2011 and PTFE/H₂/2012 samples showing the degeneration of plasma treated surfaces.

7.1.4 Thermal stability of plasma induced functional groups

Figure 7.2 (a - c) shows the C1s core level XPS spectra for pristine PTFE and plasma modified samples PTFE H₂/10h and PTFE NH₃/10h. For the pristine PTFE samples, the heating of samples up till 200 °C, (Figure 7.2 a) did not produce any appreciable change in the C1s core level XPS spectrum. However, further heating of the sample to 300 °C and beyond led to the appearance of peaks near 287.5 and 289 eV, attributed to the cross-linking in the polymer, which may occur due to either high temperature effects or as a result of X-ray exposure [210]. For plasma functionalised PTFE powders, the changes in the C1s core level spectrum are much more pronounced (see Figure 7.2 b, c). In fact, for PTFE/NH₃/10 h samples, the C1s core level signal showed a continuous reduction in the intensity of bands in the region of 285–289 eV, ascribed to C-C, C-N and C-O groups, indicating the removal of nitrogen functionalities with an increase in temperature, accompanied by a

concurrent reduction in the intensity of the N1s signal. Nevertheless, in spite of the high temperatures used during the measurement, complete removal of the polar species for both H₂ and NH₃ plasma treated samples was not observed, indicating the suitability of the plasma modification route for producing relatively stable moieties on the PTFE surfaces.

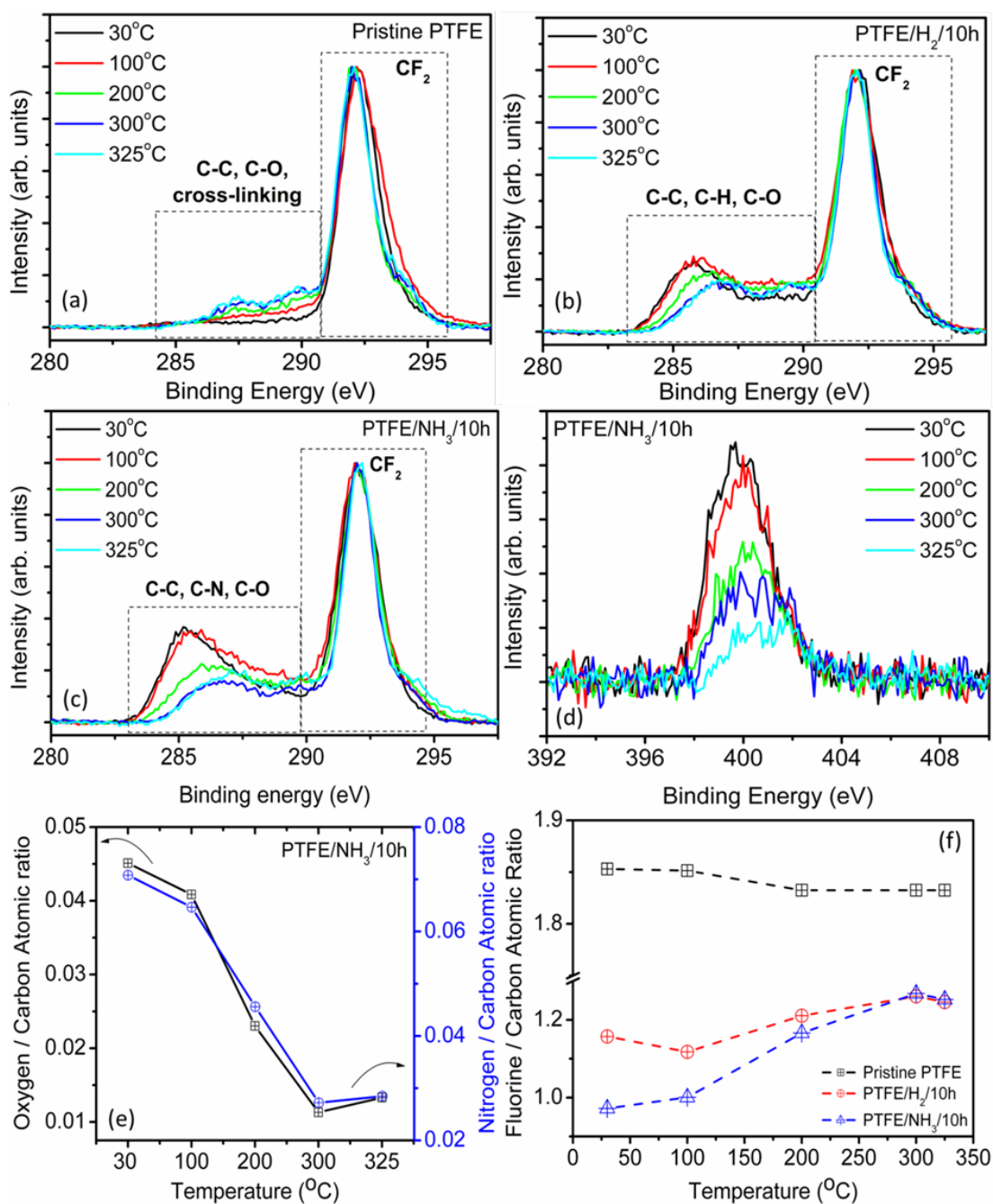


Figure 7.5 Temperature dependent XPS of pristine and plasma modified PTFE (a) C1s core level XPS spectra for pristine PTFE. (b) C1s core level XPS spectra for PTFE/H₂/10h sample. (c) C1s core level XPS spectra for PTFE/NH₃/10h sample. (d) N1s core level XPS

spectra showing the decrease in the signal intensity. **(e)** Changes in the O/C and N/C atomic ratios for PTFE/NH₃/10h sample as function of temperature. **(f)** Evolution of F/C atomic ratio for pristine and plasma treated PTFE as a function of temperature.

7.1.5 Contact angle measurement of PTFE powders

Figure 7.6 shows the results of the contact angle measurement of pristine and plasma treated PTFE samples. The wettability measurements were carried out analogical to Grundke et al. [211] for three different liquids with varying surface energies including Hexane (18.4 mJ/m²), Heptane (20.2 mJ/m²) and Dimethyl Sulfoxide, DMSO (43.6 mJ/m²). In comparison to Grundke et al. the limitation of numbers of different liquids lead to a coarser result but can already give a clear indication. Between the NH₃ and H₂ plasma treated PTFE powders, even though the NH₃ powders show much higher defluorination values as well as higher dispersion in water; the contact angle, as determined by Washburne capillary method, shows slightly lower values for H₂ plasma treated powders. In accordance with the XPS results, the addition of polar moieties via plasma treatment led to a reduction in the contact angle. The plasma functionalization of PTFE powders leads to an increase in the surface free energy enhances the dispersion of the polymer powders via increase in the dispersive component. Park *et al.* [212] have reported that there is a correlation between the incorporation of functional groups and the atomic structure and hydrophilicity (wettability). The decrease of the contact angle is mainly due to the change in the surface concentration of the polar moieties. Increasing nitrogen/oxygen functionalities on plasma treated surfaces lead to a decrease in the contact angle of the powders so that surface becomes more hydrophilic. To better visualize the change in the surface functionality and its effect on the surface wettability, pristine and plasma treated powders were dispersed in water (0.1 g/10 mL). As observed

clearly in Figure 7.6 (b), while, the pristine PTFE shows poor dispersion; the PTFE powders functionalised by H₂ and NH₃ plasmas display significantly better dispersion, which can be correlated to the presence of the polar groups.

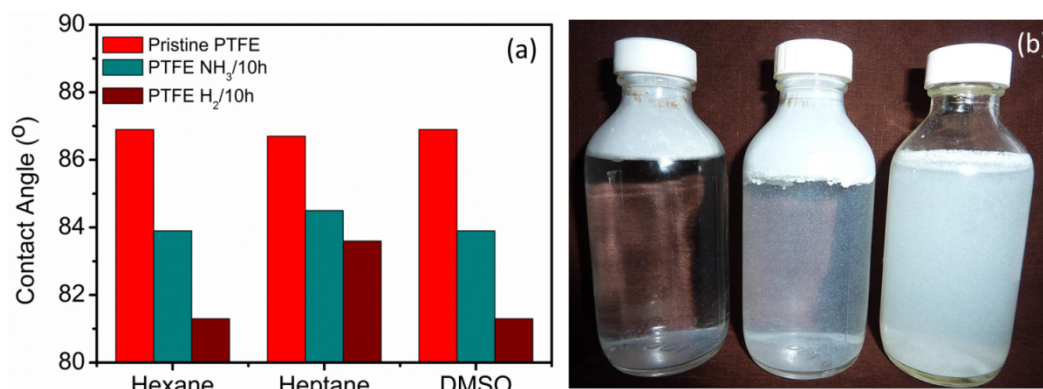


Figure 7.6 (a) Variation of contact angle for pristine and plasma treated samples in various testing media, (b) Pristine PTFE powders are poorly dispersible in water (**left**); upon H₂ (**middle**) and NH₃ plasma treatment (**right**), the dispersion is significantly improved.

7.2 Compound characterisation

7.2.1 Tensile test

Table 7.2 shows the values obtained from the tensile test according to DIN ISO 527 and the MVR flow test values according to DIN ISO 1133. It can be clearly observed that the impact modification of PA66 significantly decreases both the Young's modulus as well as tensile strength. While, commercially available PA66 (sample 31-PA66) exhibits a Young's modulus of 3.5 MPa and a tensile strength of 90.0 MPa; upon impact modification the corresponding values are reduced to 1.76 and 44.0 MPa, respectively. This dramatic drop in the mechanical properties can be ascribed to the formation of a two-phase system in impact modified PA66. Due to the significant difference in the surface energies of Polyamide and α -olefin copolymer, there exists only weak interfacial interaction between the two phases leading to the lower mechanical properties. Upon impact modification, the tensile strain at break increases from 7% to 58%; while the viscosity increases significantly due to the

rubber modification. The effect of addition of pristine PTFE on the Young's modulus and tensile strength of the PA66-PTFE compounds is small; with the tensile strength reducing from 43.6 MPa (for impact modified PA66, 1-PA66-T0) to 39.9 MPa (10 wt% pristine PTFE, 2-PA66-T2) and the corresponding Young's modulus decreasing from 1.76 GPa to 1.74 GPa, respectively.

Table 7.3 Mechanical properties of PA66i samples

PA66i samples	Young's modulus (MPa)	Tensile strength (MPa)	Tensile strain at break (in %)	MVR range (275°C / 5 kg cm ³ / 10 min)
	ISO 527-1/2	ISO 527-1/2	ISO 527-1/2	ISO 1133
31-PA66	3.500	90.00	7.00	136
1-PA66-T0	1.758	43.63	57.84	3.84
2-PA66-T2	1.744	39.92	45.07	3.30
6-PA66-H2	1.758	40.18	46.60	3.34
28-PA66-NH3	1.733	41.45	38.28	3.98

From Table 7.3, it can be clearly observed that for compounds of PESU with pristine PTFE, the Young's modulus is decreasing with the increasing content of PTFE. While the pristine PESU sample (14-PESU-T0) exhibits an E-modulus of 2.65 MPa, the 10% pristine PTFE containing composite (15-PESU-T2) exhibits a value of 2.44 MPa only. The conjunction of poor mechanical properties of PTFE with the wide differences in the surface energies of PESU and PTFE can clearly explain the weak interfacial interaction between pristine PESU/PTFE leading to poor mechanical properties of the compounds [35]. The measured tensile strength of the pristine PESU sample (14-PESU-T0) is 62.6 MPa, which increases to 64.9 MPa with the addition of 10wt% pristine PTFE. In the case of addition of 10wt% plasma modified PTFE powders to PESU, the Young's modulus of the compounds showed nearly similar values of ~2.44 MPa for both 19-PESU-H₂ and 30-PESU-NH₃ samples. In

terms of tensile strength, the H₂ plasma treated PTFE-PESU compound, 19-PESU-H₂, exhibits a tensile strength of 71.2 MPa which is nearly 8,6 MPa higher than that of pristine PESU (14-PESU-T0).

Table 7.4 Mechanical properties of PESU samples

PESU samples	Young's modulus (MPa)	Tensile strength (MPa)	Tensile strain at break in %	Melt volume-flow range 360° C / 10 kg cm ³ / 10 min
	ISO 527	ISO 527	ISO 527	ISO 1133
14-PESU-T0	2.65	62.6	6.9	63
15-PESU-T2	2.52	64.9	7.50	77
19-PESU-H ₂	2.44	71.2	9.44	60
30-PESU-NH ₃	2.43	68.2	9.44	64

Similarly, the tensile strain at break value also increases from 6.9% for pristine PESU (14-PESU-T0) to 7.5% for 10% pristine PTFE-PESU (14-PESU-T0) compounds. Upon the addition of plasma modified PTFE to PESU, the tensile strain at break is increased to nearly 9.44% with a corresponding increase in the tensile strength. According to Pukanszky et al, the higher tensile values can be attributed to the improved interfacial interaction between the plasma modified PTFE and PESU matrix, induced due to the incorporation of functional groups [174]. The decrease of Young's modulus of the compound containing 10 % PTFE modification is nearly similar for standard PTFE or plasma altered PTFE. So the plasma treatment of the PTFE modification has just minor influence on the Young's modulus.

7.2.2 Melt volume-flow rate (MVR)

For pristine PTFE-PESU compounds, the melt flow values (see Table 7.4) increase with an increase in the PTFE content. The standard PESU sample (14-PESU-T0)

offers volume flow rates of value of $63 \text{ cm}^3/10 \text{ min}$, whereas the benchmark sample 1-PA66-T0 containing 10% of pristine PTFE exhibits a value of $80 \text{ cm}^3/10 \text{ min}$. The PTFE micro-powders are well known additives for improving the melt flow properties of thermoplastic resins and thus the obtained results for pristine PTFE addition are in line with the expected behaviour [34]. However, with the addition of the plasma modified PTFE powders to PESU matrix, the flow behaviour shows slightly anomalous behaviour with a reduction in the flow rates to values ($60\text{-}64 \text{ cm}^3/10 \text{ min}$) which are quite similar to the pristine PESU ($63 \text{ cm}^3/10 \text{ min}$). This may be attributed to an increased interaction between the plasma treated PTFE particles and PESU matrix which limits the segmental movement of the PESU chains thereby enhancing the viscosity of the compounds. The addition of both H_2 and NH_3 plasma treated PTFE powders to the polyamide 66i compounds did not led to any significant improvements in the melt flow properties. All Pa66i compounds exhibit nearly the same melt volume flow rate.

Table 7.5 Melt volume rate of PESU and PA66i samples

PA66i samples	MVR range ($275^\circ\text{C} / 5 \text{ kg}$ $\text{cm}^3 / 10 \text{ min}$)
	ISO 1133
1-PA66-T0	3.84
2-PA66-T2	3.30
6-PA66-H2	3.34
28-PA66-NH3	3.98
PESU samples	Melt volume-flow range $360^\circ \text{C} / 10 \text{ kg}$ $\text{cm}^3 / 10 \text{ min}$
	ISO 1133
14-PESU-T0	63
15-PESU-T2	77
19-PESU-H ₂	60
30-PESU-NH ₃	64

7.2.3 Dart drop test

Figure 7.6 shows the time force diagram of dart the drop test for PESU-PTFE compounds. As the integral area for the neat PESU, represented by the area under the curve (blue line), is larger than those of the other compounds, the energy absorption for PESU is higher. PTFE modified compounds can be considered as two phase compounds, which exhibit lower ability of energy absorption due to the weaker interfacial bonding of the two phases. From the shape of the curve of pristine PESU, sample 14-PESU-T0, it can be observed that the pristine PESU shows ductile-brittle fracture behaviour. As observed clearly from Figure 7.6, the incorporation of pristine PTFE generally lowers the maximum force (F_m) and energy absorption (E_m) values significantly. In fact, pristine PESU sample 14-PESU-T0 absorbs a maximum force (F_m) of 5.6 kN and an energy at maximum force (E_m) of 51.6 J; whereas the addition of 10wt% pristine PTFE (15-PESU-T2) reduces these values of 0.96 kN and 2.63 J, which are only 17% and 5% of the original values, respectively.

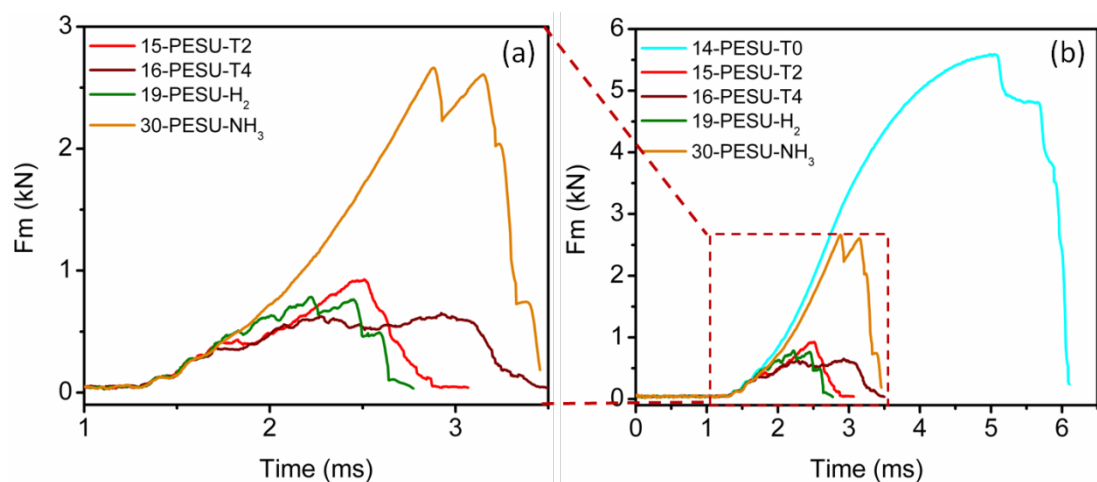


Figure 7.7 (a) Magnification of impact data of PESU-PTFE compounds with 10% modification (pristine and plasma treated), (b) Impact test data of all PESU and PESU-PTFE compounds.

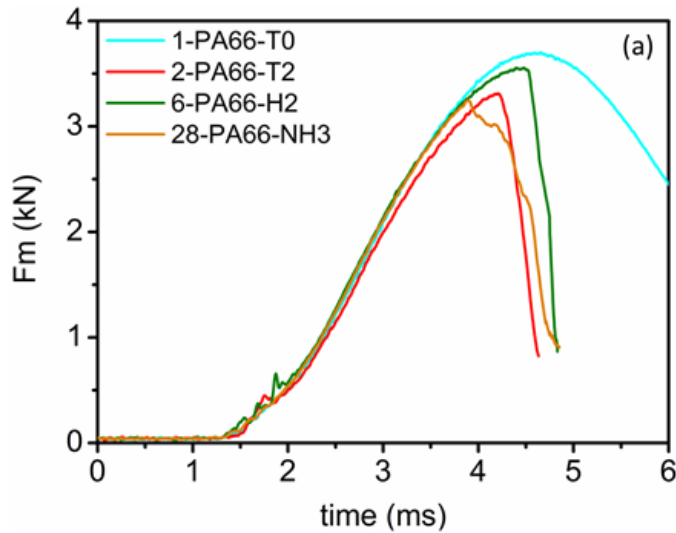


Figure 7.8 Impact test data of all Pa66i compounds.

Figure 7.7 shows the force-time diagram for the impact modified PA66 and pristine, plasma treated PTFE-impact modified PA66 compounds. While the impact modified PA66 (sample 1-PA66-T0) shows a typical ductile fracture behaviour, the addition of PTFE, both pristine and plasma treated, changes this to ductile brittle behaviour, as observed in the abrupt loss of values after having reached the values of maximum force (F_m). All curves with PTFE modification follow this trend. As observed clearly from figure 7.7 the incorporation of pristine unmodified PTFE only marginally lowers the maximum force (F_m) and energy absorption (E_m) values. While the pristine impact modified PA66 (1-PA66-T0) exhibits a maximum force of 3.7 kN and an energy absorption of 26.4 J; the corresponding values for pristine PTFE-impact modified PA66 (2-PA66-T2) are 3.3 kN and 20.8 J, respectively. However, the addition of plasma treated PTFE seems to provide a beneficial effect to the multi-axial impact behaviour. In fact, both the F_m and E_m values for H₂ (6-PA66-H2) are higher than that of pristine PTFE-impact modified PA66 samples. While the pristine PTFE-impact modified PA66 compound (2-PA66-T2) exhibits a maximum force of 3.35 kN and an energy absorption of 20.8 J; the corresponding values for H₂ plasma

treated PTFE-impact modified PA66 samples are 3.57 kN and 25.0 J, respectively. The F_m and E_m values for NH_3 plasma treated PTFE-impact modified PA66 samples (28-PA66-NH3) are only marginally higher than those of the pristine PTFE-impact modified PA66 samples. Although the value of maximum force (F_m) and energy absorption (E_m) of the compound containing the hydrogen treated PTFE (6-PA66-H2) does not completely reach the values of compound 2-PA66-T0, we have to take into consideration that the total modification content (soft phase) of the PTFE containing compounds is 30 wt%, and therefore 10 wt% higher than the pristine impact modified compounds. This beneficial effect can be attributed to the incorporation of the functional groups in the PTFE modification. The higher surface energy of the plasma modified PTFE enables a better dispersion in the polyamide-rubber-matrix and therefore promotes improved multi-axial impact behaviour.

7.2.4 Dynamic-mechanical thermal analysis (DMA)

The maximum of the $\tan \delta$ curve represents the glass transition (T_g) temperature region of the compounds. Figure 6.10 shows the results of DMTA measurement of polyamide compounds. Maximum values of $\tan \delta$ graphs indicating the glass transition temperatures. The differences in the storage modulus and $\tan \delta$ values of the impact modified polyamide 66 upon compounding with different plasma altered PTFE can clearly be seen.

Table 7.6 Glass transition temperature of impact polyamide samples

Sample name	Glass transition temperature T_g ($^{\circ}\text{C}$)
1-PA66-T0	88.40
2-PA66-T2	85.10
6-PA66-H2	81.20
28-PA66-NH3	85.40

The addition of PTFE to the matrix polymer (in figure 7.9 α -olefin impact modified polyamide 66) reduces the storage modulus E' and glass transition temperature. This reduction can be ascribed to the addition of “soft” PTFE material in conjunction with the presence of the α -olefin elastomer. However, the addition of NH_3 plasma treated PTFE to the impact modified PA66 was able to reverse this trend by enhancing the T_g to 85.40°C , which is quite close to the values observed for the addition of pristine PTFE. The presence of hydrogen bonding and possible interaction between the amine groups of PA66 with the polar groups of NH_3 treated PTFE increase the hindrance of the main chain motion of PA66. This increased hindrance results in the relaxation peak of PA66 being shifted back to higher temperatures, resulting in the increased T_g as well as higher value of $\tan \delta$, as compared to pristine and H_2 plasma

treated PTFE composites [12]. The trend was replicated in the storage modulus as well wherein the NH_3 plasma treated PTFE composites showed higher storage modulus in the glassy as well as rubbery regions as compared to H_2 plasma treated composites.

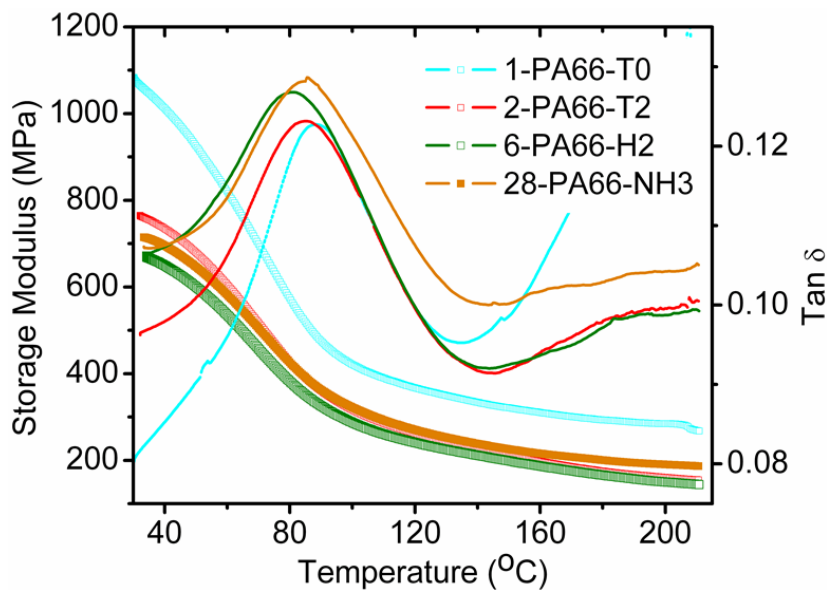


Figure 7.9 Plots of storage modulus and $\tan \delta$ versus temperature for impact modified PA66 and its compounds with pristine and plasma treated PTFE powders.

7.2.5 Scanning electron microscopy (SEM)

Figure 7.10 shows the SEM images of fractured surfaces from composite tensile test bars. For PESU composite with standard PTFE (Fig. 7.10 left), large voids due to the agglomeration and subsequent removal of PTFE particles during fracture could be observed. Moreover, these voids are quite separated from each other suggesting at the lack of interaction between the PTFE powder and PESU matrix. Due to the large differences in the surface energies of PESU and PTFE, the injection moulding skin largely seemed to be consisting of PESU only with the PTFE being present on the

inside of the fracture surface. For the composite samples containing the plasma treated PTFE (H_2 treated (Fig. 7.10 middle) and NH_3 treated (Fig. 7.10 right), the fracture surface was significantly different from pristine PTFE-PESU compounds. Especially for the NH_3 treated samples, the distribution of the PTFE particles was much more uniform across the PESU matrix. The uniform distribution of PTFE in conjunction with the smaller size of the voids suggests that the incorporation of functional groups enables a better interface interaction between the PESU matrix and the PTFE modification and is therefore beneficial for the mechanical properties.

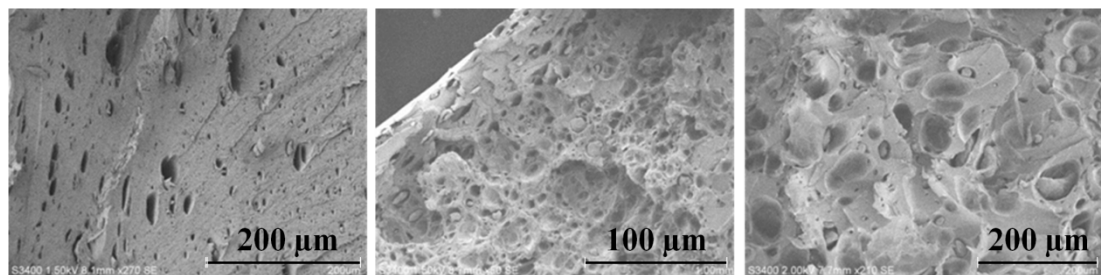


Figure 7.10 SEM pictures of the fractured surface of tensile test bars. PESU-PTFE composites with 10% pristine PTFE (left), PESU- H_2 (middle) and PESU- NH_3

Figure 7.11 (a-h) shows the SEM images of the fracture surface for pristine and plasma modified impact modified PA66 compounds. For impact modified PA66 samples, plastic deformation and fibrillation of the PA66 matrix is the dominant mechanism which leads to the failure of the material. The rubber modification provides sites to induce multiple crazing and shear yielding which can effectively diffuse the fracture energy throughout the polymer matrix [213]. During the tensile testing, the interface between the PTFE particles and the impact modified PA66 matrix plays a key role for crack initiation and propagation. For pristine PTFE compounds (2-PA66-T2), there exists no chemical interaction between the polymer matrix and the PTFE particles and the tensile force experienced during the testing

leads to a separation between the filler material and the matrix which can lead to the extracting of the soft filler phase as observed in Fig. 7.10 (c, d). While the fracture mechanism is still dominated by the plastic deformation of the PA66 matrix, the extraction of PTFE particles (Fig. 7.10 (d)) also plays a significant role in lowering the tensile strength of the compounds at the interface. In the case of plasma treated PTFE compounds, it was observed that the distribution and de-agglomeration of PTFE particles in the matrix was significantly better, especially for NH₃ plasma treated PTFE powders. For both the H₂ and NH₃ plasma treated PTFE impact modified compounds, the tensile failure was still caused by the conjunction of plastic deformation and extraction of PTFE particles from the matrix. However, due to the improved dispersion of the PTFE particles, the extraction of the PTFE particles for NH₃ plasma treated sample was not as severe and the de-agglomeration ensured that

the fracture energy was distributed all across the surface (Fig. 7.10 g, h).

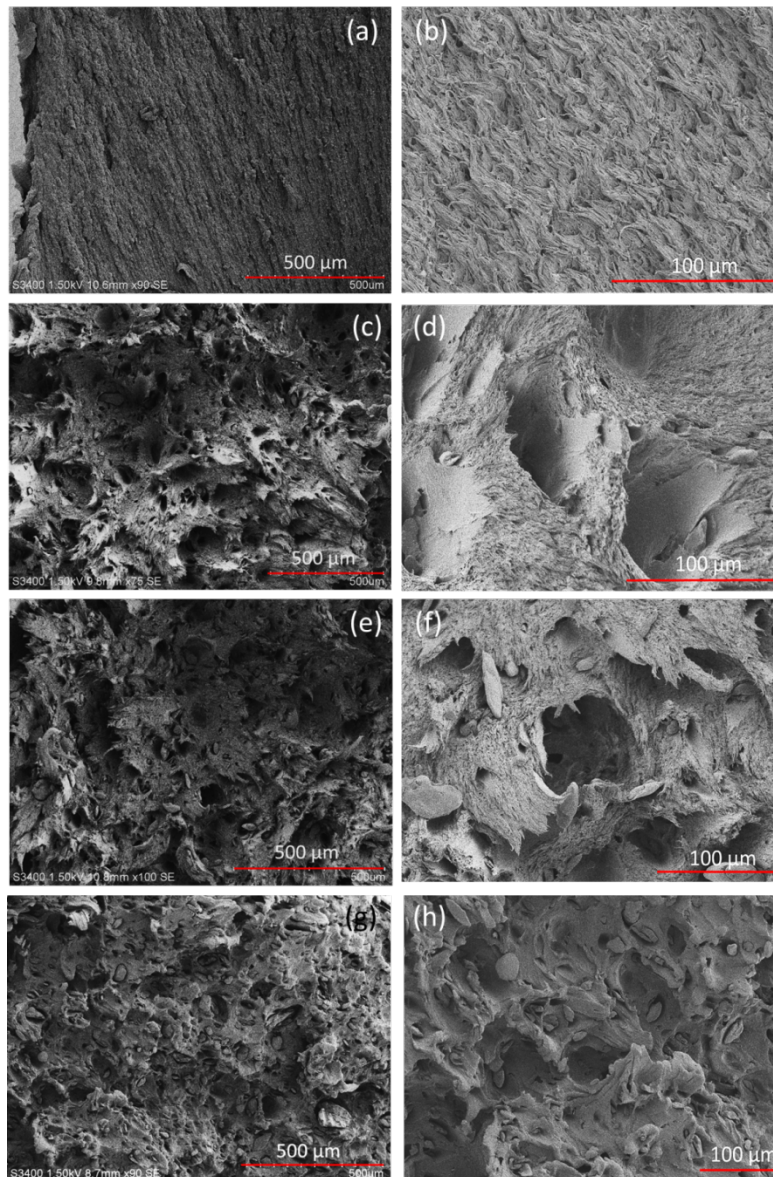


Figure 7.11 SEM analysis of the fracture surface of (a, b) 1-PA66-T0, (c, d) 2-PA66-T2, (e, f) 6-PA66-H2 and (g, h) 28-PA66-NH3 samples.

7.3 Tribological testing

7.3.1 Pin-on-disc test

For pristine PESU samples (14-PESU-T0), the tribological measurement using plastic pin on steel disc setup failed after 30 metres of sliding distance due to the strong stick-slip behaviour and hence no measurable values of coefficient of friction

and wear rate could be calculated. A measurement of coefficient of friction was only possible in a preliminary plastic ball (pristine PESU) on plastic plate (pristine PESU) test with a high value of 0.55, which matches closely to that measured by Duan et al. [50] of 0.5 and Kalacska [119] of 0.54. However, as seen in Figure 7.12, upon the addition of both the pristine PTFE and plasma treated PTFE, the values of coefficient of friction reduced drastically to the range of 0.20-0.26, which is nearly half of the value of pristine PESU. The compound 15-PESU-T2, containing 10 wt% pristine PTFE, shows a coefficient of friction curve with a run-in phase up to 2000 meter, followed by a steady state phase, with a constant coefficient of friction. The maximum value of mean friction coefficient of 0.24 at the beginning of the sliding distance reduces to a constant level of nearly 0.20 due to the formation of a PTFE friction film. During sliding, the PTFE molecules orient a fine coherent transfer film onto the counter face; this self-lubricating effect of PTFE modification [214] lowers the adhesion between the two sliding partner PESU and steel thereby decreasing the friction coefficient from 0,55 for pristine PTFE to 0,20 for PESU with 10% PTFE. Tanaka et al [68] too have reported an increase in the wear resistance of PESU with an increasing percentage of PTFE with a concurrent decrease in the coefficient of friction. As compared to the addition of pristine PTFE, the effect of addition of plasma modified PTFE to PESU showed slightly higher mean friction coefficients than the benchmark pristine PTFE sample (14-PESU-T2). Due to the presence of the functional groups on the plasma treated polymer, the formation of thin transfer film of PTFE was possibly hindered thereby leading to an increase in the observed CoF values [64]. As seen in Figure 6, while, the coefficient of friction of the H₂ treated PTFE-PESU compound (19-PESU-H₂) is decreasing in the run-in phase from 0.260 to 0.250 and further down to 0.23, but increases to 0.24 again after the half of the total sliding distance; the coefficient of friction of the compound containing the NH₃

treated PTFE (30-PESU-NH₃), is increasing over the whole of measured sliding distance from 0.240 up to 0.255. The change in the chemical PTFE structure with significant defluorination and the attachment of oxygen and nitrogen moieties in the side chain, renders the PTFE to have a higher interaction with the PESU and potentially the steel counter surface, which causes slightly higher coefficient of friction and a potential higher tendency of stick-slip behaviour.

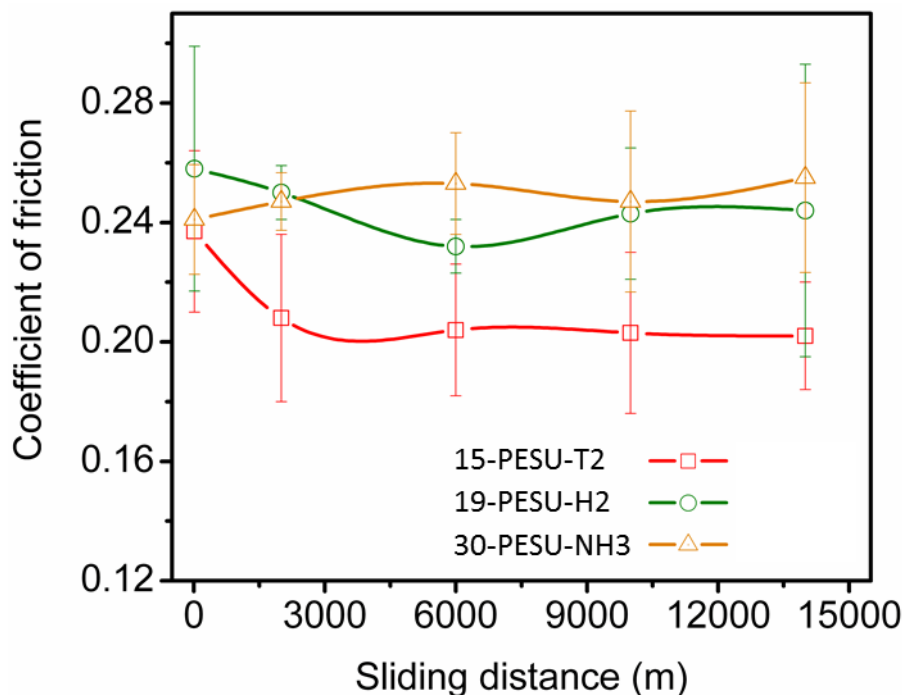


Figure 7.12 Mean friction coefficient as a function of time of PESU-PTFE compounds

Figure 7.13 shows the wear loss as a function of sliding distance. The compound containing the NH₃ plasma treated PTFE exhibits the lowest wear loss behaviour of all three PTFE lubricated compounds, followed by the compound containing the H₂ plasma treated PTFE. The benchmark sample 15-PESU-T2, with 10% pristine PTFE exhibits the highest wear loss curve over the sliding distance, representing the highest wear. The composite containing the nitrogen treated PTFE modification shows a linear gradient which characterises constant wear loss behaviour. The

improved ability of the plasma treated PTFE to form intermolecular bonds between the friction film and the PESU and the friction film and the counter face, develops a uniform friction film, which reduces the removal of PTFE during repetitive sliding and therefore improves the wear resistance [215]. The specific wear rates k , measured in the pin on disc set up, exhibit the lowest specific wear rate of $3.42 \pm 0.51 \times 10^{-6} \text{ mm}^3/\text{Nm}$ for the composite containing NH_3 treated PTFE modification (30-PESU-NH3), followed by the specific wear rate of $4.70 \pm 0.70 \times 10^{-6} \text{ mm}^3/\text{Nm}$ for the composite containing H_2 plasma treated PTFE (19-PESU-H2). The specific wear rates measured for the pristine PTFE-PESU samples was $5.75 \pm 0.58 \times 10^{-6} \text{ mm}^3/\text{Nm}$. Thus, the composites containing the standard PTFE exhibit higher specific wear rates than the plasma treated PTFE samples. The improvement of wear resistance of composites containing the plasma modified PTFE can be ascribed to the electro-negativity of the oxygen and the nitrogen atoms in the altered PTFE, which can form hydrogen bonds to the PESU [216] and the steel [215].

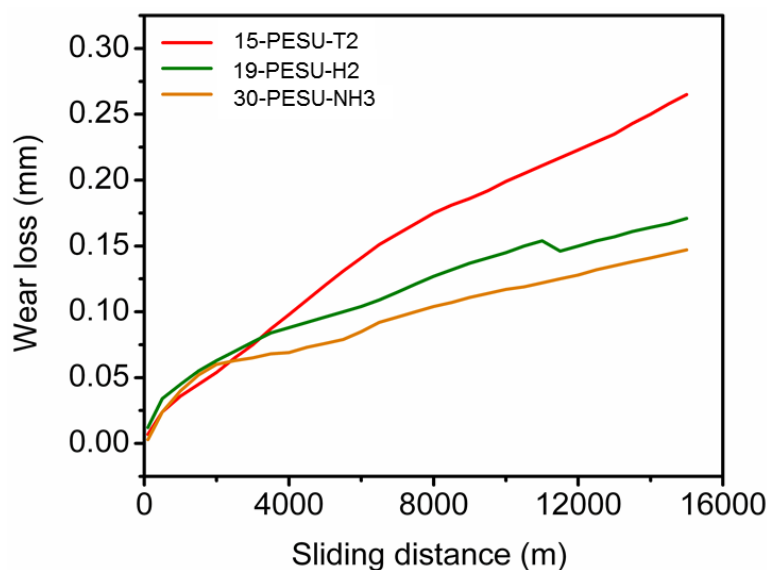


Figure 7.13 Wear loss of PESU-PTFE compounds vs. sliding distance in pin on disc set up

7.3.2 Block-on-ring test

The PTFE lubricated impact modified polyamide 66 is a three-phase system, consisting of two soft phases, the PTFE and the α -olephin-copolymer and one hard phase, the Polyamide 66. A more sophisticated block on ring tribo tester with four parallel measurement areas was used and different sliding velocities were applied in order to detect the effect of plasma treatment in this more difficult to measure three phase system. In general, polyamide 66 without any impact or friction modifier exhibits a rather high coefficient of friction, as can be seen in figure 7.14. The CoF of neat PA66 (31-PA66) starts out at 0.52 at 1 m/s sliding velocity, which is higher than the usually reported span of 0.25 – 0.40 for PA66 vs. steel in pin on disc or thrust washer tests. This discrepancy is a frequently observed by the utilized block on ring test method and it is especially characteristic for the specific combination of tribometer and steel counter body that has been used for the tests. With increasing sliding speed, the CoF increases even further until it reaches 0.82 at 3 m/s sliding velocity. This increase of friction with increasing sliding speed can also be observed for the other four investigated materials. This behavior is in good agreement with values reported by Biswas and Kalyani [217]. The observed high CoFs of neat PA66 resulted in elevated counter body temperatures of up to 108 °C at 3 m/s (see table 7.7). With the addition of the impact modifier (sample 1-PA55-T0), coefficient of friction was reduced significantly on average by 25 % over all samples, which also resulted in significantly lower counter body temperatures. This has also been reported by Yu et al. [38].

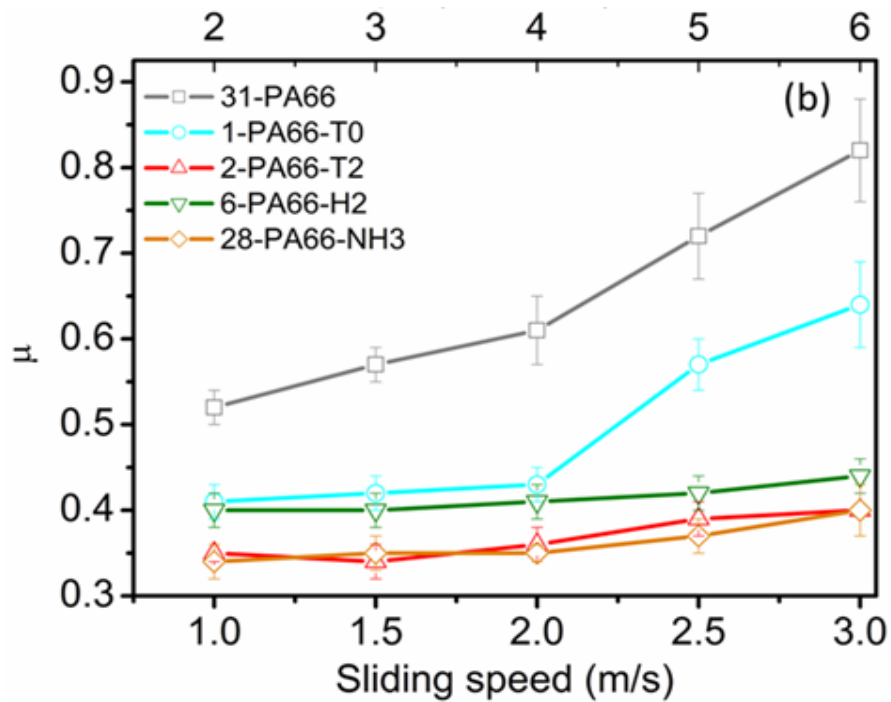


Figure 7.14 Mean friction coefficient as a function of time of PA66i-PTFE compounds

When adding pristine PTFE to the impact modified PA66, a rather small reduction of the coefficient of friction from 0.41 (sample 1-PA66-T0) to 0.35 (2-PA66-T2) is observed at 1 m/s sliding velocity. However at higher sliding speeds, the PTFE is able to significantly abate the over proportional increase in friction and temperature that is observed for neat and impact modified PA66.

Table 7.7 Coefficients of friction of the samples as a function of sliding speed

Sliding speed [m / s]	pv [MPa · m/s]	31-PA66	1-PA66-T0	2-PA66-T2	6-PA66-H2	28-PA66-NH3
		CoF	CoF	CoF	CoF	CoF
1.0	2	0.52 ± 0.02	0.41 ± 0.02	0.35 ± 0.01	0.40 ± 0.02	0.34 ± 0.02
1.5	3	0.57 ± 0.02	0.42 ± 0.02	0.34 ± 0.02	0.40 ± 0.02	0.35 ± 0.02
2.0	4	0.61 ± 0.04	0.43 ± 0.02	0.36 ± 0.02	0.41 ± 0.02	0.35 ± 0.01
2.5	5	0.72 ± 0.05	0.57 ± 0.03	0.39 ± 0.02	0.42 ± 0.03	0.37 ± 0.02
3.0	6	0.82 ± 0.06	0.64 ± 0.05	0.40 ± 0.03	0.44 ± 0.02	0.40 ± 0.03

Table 7.8 Counter body temperatures of the samples as a function of sliding speed.

Velocity [m / s]	pv	31-PA66 temperature [°C]	1-PA66-T0 temperature [°C]	2-PA66-T2 temperature [°C]	6-PA66-H2 temperature [°C]	28-PA66-NH3 temperature [°C]
1.0	2	61 ± 2	40 ± 1	41 ± 2	44 ± 2	40 ± 2
1.5	3	65 ± 2	47 ± 2	46 ± 1	49 ± 2	45 ± 1
2.0	4	70 ± 2	55 ± 2	49 ± 3	53 ± 3	49 ± 2
2.5	5	82 ± 3	71 ± 6	56 ± 3	58 ± 4	55 ± 3
3.0	6	108 ± 5	88 ± 7	62 ± 3	65 ± 4	61 ± 5

Compared to pristine PTFE the addition of plasma modified PTFE, both H₂- or NH₃-treated, does not result in further reduction of the coefficient of friction. As reported in a prior work, the plasma treated PTFE contains incorporated functional groups and therefore showing a lower contact angle [218]. This was also reported by Shojaei et al. [110] as a consequence of chemical treatment of PTFE by sodium naphthalene, resulting in an increased adhesion of PTFE reported by Kim et al. [15]. The improved adhesion results in a higher coefficient of friction. Lucas et al. have observed similar increase of coefficient of friction for short-term plasma treatment of LDPE [23]. The sample containing the hydrogen treated PTFE (6-PA66-H2) exhibit consistently higher cof 's throughout all sliding velocities than the samples containing the non-treated PTFE (2-PA66-T2). The sample containing the ammonia treated PTFE (28-PA66-NH₃) showing a trend of having lower coefficient of friction (0.35 ± 0.01) starting from a sliding speed of 2.0 m/sec. than for the reference containing pristine PTFE (0.36 ± 0.02).

Figure 7.15 exemplarily shows the results of the friction and wear tests for impact modified but PTFE-free PA66 (sample 1-PA66-T0). As mentioned in the experimental section, all tests were done in octuplicate due to the limited repeatability of friction and wear tests (especially when operating at high pv

products). The curves represent average curves of all valid individual curves, i.e. all curves not belonging to values designated to be outlying.

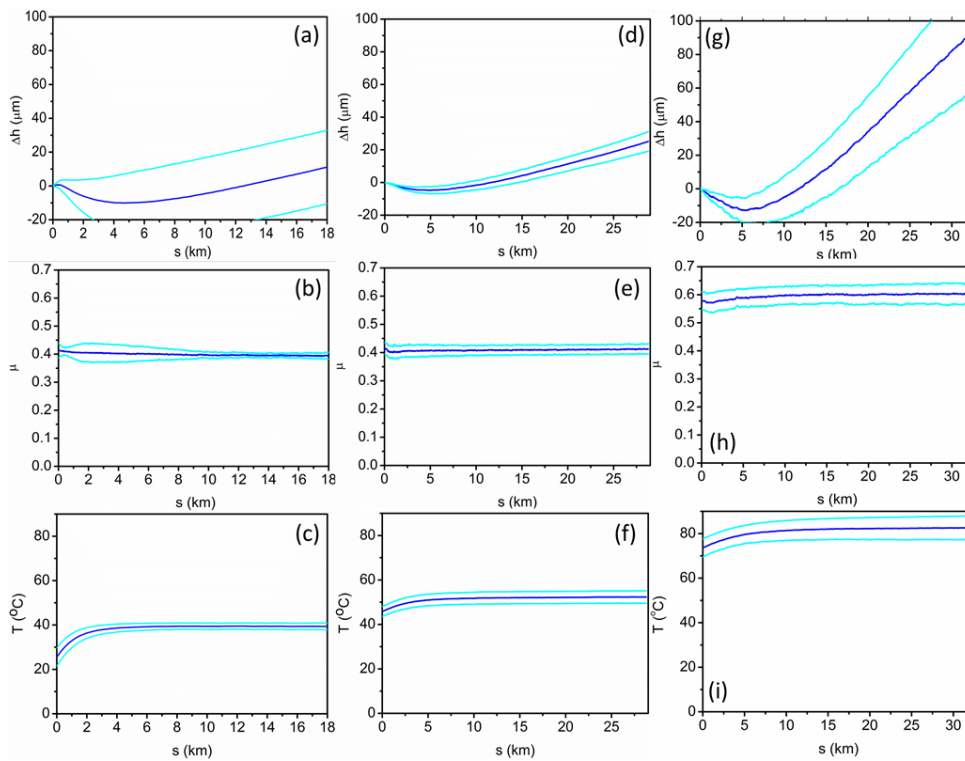


Figure 7.15 Average curves (dark blue) of test specimen height loss (top), CoF (middle) and counter body temperature (bottom) and upper and lower boundaries (light blue) of the corresponding confidence intervals. From left to right sliding speed increases from 1 m/s to 3 m/s in steps of 1 m/s.

At the beginning of all five speed segments the (average) height loss rate is negative because of the thermal expansion of the specimens and the test setup. When the corresponding thermal equilibrium is reached, thermal expansion stops and the height loss rates become positive. In all cases it was fully sufficient to ignore the first half of each segment. During the second half of each segment, no significant changes of either friction, wear and temperature could be observed, which can be considered to be proof of having chosen sufficiently long test durations for every segment. As

can be seen from table 7.9, neat PA66, i.e. without any impact or friction modifier, exhibited rather high friction and wear. Up to 2 m/s (= 4 MPa m/s) its specific wear rate amounts to about $1.4 \cdot 10^{-6}$ mm³/Nm and rises quickly when v is increased further.

Table 7.9 Linear wear rate w_t in [$\mu\text{m}/\text{h}$] and specific wear rate w_s in [10^{-6} mm³/Nm] of the samples as a function of sliding speed.

velocity	pv	31-PA66		1-PA66-T0		2-PA66-T2		6-PA66-H2		28-PA66-NH3	
		w_t	w_s	w_t	w_s	w_t	w_s	w_t	w_s	w_t	w_s
1.0	2	10 ± 1	1.4 ± 0.1	7 ± 1	1.0 ± 0.1	4 ± 1	0.6 ± 0.1	4 ± 1	0.6 ± 0.1	4 ± 1	0.6 ± 0.1
1.5	3	15 ± 2	1.4 ± 0.2	9 ± 2	0.8 ± 0.2	6 ± 1	0.6 ± 0.1	6 ± 1	0.6 ± 0.1	5 ± 1	0.5 ± 0.1
2.0	4	22 ± 4	1.5 ± 0.3	11 ± 2	0.8 ± 0.1	8 ± 2	0.6 ± 0.1	7 ± 2	0.5 ± 0.1	6 ± 1	0.4 ± 0.1
2.5	5	50 ± 6	2.8 ± 0.3	24 ± 4	1.3 ± 0.2	12 ± 3	0.7 ± 0.2	10 ± 2	0.6 ± 0.1	9 ± 2	0.5 ± 0.1
3.0	6	215 ± 20	10 ± 1	50 ± 9	2.3 ± 0.4	24 ± 4	1.1 ± 0.2	16 ± 3	0.7 ± 0.1	12 ± 2	0.6 ± 0.1

Therefore 4 MPa m/s can be considered to be the critical pv value (value of product: pressure x velocity) for the sample 31-PA66. The addition of the impact modifier (sample 1-PA66-T0) does not only significantly reduce wear but also increases limiting pv to 5 MPa m/s, beyond which the specific wear rate nearly doubles when increasing v from 2.5 m/s to 3.0 m/s.

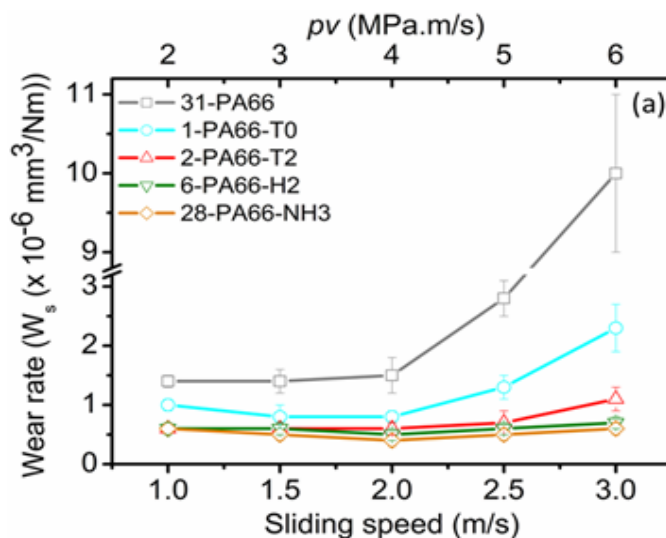


Figure 7.16 Wear rate of PA66i-PTFE compounds vs. sliding speed

Adding 10 % pristine PTFE to the impact modified material led to a further reduction of wear e.g. from $11 \pm 2 \mu\text{m/h}$ to $18 \pm 2 \mu\text{m/h}$ for the sliding velocity of 2.0 m/sec. Again, when increasing the velocity v beyond 2.5 m/s the specific wear rate for the sample 2-PA66-T2 increases significantly $12 \pm 2 \mu\text{m/h}$ to 24 ± 2 . Therefore, pv value of 5 can be considered as the critical pv value for sample 2-PA66-T2. The plasma treatment of the PTFE has no direct influence on the wear rate for the pv values between 2 and 4 (sliding speed between 1.0 m/sec and 2.0 m/sec), however when increasing the pv to a value of 6 (sliding speed 3.0 m/sec), the compound containing the standard PTFE exhibits a wear rate of $24 \pm 4 \mu\text{m/h}$ compared to a wear rate of $16 \pm 3 \mu\text{m/h}$ for the hydrogen treated PTFE and a wear rate of $12 \pm 2 \mu\text{m/h}$ for the NH_3 treated PTFE. The plasma treated PTFE types were both able to reduce wear at the highest applied sliding speed, which is a notable improvement over pristine PTFE, whose PA66 composite yields a limiting pv of 5 MPa m/s. Therefore the plasma treatment of PTFE with hydrogen or ammonia is beneficial for the use of PTFE as a lubricant in PA66i compounds. The ammonia treatment is superior to the hydrogen treatment in polyamide 66 compounds.

8 Conclusions and recommendations for further work

8.1 Contents of the work

The PTFE micro-powders were successfully plasma treated in a low-pressure 2.45 GHz microwave plasma rotating drum reactor. This has been proved by Fourier transform infrared spectroscopy (FTIR), differential scanning calorimetry (DSC) and contact angle measurement. The PTFE micro powders were then used as dry lubricants in PESU-PTFE and PA66i-PTFE compounds in order to improve the tribological behaviour. The tribological properties of the compounds were tested in pin-on-disc and block-on-ring model tests. The results reveal an improvement.

8.1.1 Goals achieved

Polar functional groups containing oxygen and nitrogen, such as double bonded oxygen C=O, amide NH₂, OH groups were incorporated onto the non-polar PTFE micro-powder surface. This was achieved by the use of ammonia and hydrogen as process gases. It was found out that under similar processing conditions, the NH₃ plasma treatment was much more effective than the H₂ plasma treatment in defluorination of PTFE and the resulting reduction in the F/C ratio.

The duration of the treatment time was found to be directly proportional with the defluorination values of the PTFE, with longer treatment times leading to higher defluorination values.

The degeneration of plasma species onto the PTFE surface was studied over time for a sample stored for one year wherein it was observed that the plasma treatment was not completely reversible.

Through temperature dependent XPS analysis it was observed that the functional groups are thermally stable and therefore can withstand the compounding process.

The addition of 10 wt% pristine PTFE to impact modified polyamide 66 and polyethersulfone dramatically lowers the mechanical properties of the composites as compared to the pristine PA66i and pristine PESU. The plasma treatment of PTFE restored the mechanical properties of these compounds, so they were significantly higher than those of the composites where pristine PTFE was used, although not to the same extent as that of pristine PA66i and PESU.

The impact of the incorporation of functional groups in the PTFE lubricant on the coefficient of friction differs, depending on the matrix polymer used. In the impact modified polyamide 66-PTFE composites, the coefficient of friction increased about 15% on the treatment with hydrogen as process gas, and remained on a similar level as compared to the pristine PTFE composites on the treatment with ammonia as process gas. Upon the treatment with hydrogen as process gas, in both matrices the impact modified polyamide 66 as well as in the polyethersulfone, the coefficient of friction increased. The specific wear rate could be improved for 40 % in the PESU-PTFE compounds with the use of ammonia treated PTFE. The PA66i-PTFE compounds exhibit similar specific wear rates of $0.6 \times 10^{-6} \text{ mm}^3/\text{Nm}$ for pristine PTFE as well as for ammonia and hydrogen treated PTFE on a sliding speed of 1 m/sec, but are improved by about 45 % at higher sliding speed of 3 m/sec.

8.2 Conclusions

To use chemically modified PTFE micro powder with enhanced tribological properties in thermoplastic compounds, the PTFE micro powders has been altered by plasma treatment using a 2.45 GHz microwave plasma reactor. A rotating drum reactor as plasma chamber was used. Hydrogen and ammonia were used as the process gases in order to determine the incorporation of functional groups as well as the impact of the treatment time. It was observed that as compared to the H₂ plasma treatment, which resulted in a fluorine to carbon ratio of 1.30; the NH₃ plasma treatment resulted in a fluorine to carbon ratio of 1.13, and hence was much more effective at defluorination of PTFE. A variation of the plasma treatment time from 2.5 hours to 10 hours, resulted in the fluorine to carbon ratio of 1.48 and 1.13, respectively, thereby confirming that the defluorination of PTFE was directly proportional to the treatment time.

The influence of long term ambient storage on the plasma induced functionalities of H₂ plasma treated powder was demonstrated with the sample stored for a period of 12 months. The storage of hydrogen treated sample led to an increase of the fluorine to carbon ratio to 1.69 from a starting value of 1.30, but not completely back to the values of pristine PTFE (1.86).

The effect of plasma treatment could also be observed clearly in the DSC scans, where a higher defluorination value led to a lower crystallinity of the samples. The enthalpy calculated for pristine PTFE powders is ~66.0 J/g, compared to the enthalpy of H₂ plasma treated PTFE of 58.0 J/g and an enthalpy of NH₃ plasma treated PTFE of about 62.0 J/g.

Through temperature dependent XPS analysis of pristine and plasma treated PTFE, the removal of hydrogen and nitrogen functional groups from PTFE surface was observed, especially above 200 °C. However, a complete removal of the moieties was still not observed even at high temperatures (>300°C), which is indicative of the thermal stability of the functional groups on the PTFE surfaces. Even as the residence time of the materials during the compounding process is much lower than duration of the temperature dependent XPS measurement. Thus, microwave plasma treatment applying hydrogen and nitrogen as process gases is an effective method for incorporation of functional groups into PTFE micro powders.

The study of the feasibility of scaling up from the plasma treatment process was not successful. The fluorine to carbon ratio of 1.76 exhibited in the scale up reactor using hydrogen as process gas and a treatment time of ten hours was very close to the fluorine to carbon ratio of 1.86 for pristine PTFE. Even a higher energy output rate of 900 W did not lead to a greater defluorination. The residence time of the PTFE particles in the plasma area of the chamber are also lower in the larger drum. Further optimization of processing conditions is required in order to obtain optimal results for the treatment of larger quantities.

The plasma modified PTFE micro powders were further used as dry lubricants for the improvement of tribological properties of polyethersulfone. The treatment of PTFE with ammonia as the process gas led to better results in both the tribological as well as the mechanical testing compared to the results obtained when hydrogen was used as the process gas. While, the use of pristine PTFE improves the coefficient of friction from 0.55 for pristine PESU to 0.20 for PESU-PTFE, the coefficient of friction is somewhat higher for the plasma treated PESU-PTFE compounds. This is due to the incorporation of functional groups on the surface of the modified PTFE,

which affect the adhesive properties of the composite. The addition of PTFE not only eliminated the strong slip-stick behaviour of PESU but also enhanced the wear performance. The wear rates for NH₃-treated PTFE-PESU composites of 3.42×10^{-6} mm³/Nm is nearly half of those of pristine PTFE-PESU composites of 5.75×10^{-6} mm³/Nm. Furthermore, the gradient of the wear loss curve of the samples containing plasma treated PTFE is smaller and for the NH₃ treated PTFE more constant than that of the pristine PTFE-PESU composites at the same loadings. At the same time, the addition of PTFE to the PESU matrix led to a dramatic reduction in the mechanical properties. While the addition of pristine PTFE to PESU significantly lowered the maximum force and energy in the dart drop test from 5.6 kN and 51.6J (for pristine PESU) to 0.96 kN and 2.63J, respectively. The addition of NH₃ treated PTFE partially restored the values to 3.3 kN and 10.79 J. Therefore, the use of plasma treated PTFE micro powders in PESU matrix as dry lubricants is beneficial for both the mechanical and tribological properties.

In the evaluation of the use of plasma treated PTFE powders in impact modified polyamide 66 composites, it should be considered that there are three phases in the composite: the matrix (polymer polyamide 66), the α -olefin-copolymer (impact modifier) and the PTFE. The results in the mechanical evaluation are quite different for the composite materials based on hydrogen plasma treated and NH₃ plasma treated PTFE. While the hydrogen treatment of PTFE seem to be more beneficial for the Young's modulus and the tensile strain at break, the treatment with ammonia as the process gas seems to be more beneficial for the properties of tensile strength and charpy impact strength. Therefore, the friction and wear behaviour was evaluated on different sliding speeds to evaluate different pv -values. The coefficient of friction for the sliding speed of 1 m/sec decreased on the addition of α -olefin-copolymer as the

impact modifier to the polyamide 66 matrix from 0.52 to 0.41. This shows that the impact modifier is already beneficial for the tribological behaviour. Similar behaviour is exhibited at all sliding speeds. The addition of the pristine PTFE to the impact modified polyamide 66 lowers the coefficient of friction further down to 0.35 (at a sliding speed of 1 m/sec). The behaviour is similar at all the sliding speeds. The addition of ammonia plasma treated PTFE keeps the coefficient of friction somewhat on the same level between 0.34 at a sliding speed of 1 m/sec and 0.40 at a sliding speed of 3 m/sec as compared to the pristine PTFE, exhibiting a coefficient of friction between 0.35 at a sliding speed of 1 m/sec and 0.40 at a sliding speed of 3 m/sec. The addition of hydrogen treated PTFE increases the coefficient of friction to 0.40 at a sliding speed of 1 m / sec to as compared to the pristine PTFE of 0.35. The lowest coefficient of friction of 0.34 was observed for the ammonia plasma treated PTFE at a sliding speed of 1 m/sec. The use of plasma treatment of PTFE micro powders is beneficial for the wear rates at sliding speeds between 1 m/sec and 3 m/sec and both the hydrogen and ammonia treatments are beneficial in this case. The specific wear rate of $1.4 \times 10^{-6} \text{ mm}^3 / \text{Nm}$ for polyamide 66 can be improved on the use of α -olefin-copolymer impact modification down to $1.0 \times 10^{-6} \text{ mm}^3 / \text{Nm}$ for the sliding speed of 1 m/sec. The addition of pristine PTFE lowers the specific wear rate down to $0.6 \times 10^{-6} \text{ mm}^3 / \text{Nm}$. The use of plasma modified PTFE (hydrogen as well as ammonia) does not lower the specific wear rate on a sliding speed of 1 m/sec. On the highest sliding speed of 3 m/second the wear rate is decreased from $10.0 \times 10^{-6} \text{ mm}^3/\text{Nm}$ for pristine polyamide 66, down to $2.3 \times 10^{-6} \text{ mm}^3/\text{Nm}$ for α -olefin-copolymer modified polyamide 66. The addition of pristine PTFE lowers the wear rate down to $1.1 \times 10^{-6} \text{ mm}^3/\text{Nm}$ and down to $0.7 \times 10^{-6} \text{ mm}^3/\text{Nm}$ for hydrogen treated PTFE and further down to $0.6 \times 10^{-6} \text{ mm}^3/\text{Nm}$ for ammonia plasma treated PTFE. Therefore, the treatment of PTFE with ammonia or hydrogen as the process

gas can be beneficial depending on the sliding speed. On low sliding speed of 1 m/sec, the treatment led to similar tribological properties compared to the pristine PTFE, however, on higher sliding speed, the plasma treatment is beneficial. The best performance is exhibited with ammonia as the process gas on higher sliding speed values.

It has been shown for the first time, that besides the treatment of various other polymers [19–22] with plasma techniques, also PTFE micro powders can be chemically altered. The altered PTFE micro powders can then be used in PESU and PA66i matrices, similar as conducted by Lehmann et al. [6,219,220]. As the plasma process is much cheaper, environmentally more friendly compared the electron beam modification, this procedure will be commercialized by the author. The plasma modified PTFE micropowders will also be used in further polymer matrices such as PEEK and PPS.

8.3 Recommendations for further work

From the results obtained during the course of this project, it can be clearly said that the microwave plasma modification by means of hydrogen and ammonia as process gases is an effective method to incorporate polar surface functionalities onto the polytetrafluoroethylene (PTFE) micro-powder surfaces. The compounds lubricated with plasma treated PTFE need to be investigated more in detail by applying different tribological settings. PESU-PTFE compounds should also be investigated under different sliding speeds in order to investigate its effect on the tribological properties. Furthermore, both the PESU-PTFE and PA66i-PTFE composites should also be tested under higher temperature tribological tests to see temperature dependent differences. It would also be of great interest to test plasma treated PESU

and polyamide compounds in other test set-ups, such as ball on prism set up, or ring on disc with different contact area.

Furthermore, a more detailed investigation of the frictional film formation would be beneficial to increase the knowledge of the role of chemical altered PTFE in tribological applications. Therefore, XPS characterization of counter-surfaces and sliding areas for chemical evaluation of the friction films is proposed. For the composites, the effect of lower PTFE loading should also be studied, as this approach may be more efficient in terms of loss of mechanical performance while keeping the tribological performance. It would be also of great interest to investigate plasma treated PTFE in other high performance polymers, such as polyphenylene sulphide or polyetheretherketone and compounds containing fibre reinforcements such as glass or carbon fibres.

In order to commercialize the plasma treatment of PTFE, further investigations on the optimisation of the plasma treatment process must be carried out. The key parameters should be selected and optimised in order to make the treatment even more effective. It seems that the treatment time needs to be significantly reduced and for this purpose other process gases should be investigated and different power settings should be evaluated. Furthermore, the feasibility of scaling up the plasma treatment process using a larger drum is necessary in order to treat large amounts of PTFE powders for commercial production.

The commercialisation of compounds containing plasma treated PTFE will now be started with high heat polymers at Lehmann & Voss, Hamburg.

A.5 Non published results

A.5.1 SEM images of counter discs

After the pin on disc tests, the transfer film on the 100 Cr⁶ counter discs was examined by SEM microscopy. Therefore a SEM microscope Hitachi S3200 was used. The films on the counter discs were sputter coated with gold for imaging as polymer is usually electrically insulating. The samples were measured using an excitation voltage of 1.5kV to the electron gun and the beam current was approx. 60 uA.

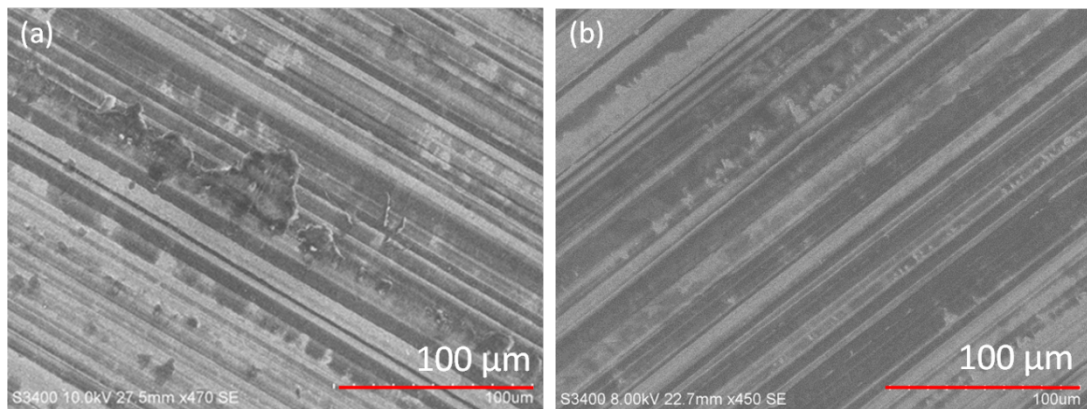


Figure 8.1 SEM pictures of transfer film on discs after sliding against (a) sample 15-PESU-T2, (b) sample 30-PESU-NH3

A.6 Statistical values

A.6.1 r-table

f	statistical certainty		
	95%	99%	99,9%
1	1409	1414	1414
2	1645	1715	1730
3	1757	1918	1982
4	1814	2051	2178
5	1848	2142	2329
6	1870	2208	2447
7	1885	2256	2540
8	1895	2294	2616
9	1903	2324	2678
10	1910	2348	2730
11	1916	2368	2774
12	1920	2385	2812
13	1923	2399	2845
14	1926	2412	2874
15	1928	2423	2899
16	1931	2432	2921
17	1933	2440	2941
18	1935	2447	2959
19	1936	2454	2975
20	1937	2460	2990
25	1942	2483	3047
30	1945	2498	3085
35	1948	2509	3113
40	1949	2518	3134
45	1950	2524	3152
50	1951	2529	3166
100	1956	2553	3227
200	1958	2564	3265
300	1958	2566	3271
400	1959	2568	3275
500	1959	2570	3279
600	1959	2571	3281
700	1959	2572	3283
800	1959	2573	3285
1000	1960	2576	3291

A.6.2 Table of student t-factor

v	95,000 %	99,000 %	99,900 %
1	12,706	63,657	636,619
2	4,303	9,925	31,599
3	3,182	5,841	12,924
4	2,776	4,604	8,610
5	2,571	4,032	6,869
6	2,447	3,707	5,959
7	2,365	3,499	5,408
8	2,306	3,355	5,041
9	2,262	3,250	4,781
10	2,228	3,169	4,587
12	2,179	3,055	4,318
15	2,131	2,947	4,073
20	2,086	2,845	3,850
30	2,042	2,750	3,646
40	2,021	2,704	3,551
50	2,009	2,678	3,496
60	2,000	2,660	3,460
100	1,984	2,626	3,390

9 References

- [1] PlasticsEurope. *Plastics – the Facts 2014: An analysis of European plastics production, demand and waste data*. Brussels, 2014.
- [2] Basavaraj E, Ramaraj B, Lee J, Siddaramaiah. Polyamide 6/carbon black/molybdenum disulphide composites: Friction, wear and morphological characteristics. *Materials Chemistry and Physics* 2013;138(2-3):658–65.
- [3] Unal H, Mimaroglu A. Friction and wear performance of polyamide 6 and graphite and wax polyamide 6 composites under dry sliding conditions. *Wear* 2012;289:132–7.
- [4] Chang L, ZHANG Z, Zhang H, Schlarb AK. On the sliding wear of nanoparticle filled polyamide 66 composites. *Composites Science and Technology* 2006;66(16):3188–98.
- [5] Basavaraj E, Ramaraj B, Siddaramaiah M. Investigations on the influence of polytetrafluoroethylene powder as a filler on physico-mechanical and wear characteristics of nylon 66/graphite composites. *High Performance Polymers* 2012;24(7):616–24.
- [6] Franke R, Lehmann D, Kunze K. Tribological behaviour of new chemically bonded PTFE polyamide compounds. *Wear* 2007;262(3-4):242–52.
- [7] Mens J, Gee A de. Friction and wear behaviour of 18 polymers in contact with steel in environments of air and water. *Wear* 1991;149(1-2):255–68.
- [8] Caro JC, Lappan U, Lunkwitz K. Insertion of sulfur-containing functional groups into polytetrafluoroethylene (PTFE) by low pressure plasma treatment. *Surface and Coatings Technology* 1999;116-119:792–5.
- [9] Inagaki N, Tasaka S, Narushima K, Teranishi K. *J. Appl. Polym. Sci.*:340–8.

- [10] Pringle SD, Joss VS, Jones C. Ammonia Plasma Treatment of PTFE Under Known Plasma Conditions. *Surf. Interface Anal.* 1996;24(12):821–9.
- [11] Klüpfel B, Lehmann D. Functionalization of irradiated PTFE micropowder with methacryl- or hydroxy groups for chemical coupling of PTFE with different matrix polymers. *J. Appl. Polym. Sci.* 2006;101(5):2819–24.
- [12] Bürger W, Lunkwitz K, Pompe G, Petr A, Jehnichen D. Radiation degradation of fluoropolymers: Carboxylated fluoropolymers from radiation degradation in presence of air. *J. Appl. Polym. Sci.* 1993;48(11):1973–85.
- [13] Morra A, Occhiello E, Garbassi F. Wettability and surface chemistry of irradiated PTFE. *Angew. Makromol. Chemie* 1990;180(1):191–8.
- [14] Huang C, Chiang W. Chemical surface treatment of poly(tetrafluoroethylene) powder. *Angew. Makromol. Chemie* 1993;209(1):9–23.
- [15] Kim SR. Surface modification of poly(tetrafluoroethylene) film by chemical etching, plasma, and ion beam treatments. *J. Appl. Polym. Sci.* 2000;77(9):1913–20.
- [16] McKeen LW:15–36.
- [17] Dorschner H, Lappan U, Lunkwitz K. Electron beam facility in polymer research: radiation induced functionalization of polytetrafluoroethylene. *Nuclear Instruments and Methods in Physics Research Section B: Beam Interactions with Materials and Atoms* 1998;139(1-4):495–501.
- [18] Diener electronic GmbH + Co. KG. Plasma Technology. [May 25, 2013]; Available from:
http://www.plasmasurfacetechology.eu/media/Plasmatechnik_en_web.pdf.
- [19] Strobel M, Lyons CS, Mittal KL. Plasma surface modification of polymers: Relevance to adhesion. Utrecht, Netherlands: VSP, 1994.

- [20] Baumgärtner K, Schneider J, Schulz A, Feichtinger J, Walker M. Short-time plasma pre-treatment of polytetrafluoroethylene for improved adhesion. *Surface and Coatings Technology* 2001;142-144:501–6.
- [21] Teodoru S, Kusano Y, Rozlosnik N, Michelsen PK. Continuous Plasma Treatment of Ultra-High-Molecular-Weight Polyethylene (UHMWPE) Fibres for Adhesion Improvement. *Plasma Processes Polym.* 2009;6(S1):S375–S381.
- [22] Anagreh N, Dorn L, Bilke-Krause C. Low-pressure plasma pretreatment of polyphenylene sulfide (PPS) surfaces for adhesive bonding. *International Journal of Adhesion and Adhesives* 2008;28(1-2):16–22.
- [23] Lucas EF, Rabello M, Mallon P, Kovačević V, Bismarck A, Brostow W, Chiu R, Hagg Lobland, Haley E., Ho KK. Effects of surface plasma treatment on tribology of thermoplastic polymers. *Polym. Eng. Sci.* 2008;48(10):1971–6.
- [24] Yasuda H, Marsh HC, Brandt ES, Reilley CN. ESCA study of polymer surfaces treated by plasma. *J. Polym. Sci. Polym. Chem. Ed.* 1977;15(4):991–1019.
- [25] Hall JR, Westerdahl CAL, Bodnar MJ, Levi DW. Effect of activated gas plasma treatment time on adhesive bondability of polymers. *J. Appl. Polym. Sci.* 1972;16(6):1465–77.
- [26] Chien H, Ma K, Kuo C, Huang S. Effects of plasma power and reaction gases on the surface properties of ePTFE materials during a plasma modification process. *Surface and Coatings Technology* 2013;228:S477–S481.
- [27] Vargo TG, Gardella JA, Meyer AE, Baier RE. *J. Polym. Sci. A Polym. Chem.*:555–70.
- [28] Bretagnol F, Tatouliau M, Arefi-Khonsari F, Lorang G, Amouroux J. Surface modification of polyethylene powder by nitrogen and ammonia low pressure

- plasma in a fluidized bed reactor. *Reactive and Functional Polymers* 2004;61(2):221–32.
- [29] Arpagaus C, Rossi A, Rudolf von Rohr P. Short-time plasma surface modification of polymer powders in a down flowing tube reactor. *Surface and Coatings Technology* 2005;200(1-4):525–8.
- [30] Loh I, Cohen RE, Baddour RF. *J. Appl. Polym. Sci.*:901–10.
- [31] Katrin Rieß. *Plasmamodifizierung von Polyethylen*. Halle, 2001.
- [32] Leroy JB, Fatah N, Mutel B, Grimblot J. Treatment of a Polyethylene Powder Using a Remote Nitrogen Plasma Reactor Coupled With a Fluidized Bed: Influence on Wettability and Flowability. *Plasmas and Polymers* 2003;8(1):13–29.
- [33] Koberstein JT. *Surface Properties*.
- [34] Ebnesajjad S, Morgan RA. *Fluoropolymer additives*, 1st ed. Oxford: William Andrew, 2012.
- [35] Dasgupta S, Hammond WB, Goddard WA. Crystal Structures and Properties of Nylon Polymers from Theory. *J. Am. Chem. Soc.* 1996;118(49):12291–301.
- [36] Margolis JM. *Engineering thermoplastics: Properties and applications*. New York: Dekker, ©1985.
- [37] Roberts R. *Fatigue Crack Propagation in Nylon 66 Blends: Fracture Mechanics*: American Society for Testing and Materials, 1980.
- [38] Yu S, Hu H, Yin J. Effect of rubber on tribological behaviors of polyamide 66 under dry and water lubricated sliding. *Wear* 2008;265(3-4):361–6.
- [39] Xing Y, Zhang G, Ma K, Chen T, Zhao X. Study on the Friction and Wear Behaviors of Modified PA66 Composites. *Polymer-Plastics Technology and Engineering* 2009;48(6):633–8.

- [40] Chen YK, Kukureka SN, Hooke CJ. The wear and friction of short glass-fibre-reinforced polymer composites in unlubricated rolling-sliding contact. *J Mater Sci* 1996;31(21):5643–9.
- [41] Jia B, Li T, Liu X, Cong P. Tribological behaviors of several polymer–polymer sliding combinations under dry friction and oil-lubricated conditions. *Wear* 2007;262(11-12):1353–9.
- [42] Dallner C, Kunkel R., Ehrenstein G. W., Lehmann D., Klupfel B. *Triebologie und Schmierungstechnik*:25–31.
- [43] Chen Z, Li T, Yang Y, Liu X, Lv R. Mechanical and tribological properties of PA/PPS blends. *Wear* 2004;257(7-8):696–707.
- [44] Rajesh JJ, Bijwe J, Tewari US. Influence of fillers on abrasive wear of short glass fibre reinforced polyamide composites. *Journal of Materials Science* 2001;36(2):351–6.
- [45] Lehmann D, Hupfer B, Lappan U, Pompe G, Häußler L, Jehnichen D, Janke A, Geißler U, Reinhardt R, Lunkwitz K, Franke R, Kunze K. New PTFE-polyamide compounds. *des monomers polym* 2002;5(2):317–24.
- [46] Pompe G, Häußler L, Lehmann D. Poly(tetrafluorethylen)/Polyamid (PTFE/PA)-Compounds - Charakterisierung der dispersen PTFE-Phase und der in-situ-reaktion zwischen PTFE und Polyamid: Jahresbericht 2003, IPFDD.
- [47] Duan Y, Cong P, Liu X, Li T. Comparative Study of Tribological Properties of Polyphenylene Sulfide (PPS), Polyethersulfone (PES), and Polysulfone (PSU). *J. of Macromolecular Sc., Part B* 2009;48(2):269–81.
- [48] R. Künkel. Auswahl und optimierung von Kunststoffen für tribologisch beanspruchte Systeme. Erlangen: Univ., Lehrstuhl für Kunststofftechnik, 2005.
- [49] Atkins AG, Omar MK, Lancaster JK. Wear of polymers. *J Mater Sci Lett* 1984;3(9):779–82.

- [50] Duan Y, Cong P, Liu X, Li T. Comparative Study of Tribological Properties of Polyphenylene Sulfide (PPS), Polyethersulfone (PES), and Polysulfone (PSU). *J. of Macromolecular Sc., Part B* 2009;48(2):269–81.
- [51] Duan Y, Cong P, Liu X, Li T. Friction and Wear of Polyphenylene Sulfide (PPS), Polyethersulfone (PES) and Polysulfone (PSU) Under Different Cooling Conditions. *J. of Macromolecular Sc., Part B* 2009;48(3):604–16.
- [52] Bijwe J, Rajesh J, Jeyakumar A, Ghosh A, Tewari U. Influence of solid lubricants and fibre reinforcement on wear behaviour of polyethersulphone. *Tribology International* 2000;33(10):697–706.
- [53] Aurilia M, Sorrentino L, Sanguigno L, Iannace S. Nanofilled polyethersulfone as matrix for continuous glass fibers composites: Mechanical properties and solvent resistance. *Adv. Polym. Technol.* 2010;29(3):146–60.
- [54] Bijwe J, Awtade S, Satapathy BK, Ghosh A. Influence of Concentration of Aramid Fabric on Abrasive Wear Performance of Polyethersulfone Composites. *Tribology Letters* 2004;17(2):187–94.
- [55] Bijwe J, Sharma M. Nano and Micro PTFE for Surface Lubrication of Carbon Fabric Reinforced Polyethersulphone Composites:19–39.
- [56] Jost HP. Lubrication (tribology) education and research. A report on the present position and the industry's needs. London, UK: Department of Education and Science: Her Majesty's Stationery Office (HMSO), 1966.
- [57] Mang T, Bobzin K, Bartels T. *Industrial Tribology: Tribosystems, Friction, Wear and Surface Engineering, Lubrication*, 4th ed. s.l: Wiley-VCH, 2011.
- [58] Biresaw G, Mittal KL. *Surfactants in tribology*.
- [59] Amontons G. De la résistance cause dans les machines. *Mémoire de l'Académie Royale* 1699(1):275–82.
- [60] Bhushan B. *Introduction to tribology*: John Wiley & Sons, 2013.

- [61] Taylor RI, Nagatomi E, Doki S, Dixon RT. Tribology and Energy Efficiency. World Tribology Congress. Kyoto, 2009.
- [62] Holmberg K, Andersson P, Erdemir A. Global energy consumption due to friction in passenger cars. *Tribology International* 2012;47:221–34.
- [63] Alexander B. Buechler. Benchmarking Golf VII; Available from: <http://www.plastics.gl/automotive/benchmarking-golf-vii/>.
- [64] Sinha SK. Polymer tribology. London: Imperial College Press, 2009.
- [65] Myshkin N, Petrokovets M, Kovalev A. Tribology of polymers: Adhesion, friction, wear, and mass-transfer. *Tribology International* 2005;38(11-12):910–21.
- [66] Czichos H. Tribology: A systems approach to the science and technology of friction, lubrication, and wear, 3rd ed. Amsterdam, New York, New York: Elsevier Scientific Pub. Co; Distributors for the U.S. and Canada, Elsevier North Holland, 1978.
- [67] Uetz H, Wiedemeyer J. Tribologie der Polymere: Grundlagen und Anwendung in der Technik: Reibung, Verschleiss, Schmierung. München, Wien: Carl Hanser, op. 1985.
- [68] Tanaka K, Yamada Y, Ueda S. Effect of temperature on the friction and wear of heat-resistant polymer-based composites. *J. Synth. Lubr.* 1992;8(4):281–94.
- [69] Chang L, Zhang Z, Ye L, Friedrich K. Tribological properties of high temperature resistant polymer composites with fine particles. *Tribology International* 2007;40(7):1170–8.
- [70] Czichos H, Habig K. Tribologie-Handbuch: Tribometrie, Tribomaterialien, Tribotechnik ; mit 123 Tabellen, 3rd ed. Wiesbaden: Vieweg + Teubner, 2010.

- [71] Unal H, Sen U, Mimaroglu A. Dry sliding wear characteristics of some industrial polymers against steel counterface. *Tribology International* 2004;37(9):727–32.
- [72] Suh NP, Sin H. The genesis of friction. *Wear* 1981;69(1):91–114.
- [73] Lehmann&Voss&Co. KG. Tribological properties of modified high-performance thermoplastics. Hamburg, 2012.
- [74] Belyj V, Sviridenok AI, Petrokovets MI, Savkin VG. Friction and wear in polymer-based materials. Oxford a.o: Pergamon Press, 1982.
- [75] Owens DK, Wendt RC. Estimation of the surface free energy of polymers. *J. Appl. Polym. Sci.* 1969;13(8):1741–7.
- [76] Wu S. Polymer interface and adhesion. New York: M. Dekker, 1982.
- [77] Erhard G. Zum Reibungs- und Verschleißverhalten von Polymerwerkstoffen. Karlsruhe, 1980.
- [78] Ludema KC. Friction, wear, lubrication: A textbook in tribology. Boca Raton: CRC Press, 1996.
- [79] Erhard G. Konstruieren mit Kunststoffen: Mit 58 Tabellen, 2nd ed. München, Wien: Hanser, 1999.
- [80] Bowden FP, Tabor D. The friction and lubrication of solids. Oxford, New York: Clarendon Press; Oxford University Press, 2001, c1954.
- [81] Briscoe BJ, Sinha SK. Wear of polymers. *Proceedings of the Institution of Mechanical Engineers, Part J: Journal of Engineering Tribology* 2002;216(6):401–13.
- [82] Blau PJ. Wear testing: in *Metals handbook*, 2nd ed. Materials Park, Oh.: ASM International, 1998.
- [83] McKeen LW. Fatigue and tribological properties of plastics and elastomers, 2nd ed. Amsterdam, Oxford: William Andrew, 2010.

- [84] Theiler GE. PTFE- and PEEK-matrix composites for tribological applications at cryogenic temperatures and in hydrogen. Bremerhaven: Wirtschaftsverl. NW, Verl. für neue Wiss, 2005.
- [85] WIELEBA W. The Mechanism of Tribological Wear of Thermoplastic Materials. Archives of Civil and Mechanical Engineering 2007;7(4):185–99.
- [86] Suh NP, Saka N (eds.). Fundamentals of tribology: Proceedings of the International Conference on the Fundamentals of Tribology, held at the Massachusetts Institute of Technology, Cambridge, Massachusetts, June 1978. Cambridge, Mass: MIT Press, 1980.
- [87] Szameitat M. Reibung und Verschleiß von Mischungen aus hochtemperaturbeständigen thermoplastischen Kunststoffen. Erlangen-Tennenlohe: Univ., Lehrstuhl für Kunststofftechnik, 1997.
- [88] Zum Gahr K. Microstructure and wear of materials. Amsterdam, New York: Elsevier, 1987.
- [89] DIN Deutsches Institut für Normung e.V. Plain bearings - Testing of the tribological behaviour of bearing materials - Part 2: Testing of polymer-based bearing materials, 1999th ed.(ISO 7148-2). Berlin: Beuth Verlag, 2001.
- [90] RYMUZA Z. Tribology of Polymers. Archives of Civil and Mechanical Engineering 2007;7(4):177–84.
- [91] Hergenrother PM. The use, design, synthesis, and properties of high performance/high temperature polymers: an overview. High Performance Polymers 2003;15(1):3–45.
- [92] Ehrenstein GW. Mit Kunststoffen konstruieren: Eine Einführung ; mit 33 Tabellen. München, Wien: Hanser, 1995.
- [93] Campo EA. Selection of Polymeric Materials: How to Select Design Properties from Different Standards: Elsevier Science, 2008.

- [94] Friedrich K. Friction and wear of polymer composites. Amsterdam, New York: Elsevier, 1986.
- [95] Stachowiak G, Batchelor AW. Engineering Tribology: Elsevier Science, 2011.
- [96] Li D, Xie Y, Li W, You Y, Deng X. Tribological and mechanical behaviors of polyamide 6/glass fiber composite filled with various solid lubricants. *TheScientificWorldJournal* 2013;2013:320837.
- [97] Morton-Jones DH, Ellis JW. Plastics Gears. In: *Polymer Products*: Springer, 1986. pp. 42–64.
- [98] Bahadur S, Tabor D. Role of Fillers in the Friction and Wear Behavior of High-Density Polyethylene;287:253–68.
- [99] Studies on abrasive wear of carbon fibre (short) reinforced polyamide composites. *Composites* 1992;23(4):281.
- [100] Flöck J. Beitrag zur experimentellen und modellhaften Beschreibung der Gleitverschleissmechanismen kohlenstoffaserverstärkter Polyetheretherketon-(PEEK)-Verbunde. Kaiserslautern: IVW, 2001.
- [101] Sutor S, Gebhard S. On the impact of selected solid lubricants on the dry and diesel fuel lubricated friction and wear behavior of Polyetheretherketone (PEEK). Kaiserslautern, 2011.
- [102] Borggreve R, Gaymans RJ. Impact behaviour of nylon-rubber blends: 4. Effect of the coupling agent, maleic anhydride. *Polymer* 1989;30(1):63–70.
- [103] Kohan MI. Nylon plastics handbook. Munich, New York, Cincinnati: Hanser Publishers; Distributed in the USA and in Canada by Hanser/Gardner Publications, ©1995.
- [104] Wunderlich W. Polyamide. Würzburg, 2008.
- [105] Kutz M (ed.). Applied plastics engineering handbook: Processing and materials. Amsterdam, Boston: William Andrew, ©2011.

- [106] Page IB. Polyamides as Engineering Thermoplastic Materials: Rapra Technology Limited.
- [107] Engineering Thermoplastics: Properties and Applications: Taylor & Francis, 1985.
- [108] Monson L, Braunwarth M, Extrand CW. Moisture absorption by various polyamides and their associated dimensional changes. *J. Appl. Polym. Sci.* 2008;107(1):355–63.
- [109] Meister J. Polymer Modification: Principles, Techniques, and Applications: Taylor & Francis, 2000.
- [110] Shojaei A, Gholamalipour S. Effect of chemical treatment of Teflon powder on the properties of polyamide 66/Teflon composites prepared by melt mixing. *Macromol. Res.* 2011;19(6):613–21.
- [111] Lehmann D, Hupfer B, Staudinger U, Hupfer L, Jehnichen D, Janke A, Kunze K, Franke R, Haase I. Reibungs- und Verschleissverhalten von chemisch gekoppelten PTFE-PA-6.6-Materialien. *Mat.-wiss. u. Werkstofftech.* 2004;35(10-11):696–706.
- [112] Gomari S, Ghasemi I, Karrabi M, Azizi H. Organoclay localization in polyamide 6/ethylene-butene copolymer grafted maleic anhydride blends: the effect of different types of organoclay. *J Polym Res* 2012;19(1).
- [113] Tomova D, Radusch H. Morphology and properties of ternary polyamide 6/polyamide 66/elastomer blends. *Polym. Adv. Technol.* 2003;14(1):19–26.
- [114] Chen Z, Li T, Yang Y, Zhang Y, Lai S. The Effect of Phase Structure on the Tribological Properties of PA66/HDPE Blends. *Macromol. Mater. Eng.* 2004;289(7):662–71.

- [115] Ittemann PD, Heinz GD. High-temperature resistant polyether sulphone polyether ketone block copolycondensates: Google Patents, 1988; Available from: <http://www.google.com/patents/EP0265842A2?cl=en>.
- [116] Cheremisinoff NP. Advanced polymer processing operations. Westwood, N.J., U.S.A.: Noyes Publications, 1998.
- [117] Staff PD. Fatigue and Tribological Properties of Plastics and Elastomers: Elsevier Science, 2013.
- [118] Platt DK. Engineering and High Performance Plastics Market Report: A Rapra Market Report: Rapra Technology Limited, 2003.
- [119] Kalacska G. An engineering approach to dry friction behaviour of numerous engineering plastics with respect to the mechanical properties. *expresspolymlett* 2012;7(2):199–210.
- [120] Woo H, Li H. Advanced functional materials. Hangzhou, Berlin: Zhejiang University Press; Springer, 2011.
- [121] Kaiser W. Kunststoffchemie für Ingenieure: Von der Synthese bis zur Anwendung, 3rd ed. München: Hanser, 2011.
- [122] Drobny JG. Fluoroplastics. Shawbury, Shrewsbury, Shropshire, U.K: Rapra Technology Ltd., 2006.
- [123] Ebnesajjad S, Khaladkar P. Fluoroplastics, Volume 2: Melt Processible Fluoroplastics: The Definitive User's Guide (Fluoropolymers): Elsevier Science, 2008.
- [124] Xanthos M. Functional fillers for plastics, 2nd ed. Weinheim: Wiley-VCH, 2010.
- [125] Burris DL, Santos K, Lewis SL, Liu X, Perry SS, Blanchet TA, Schadler LS, Sawyer WG. Chapter 17. Polytetrafluoroethylene matrix nanocomposites for tribological applications;55:403–38.

- [126] McKeen LW. Fluorinated Coatings and Finishes Handbook 1 Fundamentals:1–13.
- [127] Kutz M. Applied Plastics Engineering Handbook: Processing and Materials: Elsevier Science, 2011.
- [128] Johns K, Stead G. Journal of Fluorine Chemistry:5–18.
- [129] Karl Harrison. Teflon; Available from:
<http://www.3dchem.com/molecules.asp?ID=200#>.
- [130] Bijwe J, Sen S, Ghosh A. Influence of PTFE content in PEEK–PTFE blends on mechanical properties and tribo-performance in various wear modes. *Wear* 2005;258(10):1536–42.
- [131] Li J. The Impact and Tribological Properties of PTFE Composites Filled with PA6. *Journal of Thermoplastic Composite Materials* 2010;23(6):807–16.
- [132] Hoffmann T, Lehmann D. Chemical modification of poly(tetrafluoroethylene) micropowder - basis for special lubricant additives. *Lubr. Sci.* 2013;25(4):313–27.
- [133] Sohail Khan M, Franke R, Lehmann D, Heinrich G. Physical and tribological properties of PTFE micropowder-filled EPDM rubber. *Tribology International* 2009;42(6):890–6.
- [134] Ting-Yung H, Eiss NS. The effects of molecular weight and cooling rate on fine structure, stress-strain behavior and wear of polytetrafluoroethylene. *Wear* 1983;84(2):203–15.
- [135] Khattab Ghazi M. A., Salatiello Peter P. Nucleated Nylon/PTFE Compositions(US4159286), 1977.
- [136] Crosby Jane M., Theberge John E. Methods of improving friction and wear properties of polymer systems(US4945126), 1987.

- [137] Stott LL. Nylon polytetrafluoroethylene composition and article(US 2975128 A): Google Patents, 1961; Available from: <https://www.google.com/patents/US2975128>.
- [138] Makuuchi K, Cheng S. Radiation Processing of Polymer Materials and Its Industrial Applications: Wiley, 2012.
- [139] Dillon Joseph A. Process for non-destructive radiation degradation of polytetrafluorethylene(US 3766031), 1972.
- [140] Chapman BN. Glow discharge processes: Sputtering and plasma etching. New York: Wiley, 1980.
- [141] Sturrock PA. Plasma physics: An introduction to the theory of astrophysical, geophysical, and laboratory plasmas. Cambridge [England], New York: Cambridge University Press, 1994.
- [142] Grace JM, Gerenser LJ. Plasma Treatment of Polymers. *Journal of Dispersion Science and Technology* 2003;24(3-4):305–41.
- [143] Vandencastele N, Reniers F. Surface characterization of plasma-treated PTFE surfaces: an OES, XPS and contact angle study. *Surf. Interface Anal.* 2004;36(8):1027–31.
- [144] Píchal J, Hladík J, Špatenka P. Atmospheric-Air Plasma Surface Modification of Polyethylene Powder. *Plasma Process. Polym.* 2009;6(2):148–53.
- [145] Liu C, Wu J, Ren L, Tong J, Li J, Cui N, Brown N, Meenan B. Comparative study on the effect of RF and DBD plasma treatment on PTFE surface modification. *Materials Chemistry and Physics* 2004;85(2-3):340–6.
- [146] Sarani A, Geyter N de, Nikiforov A, Morent R, Leys C, Hubert J, Reniers F. Surface modification of PTFE using an atmospheric pressure plasma jet in argon and argon+CO₂. *Surface and Coatings Technology* 2012;206(8-9):2226–32.

- [147] Arpagaus C, Rossi A, Rudolf von Rohr P. Short-time plasma surface modification of HDPE powder in a Plasma Downer Reactor – process, wettability improvement and ageing effects. *Applied Surface Science* 2005;252(5):1581–95.
- [148] Clark DT, Hutton DR. Surface modification by plasma techniques. I. The interactions of a hydrogen plasma with fluoropolymer surfaces. *J. Polym. Sci. A Polym. Chem.* 1987;25(10):2643–64.
- [149] van de Velde F, Baets P de. *Wear*:106–14.
- [150] Inagaki N, Tasaka S, Abe H. Surface modification of polyethylene powder using plasma reactor with fluidized bed. *J. Appl. Polym. Sci.* 1992;46(4):595–601.
- [151] Badey JP, Espuche E, Sage D, Chabert B, Jugnet Y, Batier C, Duc TM. A comparative study of the effects of ammonia and hydrogen plasma downstream treatment on the surface modification of polytetrafluoroethylene. *Polymer* 1996;37(8):1377–86.
- [152] Park SH, Kim SD. Plasma surface treatment of HDPE powder in a fluidized bed reactor. *Polymer Bulletin* 1994;33(2):249–56.
- [153] Zettsu N, Itoh H, Yamamura K. Surface functionalization of PTFE sheet through atmospheric pressure plasma liquid deposition approach. *Surface and Coatings Technology* 2008;202(22-23):5284–8.
- [154] Mutel B, Bigan M, Vezin H. Remote nitrogen plasma treatment of a polyethylene powder. *Applied Surface Science* 2004;239(1):25–35.
- [155] Vivien C, Wartelle C, Mutel B, Grimblot J. Surface property modification of a polyethylene powder by coupling fluidized bed and far cold remote nitrogen plasma technologies. *Surf. Interface Anal.* 2002;34(1):575–9.

- [156] Pavlatova M, Horakova M, Hladik J, Spatenka P. Plasma Surface Treatment of Powder Materials — Process and Application. *Acta Polytech* 2012;52(3).
- [157] Morosoff N. *Plasma Science and Technology*, Herman V. Boenig, Cornell University Press, Ithaca, New York, 1982, 299 pp. Price: \$34.50. *J. Polym. Sci. B Polym. Lett. Ed.* 1982;20(10):558–9.
- [158] Thomas M, Mittal KL. *Atmospheric Pressure Plasma Treatment of Polymers: Relevance to Adhesion*: Wiley, 2013.
- [159] Wilson DJ, Williams RL, Pond RC. Plasma modification of PTFE surfaces. Part I: Surfaces immediately following plasma treatment. *Surf. Interface Anal.* 2001;31(5):385–96.
- [160] Hansen RH, Schonhorn H. A new technique for preparing low surface energy polymers for adhesive bonding. *J. Polym. Sci. B Polym. Lett.* 1966;4(3):203–9.
- [161] Clark DT, Wilson R. Selective surface modification of polymers by means of hydrogen and oxygen plasmas. *J. Polym. Sci. Polym. Chem. Ed.* 1983;21(3):837–53.
- [162] Caro J, Lappan U, Simon F, Pleul D, Lunkwitz K. On the low-pressure plasma treatment of PTFE (polytetrafluoroethylene) with SO₂ as process gas. *European Polymer Journal* 1999;35(6):1149–52.
- [163] Gerenser LJ. X-Ray photoemission study of plasma modified polyethylene surfaces. *Journal of Adhesion Science and Technology* 1987;1(1):303–18.
- [164] Klemberg-Sapieha JE, Martinu L, Küttel OM, Wertheimer MR. Modification of Polymer Surfaces by Dual Frequency Plasma:315–29.
- [165] Wilson DJ, Williams RL, Pond RC. Plasma modification of PTFE surfaces. Part I: Surfaces immediately following plasma treatment. *Surf. Interface Anal.* 2001;31(5):385–96.

- [166] Wilson DJ, Williams RL, Pond RC. Plasma modification of PTFE surfaces. Part II: Plasma-treated surfaces following storage in air or PBS. *Surf. Interface Anal.* 2001;31(5):397–408.
- [167] Clark DT, Hutton DR. *J. Polym. Sci. A Polym. Chem.*:2643–64.
- [168] Foerch R, Beamson G, Briggs D. XPS valence band analysis of plasma-treated polymers. *Surf. Interface Anal.* 1991;17(12):842–6.
- [169] Wilson DJ, Eccles AJ, Steele TA, Williams RL, Pond RC. Surface chemistry and wettability of plasma-treated PTFE. *Surf. Interface Anal.* 2000;30(1):36–9.
- [170] Foerch R, McIntyre NS, Hunter DH. Oxidation of polyethylene surfaces by remote plasma discharge: A comparison study with alternative oxidation methods. *J. Polym. Sci. A Polym. Chem.* 1990;28(1):193–204.
- [171] Sun H, Zhang L, Chai H, Chen H. Surface modification of poly(tetrafluoroethylene) films via plasma treatment and graft copolymerization of acrylic acid. *Desalination* 2006;192(1-3):271–9.
- [172] d'Agostino R, Cramarossa F, Benedictis S de, Ferraro G. Kinetic and spectroscopic analysis of NH₃ decomposition under R.F. Plasma at moderate pressures. *Plasma Chem Plasma Process* 1981;1(1):19–35.
- [173] Clark DT, Hutton DR. Surface modification by plasma techniques. I. The interactions of a hydrogen plasma with fluoropolymer surfaces. *J. Polym. Sci. A Polym. Chem.* 1987;25(10):2643–64.
- [174] Pukanszky B and Fekete E. Adhesion and surface modification 1999;139:109–53.
- [175] Lennon P, Espuche E, Sage D, Gauthier H, Sautereau H, Valot E. *Journal of Materials Science*:49–55.

- [176] Park SH, Kim SD. Oxygen plasma surface treatment of polymer powder in a fluidized bed reactor. *Colloids and Surfaces A: Physicochemical and Engineering Aspects* 1998;133(1-2):33–9.
- [177] Put S, Bertels C, Vanhulsel A. Atmospheric pressure plasma treatment of polymeric powders. *Surface and Coatings Technology* 2013.
- [178] Weiss P. Techniques and applications of plasma chemistry, John R. Hollahan and Alexis T. Bell, Eds., 1974, Wiley, New York, 403 pp. \$22.50. *J. Polym. Sci. B Polym. Lett. Ed.* 1975;13(3):185–6.
- [179] Murata Y, Aradachi T. Change in charging characteristics of polymer powder by plasma treatment. *Journal of Electrostatics* 2001;51-52:97–104.
- [180] J. DERCO, A. LODES, L. Lapcik, J. BLECHA. *Chemical Papers*.
- [181] Cordian Arpagaus. *Plasma Surface Modification of Polymer Powders in a Downer Reactor*. Zürich, 2005.
- [182] Arpagaus C, Sonnenfeld A, von Rohr, Ph. Rudolph. A Downer Reactor for Short-time Plasma Surface Modification of Polymer Powders. *Chem. Eng. Technol.* 2005;28(1):87–94.
- [183] Berger S, Messelhauser Johannes, Schoenherr Walter. *Plasma Unit(US5925325)*, 1995.
- [184] Ihara T, Itô S, Kiboku M. LOW TEMPERATURE PLASMA OXIDATION TREATMENT OF SEVERAL ORGANIC PIGMENTS. *Chem. Lett.* 1986;15(5):675–8.
- [185] Godfrey SP, Kinmond EJ, Badyal, J. P. S., Little IR. Plasmachemical Functionalization of Porous Polystyrene Beads. *Chem. Mater.* 2001;13(2):513–8.
- [186] Sarra-Bournet C, Turgeon S, Mantovani D, Laroche G. Comparison of Atmospheric-Pressure Plasma versus Low-Pressure RF Plasma for Surface

- Functionalization of PTFE for Biomedical Applications. Plasma Process. Polym. 2006;3(6-7):506–15.
- [187] Badey JP, Urbaczewski-Espuche E, Jugnet Y, Sage D, Duc TM, Chabert B. Surface modification of polytetrafluoroethylene by microwave plasma downstream treatment. Polymer 1994;35(12):2472–9.
- [188] Kohlgrüber K. Co-Rotating Twin-Screw Extruder: Carl Hanser Verlag GmbH & Company KG, 2012.
- [189] Manas-Zloczower I. Mixing and Compounding of Polymers: Theory and Practice: Carl Hanser Verlag GmbH & Company KG, 2012.
- [190] Todd DB. Improving incorporation of fillers in plastics. A special report. Advances in Polymer Technology 2000;19(1):54–64.
- [191] Smith BC. Fundamentals of Fourier Transform Infrared Spectroscopy, Second Edition: CRC Press, 2011.
- [192] Sepe P, Rapra Technology Limited. Thermal Analysis of Polymers: Rapra Technology Limited, 1997.
- [193] Lawson G. Chemical Analysis of Polymers: Elsevier, 1991.
- [194] König U, Nitschke M, Pilz M, Simon F, Arnhold C, Werner C. Stability and ageing of plasma treated poly(tetrafluoroethylene) surfaces. Colloids and Surfaces B: Biointerfaces 2002;25(4):313–24.
- [195] Young T. An Essay on the Cohesion of Fluids. Philosophical Transactions of the Royal Society of London 1805;95(0):65–87.
- [196] Washburn EW. The Dynamics of Capillary Flow. Phys. Rev. 1921;17(3):273–83.
- [197] DIN EN ISO 527-1/-2/-3: Determination of tensile properties - Part 1. Berlin: Beuth Verlag, 2012.

- [198] DIN EN ISO 1133: Determination of the melt mass-flow rate (MFR) and melt volume-flow rate (MVR) of thermoplastics - Part 1: Standard method (ISO 1133-1:2011). Berlin: Beuth Verlag, 2012.
- [199] DIN EN 6603-2: Determination of puncture impact behaviour of rigid plastics - Part 2. Berlin: Beuth Verlag, 2002.
- [200] Soever A, Hopf M, Frommann L. *Polymer Testing*:703–8.
- [201] Liu TM, Baker WE. Instrumented dart impact evaluation of linear low density polyethylene at controlled impact energy. *Polym. Eng. Sci.* 1991;31(10):753–63.
- [202] ASTM G137 - 97(2009) Test Method for Ranking Resistance of Plastic Materials to Sliding Wear Using a Block-On-Ring Configuration. West Conshohocken, PA: ASTM International. doi:10.1520/G0137-97R09.
- [203] ASTM D 618 - Practice for Conditioning Plastics for Testing. West Conshohocken, PA: ASTM International. doi:10.1520/D0618.
- [204] Kaiser RE, Mühlbauer JA. *Elementare Tests zur Beurteilung von Messdaten: Soforthilfe für statist. Tests mit wenigen Messdaten*, 2nd ed. Mannheim, Wien, Zürich: Bibliographisches Institut, 1983.
- [205] Sarra-Bournet C, Turgeon S, Mantovani D, Laroche G. A study of atmospheric pressure plasma discharges for surface functionalization of PTFE used in biomedical applications. *J. Phys. D: Appl. Phys.* 2006;39(16):3461–9.
- [206] Heitz J, Niino H, Yabe A. Chemical surface modification on polytetrafluoroethylene films by vacuum ultraviolet excimer lamp irradiation in ammonia gas atmosphere. *Appl. Phys. Lett.* 1996;68(19):2648.
- [207] Dumitraş M, Odochian L. *Journal of Thermal Analysis and Calorimetry*:599–606.

- [208] Conte M, Pinedo B, Igartua A. Role of crystallinity on wear behavior of PTFE composites. *Wear* 2013;307(1-2):81–6.
- [209] Khan M. Friction, Wear and Mechanical Properties of Electron Beam Modified PTFE-based Rubber Compounds, 2009.
- [210] Wheeler DR. Effect of x-ray flux on polytetrafluoroethylene in x-ray photoelectron spectroscopy. *J. Vac. Sci. Technol.* 1982;20(2):226.
- [211] Grundke K, Bogumil T, Gietzelt T, Jacobasch H, Kwok DY, Neumann AW. Wetting measurements on smooth, rough and porous solid surfaces;101:58–68.
- [212] Park SH, Kim SD. *Colloids and Surfaces A: Physicochemical and Engineering Aspects*:33–9.
- [213] Pecorini TJ, Hertzberg RW. The fracture behavior of rubber-toughened, short-fiber composites of nylon 6,6. *Polym. Compos.* 1994;15(3):174–83.
- [214] K. Friedrich (ed.). *Friction and wear of polymer composites*. Amsterdam, The Netherlands: Elsevier Science Publishers, B. V., Amsterdam, 1986.
- [215] Bahadur S. The development of transfer layers and their role in polymer tribology. *Wear* 2000;245(1-2):92–9.
- [216] Hüttinger KJ, Krekel G, Zielke U. Evidence for chemical bond formation between surface treated carbon fibres and high temperature thermoplastics. *J. Appl. Polym. Sci.* 1994;51(4):737–42.
- [217] Biswas SK, Vijayan K. Friction and wear of PTFE — a review. *Wear* 1992;158(1-2):193–211.
- [218] Hunke H, Soim N, Shah T, Kramer E, Pascual A, Karuna M, Siores E. Low-Pressure H₂, NH₃ Microwave Plasma Treatment of Polytetrafluoroethylene (PTFE) Powders: Chemical, Thermal and Wettability Analysis. *Materials* 2015;8(5):2258–75.

- [219] Khan MS, Lehmann D, Heinrich G, Franke R. Tribological study of peroxide-cured EPDM rubber filled with electron beam irradiated PTFE powder. *Wear* 2009;266(1-2):200–7.
- [220] Khan MS, Franke R, Gohs U, Lehmann D, Heinrich G. Friction and wear behaviour of electron beam modified PTFE filled EPDM compounds. *Wear* 2009;266(1-2):175–83.